Université d'Ottawa • University of Ottawa

Precise Motion with Piezoelectric Actuator

by

Constantin Giurgea

Submitted
as part of requirements for a
M. A. Sc. Degree

University of Ottawa

April 2002

0-612-76583-0

Question: Can we control the motion of intelligent materials?

Answer: One of the answers is presented in this report.

Abstract

The purpose of this study is to determine the displacement performance of a high accuracy-positioning device equipped with three piezo ceramic actuators.

The displacement performance of each individual actuator is investigated in order to perform controlled motion over a very small range.

A nanometric precision three – degrees of freedom positioner was designed and fabricated. In order to design a proper closed–loop controller, the open loop characteristics of the nanopositioner were experimentally investigated.

Table of Content

Symbols

Xf	deflection
Fb	blocked force
Fr	resonant frequency
C	capacitance
Xf*	free deflection
P	polarization
μ	dipole moment per unit volume
T	constant stress for mechanically free case
E	constant field for short circuit free case
D	constant electrical displacement for open circuit case
S	constant strain for mechanically clamped case
"d"	strain constants, or d coefficients
"g"	voltage constants, or g coefficients
e	permittivity of the material
e_0	permittivity in free space
k	relative dielectric constant
V	voltage
Q	charge
E	Young's modulus
A	cross section
L	length
F	force
ρ	density
$\propto$	pyroelectric coefficient
T	difference temperature

K3	dielectric constant
X (f)	free deflection
H	hysteresis operator
M	mechanical operator
Fp	tranduced force
q_{ur}	upper right side points of a hysteresis loop
q_{ll}	lower left side points of a hysteresis loop
$\propto$, a, and b	independent characteristic quantities in a hysteresis loop, hysteresis area
ω_0	gaussian beam radius
I	intensity

Figures

Tables

Acknowledgement

The jig shown in Figure 1.0 was build by a group of mechanical engineers from JDS Uniphase. In the next chapters, the experiments will demonstrate the fact that we can control small displacements with piezoelectric actuators.

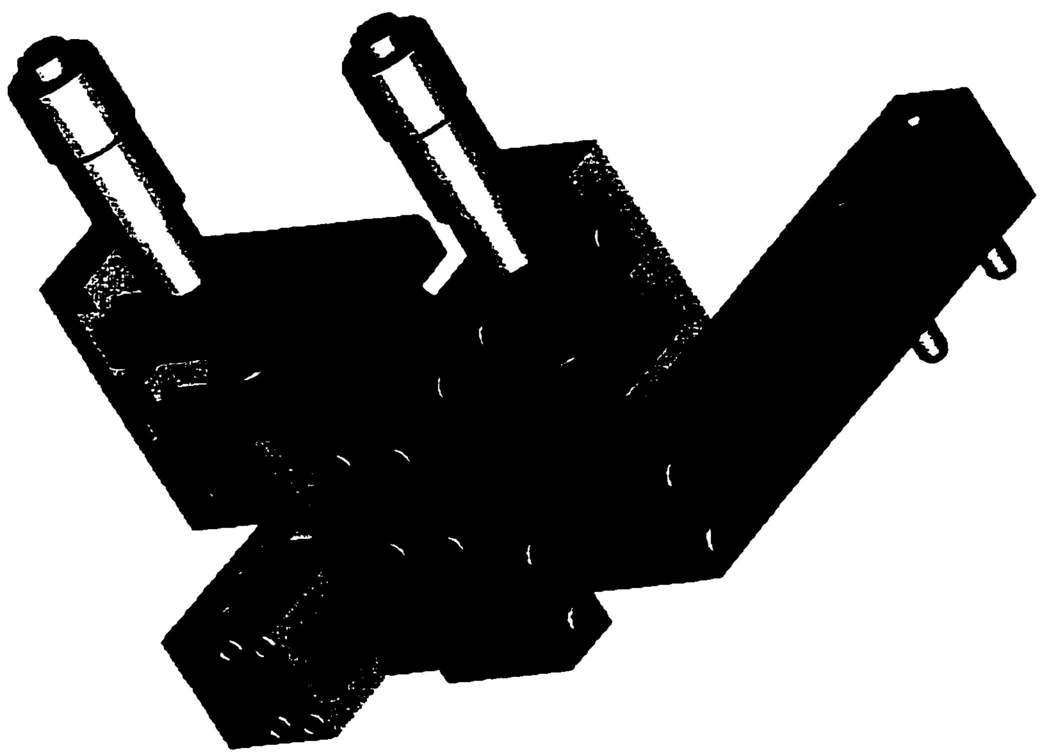

Figure 1.0: Three-axis position jig

1. Introduction

Piezoelectric actuators convert electrical energy into mechanical energy, and mechanical energy into electrical energy [20].

Intelligent material systems (IMS), also known as smart materials, have the unique property of being able to modify their external and internal behavior as a response to a signal. Figure 1.1 shows how this is achieved in a combination of a controller, actuators, materials and sensors that compose Intelligent Smart Material Structures. In the recent years, piezoelectric materials under computer control where made to act as actuators and sensors. In the semiconductor industry smart materials are used already as valves in mass flow controllers. Other applications of piezoelectric materials are in the instrumentation industry, for example pressure transducers [29]. In the aerospace industry, piezoelectric materials have been used for active dumping vibrations in large flexible structures. In the biomedical industry, ionic polymers metal composites have been studied as possible materials for the development of artificial muscle [22].

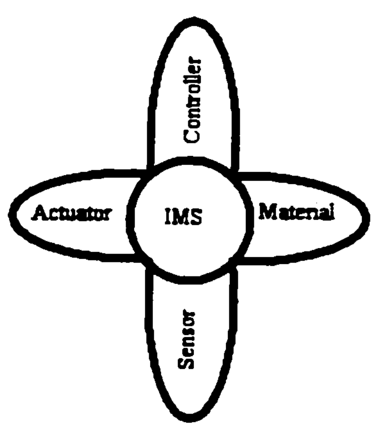

Figure 1.1: Intelligent material systems [20]

Piezoelectric materials have a history of over 100 years[43]. Pierre and Jacques Curie published the first experimental demonstration of a connection between macroscopic piezoelectric phenomena and crystallographic structure in 1880. Their experiment consisted of a conclusive measurement of surface electric charges, appearing on specially prepared crystals (tourmaline, quartz, topaz, cane sugar etc.), which were subjected to mechanical stress.

At that time, this effect was considered a significant discovery, which received the name of piezoelectricity in order to distinguish "contact electricity" (friction generated static electricity) and "pyroelectricity" (electricity generated from crystals by heating).

The Curie brothers found out the relationships between the electrical effects of temperature change and mechanical stress in a given crystal.

However, they did not predict that crystals exhibiting the direct piezoelectric effect (electricity from applied mechanical stress) would also exhibit the reverse piezoelectric mechanical effect (stress in response to applied electric field). Lippmann mathematically derived this property from fundamental thermodynamic principles, in 1881. The Curie brothers confirmed immediately afterwards the existence of the "reverse effect".

At that time, the reversible exchanges of electrical and mechanical energy in piezoelectric crystals were explained on the basis of crystal asymmetry.

Between 1882 and 1917, research work was done on 20 natural crystal classes, in which piezoelectric effects occur.

The first important applications of piezoelectric devices took place during the World War I. In 1917, P. Langevin perfected an ultrasonic submarine detector. The transducer was thin quartz crystals glued between two steel plates, with a resonant frequency of about 50 kHz, mounted in housing suitable for submersion. The goal was of emitting a high frequency "chirp" underwater and measuring depth return echo. Since then the development of sonar transducers, circuits, systems, and materials have never ceased.

The success of sonar stimulated intense development activity on all kind of piezoelectric devices, both resonating and non-resonating.

A new class of materials testing methods based on the propagation of ultrasonic waves was developed. As a result, elastic and viscous properties of liquids and gases could be measured relatively easy and flaws in solid metal structural members could be detected. Also acoustic holographic technique was successfully demonstrated and new ranges of transient pressure measurement were opened up, permitting the study of explosives and internal combustion engines, along with other previously unmeasurable vibrations, accelerations, and impacts.

By the Second World War, most of the piezoelectric applications known today, microphones, accelerometers, ultrasonic transducers, phonograph pick-ups, signal filters, etc. had been conceived.

During and after World War II, in the U.S., Japan and the Soviet Union, research groups worked on improved materials that exhibited dielectric constants up to 100 times higher than common cut crystals. The same class of materials, ferroelectric, was made to exhibit similar improvements in piezoelectric properties. The discovery of easily manufactured piezoelectric ceramics resulted in the development of new piezoelectric devices.

The major advances in material science consisted of the development of the barium titanate, lead zirconate titanate family and perovskite crystal structure. Doping these families with metallic impurities permitted to achieve desired properties such as dielectric constant, stiffness, and piezoelectric coupling coefficients.

Major applications of piezoelectric devices include the following:

- Sonar - based on new transducer geometry's (such as spheres and cylinders) and sizes achieved with ceramic casting;
- Ceramic phono cartridge;
- Piezoelectric ignition systems for single cylinder engine ignition systems, which generate spark voltages by compressing a ceramic part;
- Sonobouy, a sensitive hydrophone for listening and radio transmitting;
- Piezoceramic microphones;

- Ceramic audio tone transducer consisting of a disc of ceramic laminated to a disc of sheet metal.

In 1951 several Japanese companies and universities formed a "competitively cooperative" association the Barium Titanate Application Research Committee [BTARC].

As a result, after 1965 Japanese commercial enterprises began to produce applications and materials, following a successful fish-finder test.

New piezoceramic families free of patent restrictions entered in competition with Vernitron's PZT. Based these materials available, Japanese manufacturers developed piezoceramic signal filters used in television, radio, and communications equipment markets and piezoceramic igniters for natural gas/butane appliances.

New products using piezoceramic materials were developed, such as: audio buzzers, smoke alarms, TTL compatible tone generators, air ultrasonic transducers, television remote controls, intrusion alarm and SAW filter devices, which employed Surface Acoustic Wave effects to achieve high frequency signal filtering, etc.

After 1975 linear piezomotors have been designed using various piezoelectric actuators. Linear piezomotors with nanometer positioning resolution are unable to deliver high stiffness and large output force. The rest of the world, except Japan, was slow in developing piezoceramic applications.

After 1980, several new linear piezomotors have been developed.

Inchworm II was designed to produce a stable holding force, using preload applied springs when the device was off power.

A piezoelectric stepper motor was designed to achieve sub micrometer controlled movement. This device was inserted in a trench to constrain motion to one direction. An electrode on the bottom of a glider worked with another on the top of the trench to implement an electrostatic clamp.

Piezoelectric linear motor was design to drive a head element of a CD-ROM.

The commercial success of the Japanese efforts has attracted the attention of industries in other countries and piezoelectric materials and products are now manufactured in many countries.

2. Overview of Intelligent Materials and Actuators

2.1. Advantages of Piezoelectric Actuators

- A piezoelectric actuator (PZT) can produce extremely fine position changes down to the sub a nanometer range. The smallest changes in operating voltage are converted into smooth movements.
- PZTs can generate a force of several tens of thousand N. Acceleration rates of more than 10,000 g's can be obtained.
- The piezo effect is related to electrical fields. Piezoelectric actuators don't produce magnetic fields and are not affected by magnetic fields. They are especially well suited for applications where magnetic fields cannot be tolerated.
- The piezo effect directly converts electrical energy into motion only absorbing electrical energy during movement; holding heavy loads does not consume power.
- Piezo actuators are ceramic elements that do not need any lubricants and show no wear and abrasion. This makes them clean room compatible and ideally suited for Ultra High Vacuum applications.
- The piezo effect is based on electric fields and functions down to almost zero degree Kelvin.

2.2. Applications of Piezoelectric Actuators

Piezoelectric actuators are used in various applications in Optics, Photonics and Measuring Technology, such as:

- Image stabilization
- Scanning microscopy
- Auto focus systems
- Fiber optic alignment & switching
- Fast mirror scanners
- Adaptive and active optics
- Laser tuning
- Mirror positioning
- Holography
- Stimulation of vibrations

In Microelectronics, piezoelectric actuators are used for:

- Nano-metrology
- Wafer and mask positioning
- Critical Dimensions measurement
- Microlithography
- Inspection systems
- Vibration cancellation

Piezoelectric actuators are also used in Precision Mechanics and Mechanical Engineering:

- Vibration cancellation
- Structural deformation
- Out-of-roundness grinding, drilling, turning
- Tool adjustment
- Wear correction
- Needle valve actuation
- Micro pumps

- Linear drives
- Piezo hammers
- Knife edge control in extrusion tools
- Micro engraving systems
- Shock wave generation

Life Science, Medicine, and Biology also use piezoelectric actuators as follows:

- Patch-clamp drives
- Gene technology
- Micro manipulation
- Cell penetration
- Micro dispensing devices

2.3. Types of Intelligent Materials

Materials that are commonly used to create intelligent material systems are the following:

- Shape memory alloys
- Ionic polymer gels
- Electro and magneto-rheological fluids
- Magnetostrictive materials
- Piezoelectric materials

Shape memory alloys are materials that have a strong relationship between a temperature field and the deformation field [9].

Polymer gels are three-dimensional networks of cross-linked macromolecular polyelectrolytes that swell or shrink in aqueous solutions on addition of alkali or acids, respectively. [6]

Electro and magneto-rheological fluids are a special type of materials that are able to significantly change their properties when they are influenced by an electric or magnetic field. Electro-rheological fluids produce changes in the properties of the fluid shear yield stress and viscosity.

These types of fluids can change their properties by creating a series of dipoles that act like chain structures along the direction of the electrical field. Electro and magneto-rheological fluids have the ability to change phases from liquid to solid and vice versa in a few milliseconds.

Magneto-rheological fluids have similar property changes as the electro-rheological fluids with the exception that the change in properties of magneto-rheological fluids is due to the application of a magnetic field [15]. Magnetostrictive materials are materials that deform when subjected to a magnetic field.

Piezoelectric materials are materials that have a very strong link between an electrical field and their deformation field. They also have the ability to produce an electrical field when the piezoelectric materials are deformed. Piezoelectric phenomena are closely related to ferroelectric behavior [25].

In the next section the concepts of ferroelectricity and ferroelectric properties are presented. These properties are dependent on parameters such as solute composition, lattice structure, grain size, and grain shape. In the case of ferroelectric materials, the symmetry of the crystal, influences the elastic, dielectric, piezoelectric, and ferroelectric properties of the crystal [39].

2.4. Macro and Micro Structure of Piezoelectric Materials

The properties of materials are determined by the crystallographic arrangement of atoms. Ferroelectric crystals are those that exhibit spontaneous polarization and for which the polarized dipoles can have a change in direction under the effect of an external electrical field. Physical properties, as well as elastic, dielectric and piezoelectric properties, are due to the existence or lack of structural symmetry of the crystal. Some crystals exhibit different microstructure arrangement at different temperatures. In the case of ferroelectric materials, this temperature is known as the Curie temperature. Curie temperature is the temperature at which a paraelectric-ferroelectric phase transition occurs. A paraelectric structure is a structure, which does not exhibit ferroelectric properties. Figure 2.1 shows the crystal structure of a piezoelectric material, barium titanate. When the temperature of the structure is raised to the Curie temperature of $120^{\circ}C$, the unit cell structure of the barium titanate becomes cubic. Below the Curie temperature the structure is slightly deformed, and it is producing a dipole at the unit cell level. Pyroelectricity corresponds to the property of materials to exhibit polarization due to a change in temperature [39].

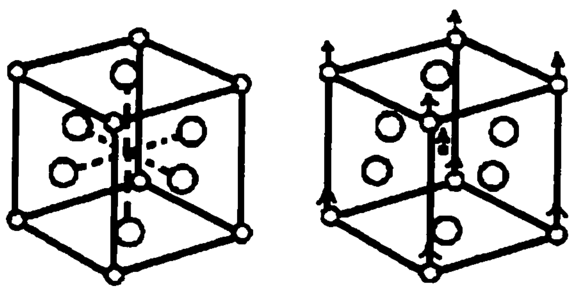

Figure 2.1: Crystal structure of barium titanate [39]

In most cases, the alignment of dipoles is localized in certain regions of the material, while in other regions the dipoles may be aligned in other directions. A ferroelectric domain (Figure 2.2) is a region of a material where all the dipoles are aligned in the same direction. There are two possible explanations regarding the causes of a ferroelectric domain. The first explanation is that the domains form a state of minimum free energy. The second explanation is that the dipoles do not align due to material imperfections. As a consequence of the presence of these regions, it can be concluded that ferroelectric crystals are anisotropic crystals due to spontaneous polarization direction of the dipoles.

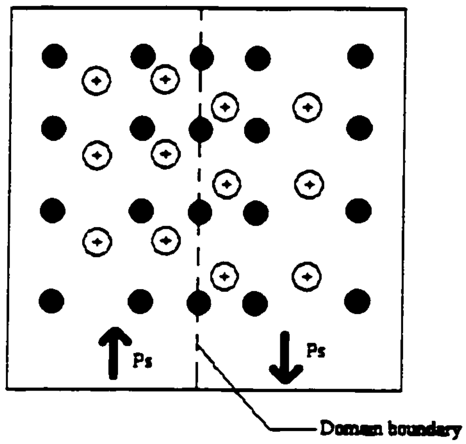

Figure 2.2: Representation of the ferroelectric regions

The ferroelectric regions can be observed by the following methods:

- Polarizing microscopy, chemically etched samples observed by polarizing microscope [36];
- Power pattern method [15];
- Liquid crystal display [14].

As a consequence of the anisotropic effects of ferroelectric materials, these materials tend to be very nonlinear.

2.5. Properties of Piezoelectric Materials

Piezoelectric materials have the property to expand and contract proportionally to an applied voltage.

A piezoceramic element, mechanically stressed by a force, generates an electric charge. A piezoceramic element, electrically stressed by a voltage, changes its dimensions. If the electrodes are not short-circuited, a voltage associated with the charge appears.

A piezoceramic material is therefore capable of acting as either a sensing or an actuating element, or both. Piezoceramic elements are capable of generating very high voltages and they are compatible with today's generation of solid-state devices, which are rugged, compact, reliable, and efficient.

The relationships between applied forces and the resultant responses depend upon the piezoelectric properties of the ceramic, the size and shape of the piece, and the direction of the electrical and mechanical excitation.

To describe directions in a piezoceramic element, three axes are used. These axis, termed 1, 2, and 3, and analog X, Y, and Z of the classical three-dimensional orthogonal set of axes.

The polar axis, or axis 3, is taken parallel to the direction of polarization within the ceramic. This direction is established during manufacturing by a high DC voltage that is applied between a pair of electrodes to activate the material. In shear operations, these poling electrodes are later removed and replaced by electrodes deposited on a second pair of faces. In this case, the axis 3 is not altered, but is then parallel to the electrode faces found on the finished element.

Piezoelectric coefficients with double subscripts link electrical and mechanical quantities. The first subscript gives the direction of the electrical field associated with the voltage applied, or the charge produced. The second subscript gives the direction of the mechanical stress or strain. Several piezoceramic material constants may be written with a "superscript", which specifies either a mechanical or electrical boundary condition. The superscripts T, E, D, and S are the following:

T = constant stress

E = constant field

D = constant electrical displacement

S = constant strain

"d" CONSTANT

The "d" coefficients or the strain constant is the piezoelectric constant relating the mechanical strain produced by an applied electric field.

d = short circuit charge density/ applied mechanical stress $\left[\frac{m}{V}\right]$

Large mechanical displacements are desirable for piezomotors. This requires large d_{ij} constants. On the other hand, the coefficient may be viewed as relating the charge collected on the electrodes to the applied mechanical stress.

When the force is in the direction 3 and the charge is collected on surfaces normal to the same direction the coefficient is named d_{33}.

d_{31} applies when the charge is collected on the same surface as before, but the force is applied at right angles to the polarization axis.

The subscripts in d_{15} indicate that the charge is collected on electrodes, which are at right angles to the original poling electrodes and that the applied mechanical stress is shear.

"g" CONSTANT

Voltage constants or "g" coefficients are the piezoelectric constants relating the electric field produced to the mechanical stress.

g = open circuit electric field / applied mechanical stress $\left[\frac{Vm}{N}\right]$

DIELECTRIC CONSTANTS

The ratio of the permittivity of the material ε, to the permittivity of free space ε_0, in the unconstrained condition is the relative dielectric constant.

$$k = \frac{permittivity-of-material}{permittivity-of-free-space} = \frac{\varepsilon}{\varepsilon_0}$$

CAPACITANCE

The capacitance in farads is given by

$$C = \frac{k\varepsilon_0 A}{t}$$

where the permittivity of free space is $\varepsilon_0 = 8.9x10^{-12}$ [farads/meter], A is the electrode surface and t is the thickness separating the electrodes.

The relative dielectric constant is strictly a material property, while the capacitance is a quantity dependent on the type of material and its dimensions.

K_3 is related to the capacitance between the original poling electrodes, while K_1 is related to the capacitance between the second pair of electrodes applied after removal of the poling electrodes for the purpose of shear excitation.

At frequencies far below resonance, piezoelectric ceramic transducers are fundamentally capacitors. Consequently, the voltage coefficients g_{ij} are related to the charge coefficients d_{ij} by the dielectric constant K_i as, in the case of a capacitor, the voltage V is related to the charge Q by the capacitance C.

$$Q = CV$$

The relationships between d and g are the following:

$$d_{33} = K_3^T \varepsilon_0 g_{33}$$

$$d_{31} = K_3^T \varepsilon_0 g_{31}$$

$$d_{15} = K_1^T \varepsilon_0 g_{15}$$

COUPLING COEFFICIENTS

The conversion of energy by the ceramic element from electrical to mechanical form or vice versa, is described by electromechanical coupling coefficients k_{33}, k_{31}, k_p, and k_{15}. The ratio of the stored converted energy of one kind (mechanical or electrical) to the input energy of the second kind (electrical or mechanical) is defined as the square of the coupling coefficient:

$$k = \sqrt{\frac{mechanical - energy - stored}{electrical - energy - applied}}$$

Subscripts are used to denote the relative directions of electrical and mechanical quantities and the kind of motion involved. They can be associated with vibration modes of certain simple transducer shapes:

- k_{33} is appropriate for a long thin bar with electrodes on the ends, polarized along the length and vibrating in a simple length expansion and contraction;
- k_{31} relates to a long thin bar with electrodes on a pair of long faces, polarized in thickness, and vibrating in simple length expansion and contraction;
- k_p signifies the coupling of electrical and mechanical energy in a thin round disc, polarized in thickness and vibrating in radial expansion and contraction;
- k_{15} describes the energy conversion in a thickness shear vibration.

Since these coefficients are energy ratios, they are dimensionless.

YOUNG'S MODULUS

The mechanical stiffness properties of piezoelectric ceramics are described by the Young's Modulus, the ratio of stress (force per unit area) to strain (change in length per unit length).

$$E = \frac{stress}{strain}$$

Young's Modulus (E) is used to describe the" stiffness" of materials. When a rod or a plate of cross section (A) and length (L) is pulled with force (F) resulting in an elongation (Δ L), the Young's Modulus can be computed as follows:

$$E = \frac{L}{A}\frac{F}{\Delta L}$$

In piezoelectric applications, $E\left[\frac{N}{m^2}\right]$ is frequently used to estimate the equivalent spring constant i.e. to the quantity (F/ΔL) of a rod or a plate of material that is in contact with a piezoelectric actuator.

The Young's Modulus with electrodes short-circuited is lower than the one with the electrodes open circuited, because mechanical stress applied to ceramic material produces an electrical response, which opposes the resultant strain. In addition, the stiffness is different in the direction 3 from that in the direction 1 or 2. Therefore, in expressing such quantities, both direction and electrical conditions must be specified. E^E_{33} is the ratio of stress to strain in the direction 3 at constant field E (electrodes shorted). E^D_{33} is the equivalent with the electrodes open circuited. E^E_{11} and E^D_{11} is the module in the direction 1 or 2. E^E_{55} and E^D_{55} are the ratios of shear stress to shear strain.

Piezoceramic properties described above are defined for ideal shapes measured under ideal mechanical and electrical boundary conditions. In practical device operating conditions, the performance can be close, but always lower then the predicted performance. Non-ideal shapes and non-ideal boundary conditions contribute to transduction losses due to standing waves, interfering vibrational modes, pseudo-clamping, stray electric and dielectric resistances, etc.

CURIE TEMPERATURE

The Curie temperature is the temperature at which the crystal structure changes from a non-symmetrical (piezoelectric) to a symmetrical (non-piezoelectric) form.

AGING RATE

Aging is the process of the ceramic material changing back to its original state prior to polarization. Aging of piezoelectric ceramics can be expressed as a logarithmic function with time. The aging rate defines change in the material parameters per decade of time.

PYROELECTRICITY

Pyroelectricity is one of the characteristics of the piezoelectric materials. When they undergo a temperature change, they produce electric charge. When their temperature is increased, a voltage is generated with the same orientation as the polarization voltage. At that moment, if the temperature is decreased, a voltage develops with an orientation opposite to the polarization voltage, creating a depolarizing field with the potential to degrade the state of polarization of the part.

The maximum electric field which arises due to a temperature shift, is determined as follows:

$$E_{piro} = \frac{\alpha(\Delta T)}{K_3 \varepsilon_0}$$

E_{pyro} is the induced electric field in [volts/meter], α is the pyroelectric coefficient in [Coulomb/° C meter ^{2}], T is the temperature difference in [°C], K_3 is the dielectric constant, and e_0 is the dielectric permittivity of free space.

For piezoceramic actuators, α is typically about 400×10^{-6} [coulomb/°C meter^2].

PERFORMANCE

Free deflection and blocked force usually can determine the characteristic of the piezoelectric actuators. Free deflection refers to the displacement at a given voltage level, with the actuator working against no external load. Blocked force refers to the force exerted at a given voltage level when the actuator is not allowed to produce any displacement.

Since the force at maximum deflection is zero, all other values of simultaneous displacement and force (for a given voltage level) are determined by a line drawn between these points on a force versus deflection. In practice, a bending motor must move a specified amount of displacement and exert a specified force, which determines its operating point on the force versus deflection diagram. Work is maximized when the deflection performed permits one half the blocked force to be developed. This occurs when the deflection equals one half of the free deflection.

Motor Transducer Relationships

Parallel expansion of a motor is given by $\Delta T = V\, d_{33}$

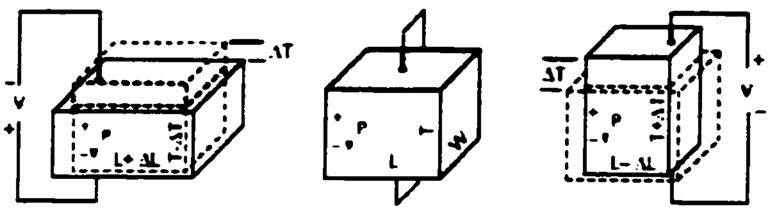

Figure 2.3: Transverse and parallel motor [43]

The transverse expansion of a motor is given by $\frac{\Delta L}{L} = \frac{\Delta W}{W} = \frac{Vd_{31}}{T}$

Shear motor

The expression of a shear motor is given by $\Delta X = Vd_{15}$

Depending on the polarization, it is achieved by a controlled deformation of the piezoelectric actuator (Δx).

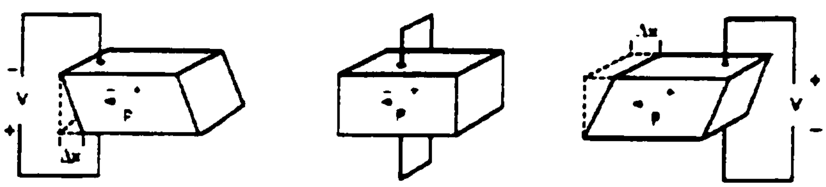

Figure 2.4: Shear motor [43]

Bending motor

1. Series connection

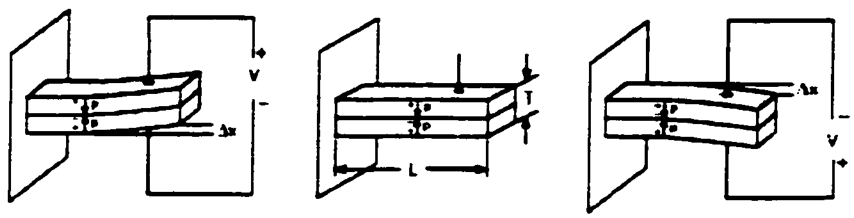

Figure 2.5: Bending motor series connection [43]

In the bending motor case for the series connection, the displacement is given by

$$X = \frac{2L^2 V d_{31}}{T^2}$$

2. Parallel connection

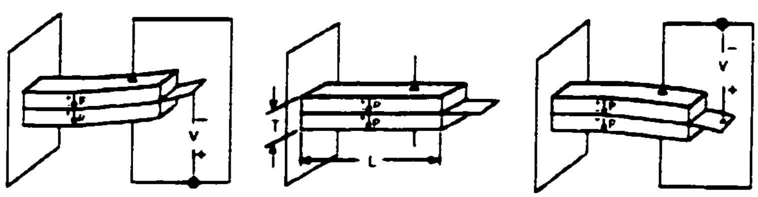

Figure 2.6: Bending motor parallel connections [43]

In the bending motor case for the parallel connection the displacement is given by

$$X = \frac{4L^2 V d_{31}}{T^2}$$

SENSITIVITY

Because of differences in the material properties and dimensions of each piezoelectric element, each responds differently to an applied voltage.

This response is conveniently measured in terms of sensitivity, a ratio of piezoelectric movement-to piezoelectric voltage, i.e., how far the piezoelectric extends or contracts per applied voltage.

Sensitivity is not a linear relationship with respect to piezoelectric element size. Because the piezo element exhibits more sensitivity (i.e., more movement per volt) at the end of a scan line than at the beginning, the relationship of movement vs. applied voltage is nonlinear.

When no voltage is applied, the piezo element is "motionless". At higher voltages the piezo element's sensitivity increases (i.e. more movement per voltage applied). By plotting each point along the curve, an exponential relationship is obtained, which provides a rough approximation of piezoelectric sensitivity, as shown in Fig 2.7.

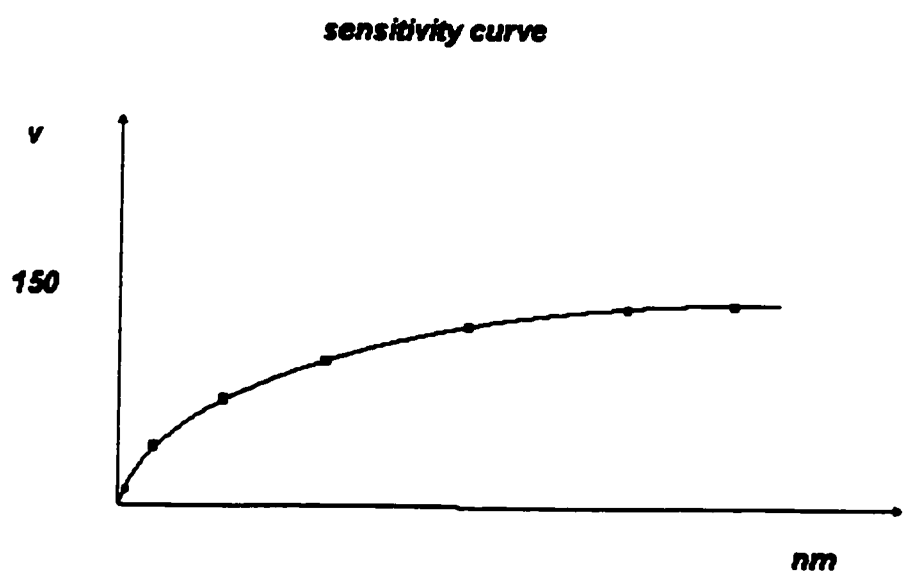

Figure 2.7: Sensitivity curve [13]

HYSTERESIS

As the piezo elements extend and retract throughout a full range, they move less per applied volt at the beginning of the extension than near the end. The same is true when the piezo element is retracting; the piezo element moves less per applied volt at the beginning of its retraction than near the end.

The direction of the polarization vector, for many domains in the crystal structure, is influenced by the strength of the electric field and temperature. Hysteresis loops are a consequence of the ability of these domains to re-align in the direction of the electric field.

Loops could be observed by means of an electric circuit. Sawyer – Tower [12] demonstrated that by monitoring the voltage with an oscilloscope the hysteresis loop could be determined. The voltage as a function of the electric field is shown in a conceptual diagram in Figure 2.8.

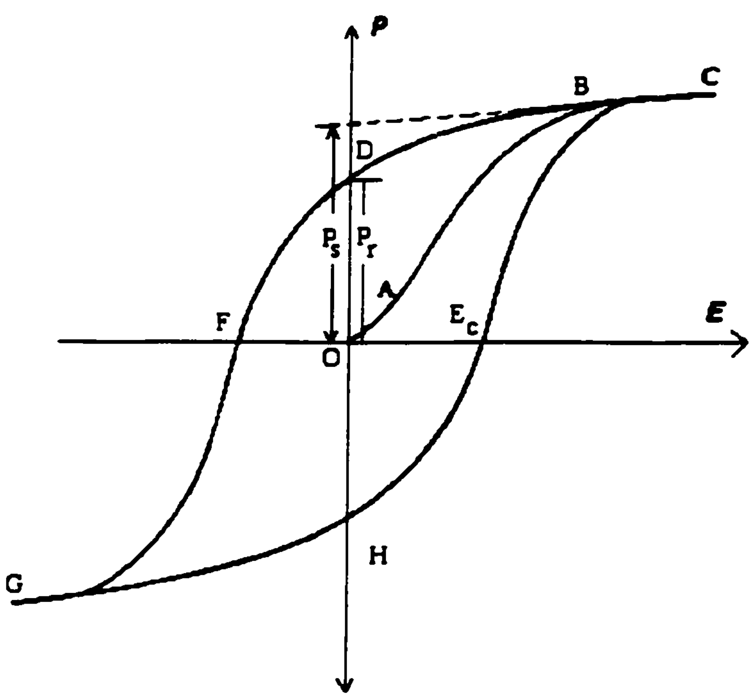

Figure 2.8: Hysteresis loops [12]

Figure 2.8 shows a typical loop. When small electric fields [E] acts on the piezoelectric material the polarization [P] is almost linear (points O-A). As the electric field forces increase, a number of the negative domains (regions with the uniform polarization, which have a polarization opposite to the direction of the field) will be switched over in the positive direction of the field and polarization will increase rapidly until all the domains are aligned in the positive direction. This is the state of saturation point C. The remaining polarization is indicated in Figure 2.8 by the distance P_r. If the electric field changes direction then the polarization past point D rapidly approaches zero, at a value of the electric field known as the coercive field strength. If the electric field increases in the negative direction then saturation of the polarization also occurs at point G. If the electric field is increased in the positive direction then a negative value of polarization will remain at an electric field value of zero. This polarization is due to the alignment of the domains even after the electric field has been removed. A final increase of the electric field in the positive direction causes the dipoles to follow the direction of the electric field until saturation occurs again at point C. The complete hysteresis curve is represented by CDFGHC.

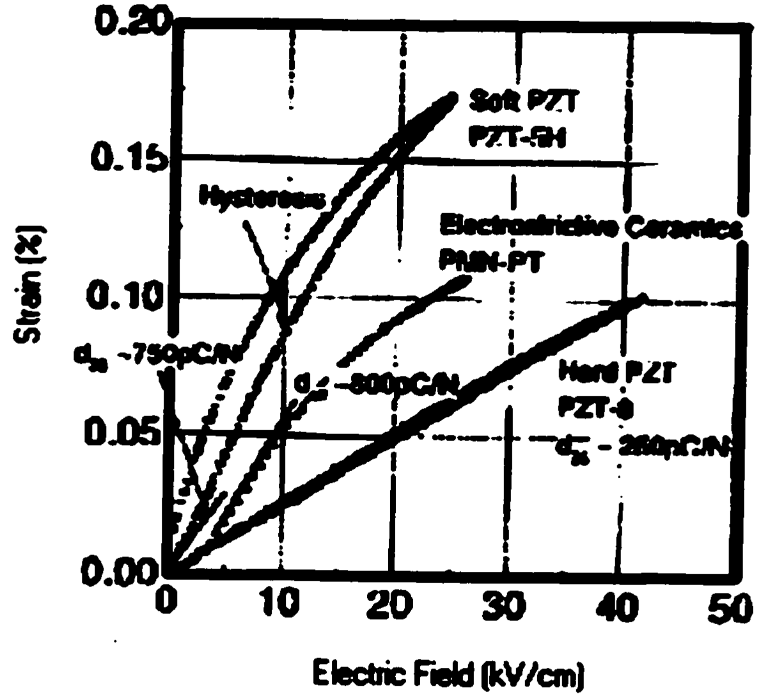

Figure 2.9: Strain vs. electric field behaviors for various electromechanical ceramics [37]

As shown in Figure 2.9 it is noticeable that "hard" piezoelectric (ceramic) tend to have very little hysteresis. The fact that hard piezoelectric have little hysteresis comes at the expense of low strain for hard piezoelectric crystals. It is believed that this low value of strain is due to a breakdown in the dielectric strength and polarization saturation. In contrast, soft piezoelectric show higher levels of strain and also very nonlinear response between the electric field and their strain. The high values of hysteresis are due to domain motion.

This high hysteresis results in poor positioning accuracy.

Shrout has shown larger strains on single crystal piezoelectric that are capable of producing strains in the order of 1.2%. This opens a wider range of uses for these materials, such as, for example, actuators.

Nonlinearity and hysteresis can cause feature distortion in the applications.

CREEP

Creep is the drift of the piezo displacement after a voltage is applied to the elements. Creep appears as an elongation and stretching of features in the direction of offset. Creep is the result of this slow movement of the piezo over their remainder of the offset distance.

Creep does not affect repeatability. Like hysteresis, creep is related to the effect of the applied voltage on the remanent polarization of the piezo ceramics. Creep decreases logarithmically with time. If the operating voltage of a (open loop) PZT is increased (decreased), the remanent polarization (piezo gain) continues to increase (decrease), manifesting itself in a slow creep (positive or negative) after the voltage change is complete.

The following equation describes the effect:

$$\Delta L \approx \Delta L\left(1 + g\lg\left(\frac{t}{0.1}\right)\right)$$

where

ΔL = displacement 0.1 seconds after the voltage change is complete [m].
g = creep factor which is dependent on the properties of the actuator (on the order of 0.01 to 0.02). Maximum creep (after a few hours) can add up to a few percentages error with regards to the desired motion.

LIFETIME OF PZTs

The lifetime of a PZT is not limited by wear. Tests have shown that PZTs can perform billions of cycles without loss of performance if operated under suitable conditions. Generally, as with capacitors, the lifetime of a PZT is a function of the applied voltage. The average voltage should be kept as low as possible.

There is no generic formula to determine the lifetime of a PZT because of the many parameters such as temperature, humidity, voltage, acceleration, load, operating frequency, insulation materials, etc., which have a (nonlinear) influence. PZTs are built for maximum lifetime under actual operating conditions. The operating voltage range figures in the technical data tables are based on years of experience.

Statistics show that most failures with piezoelectric actuators occur because mechanical installation guidelines are not observed and mechanical stress, shear forces and torque exceed the permissible limits.

2.6. Configurations of Piezoelectric Actuators

The same piezoceramic element can be used as a piezo actuator and as a piezo sensor. [43]

Single piezoceramic sheets can be energized to produce motion in the thickness, length, and width directions. Conversely, they may be stretched or compressed to generate electrical output.

Two layer elements represent the most versatile configuration. They may be used as two layers for bending or for extending.

Multilayered piezoceramic stacks can deliver and support high force loads with minimal compliance, but they deliver small displacements.

In order to clarify how the piezoelectric phenomena are produced, the single sheets will be presented first.

2.6.1. Single-Layer Actuator

If we apply an electrical field having the same polarity and orientation as the original polarization field to single-layer actuators, the piezoceramic element will be deformed. In this case, a extension in the "longitudinal " direction and a compression in the "transverse" direction will occur. If the field is reversed, the motion will be reversed. The motion of a sheet in the thickness direction is extremely small (in the order of tens of nanometers) but, the motion along the length is generally larger (in the order of microns to tens of microns). If the single layer actuator operates on a sheet laminated to the surface of a structure, a stretch or a bend can result.

In Figure 2.10 is shown a longitudinal actuator and in Figure 2.11 a transverse actuator in contraction. Both piezoceramic actuators react to the electrical field (V_{in}) and change the shape with ΔT in thickness or ΔL in length. The pizoceramic element expands or contracts for opposing field.

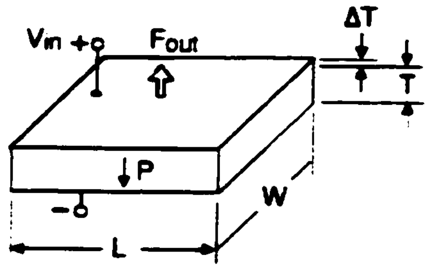

Figure 2.10: Longitudinal actuator [43]

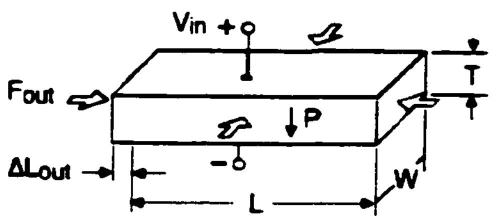

Figure 2.11: Transverse actuator[43]

2.6.2. Two-Layer Actuator

Depending on the polarization and wiring configuration of the layers, two-layer elements can be made to elongate, bend or twist

For parallel operation, the two layers offer the opportunity to reduce drive voltage by half when it is configured.

The most useful "2-layer" element actually has stacks of nine layers, consisting of four electrode layers, two piezoceramic layers and two adhesive layers.

Figure 2.12 shows a two-layer transverse actuator, expanding lengthwise; the piezoceramics elements react to the electrical field (V_{in}) and change longitudinally the shape by ΔL.[43]

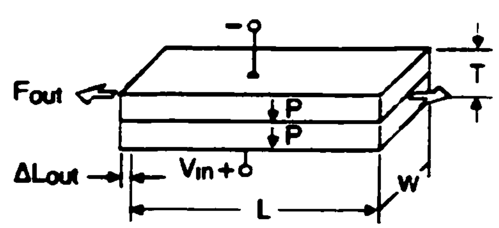

Figure 2.12: Two-layer transverse actuators[43]

2.6.3. Extension Actuator

A two-layer element behaves like a single layer when both layers expand (or contract) together.

2.6.4. Bending Actuator, Cantilever Mount

A two-layer element produces a curvature when one layer expands while the other layer contracts. These transducers are often referred to as benders, or flexural elements. Bender motion in the order of hundreds to thousands of microns, and bender force from tens to hundreds of Newton, are typical.

Figure 2.13 shows the bending motor expanding lengthwise in cantilever mount. The piezoceramics react to the electrical field (V_{in}) by producing the deflection ΔX. [43]

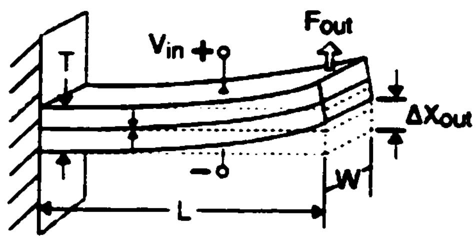

Figure 2.13: Bending motor, cantilever mounts [43]

2.6.5. Bending Actuator, Simple Support Beam Mount

In Figure 2.14 the bending actuator is a simple supported beam mount. The piezoceramics element reacts to the electrical field (V_{in}) by producing a deflection ΔX. The deflection ΔX is more active in the center of the piezoceramics actuator and the center moves up and down along a vertical plane.

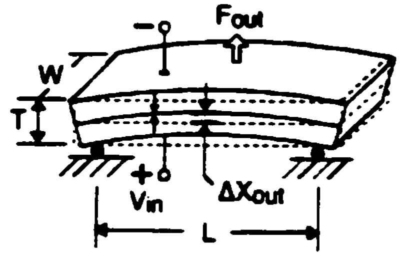

Figure 2.14: Bending actuator, simple supported beam mount[43]

2.6.6. Multi-Layer Actuator

Many layer actuators can be stacked on top of one another such as shown in Figure 2.15. Increasing the volume of piezoceramic increases the energy that may be delivered to a load. As the number of layers grows, so does the difficulty of accessing and wiring all the layers. As a result, the construction with more than four layers becomes impractical. [43]

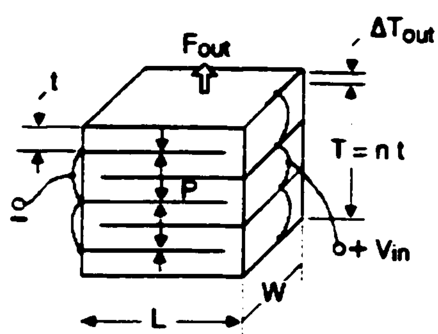

Figure 2.15: Multi-layer actuator [43]

2.6.7. Actuator Performance

Piezoelectric actuators are usually specified in terms of free deflection (Xf), which refers to displacement attained at the maximum recommended voltage level, when the actuator is completely free to move and it is not asked to exert any force.

Blocked force (Fb) is the force exerted at the maximum recommended voltage level, when the actuator is totally blocked and not allowed to move.

Deflection is at a maximum, when the force is zero, and force is at a maximum, when the deflection is zero.

Generally, a piezoelectric actuator must move over a specified distance and exert a specified force, which determines its operating point on the force versus deflection line. An actuator is considered optimized for a particular application if it delivers the required force corresponding to the half of the maximum of deflection. All other actuators satisfying the design criteria will be larger, heavier, and consume more power.

2.6.8. Series and Parallel Operation

When the supply voltage is applied across all piezoelectric layers at once we have the Series Operation case. The voltage on any individual layer is the supply voltage divided by the total number of layers. A 2-layer device wired for series operation uses only two wires, one attached to each outside electrode (Figure 2.16). [43]

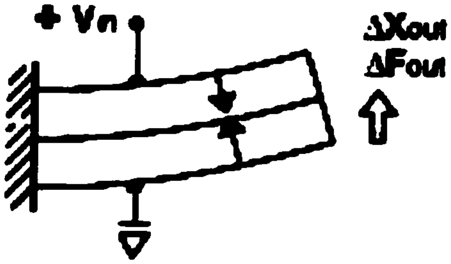

Figure 2.16: Two-layer bending element, poled for series operation [43]

When the supply voltage is applied to each layer individually, we have the Parallel Operation case. This requires access and attachment wires to each layer. A 2-layer bending element wired for parallel operation requires three wires, one attached to each outside electrode and one attached to the center shim. For the same motion, a 2-layer element poled for parallel operation needs only half the voltage required for series operation (Figure 2.17).

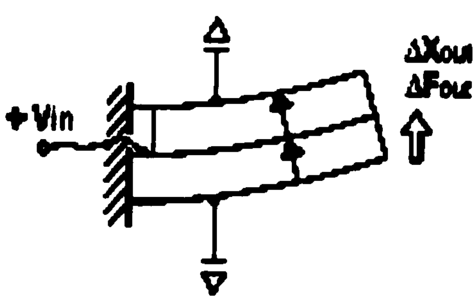

Figure 2.17: Two-layer bending element poled for parallel operation[43]

3. Design of Three-Axis Piezoelectric Actuator

Linear piezoelectric motors with high stiffness and nanoprecision have received increased attention due to needs of the semiconductor optical fiber communication and machine tool industries. Positioning systems based on piezoelectric actuators gave certain advantages such as unlimited resolution, large force, fast expansion, and no magnetic field, but their positioning range is extremely small. Efforts have been made to increase the positioning range, which results in the linear piezomotor technique and its application in precision instrument.

The advantages of piezoelectric motors are the following:

- no backlash and no friction in the actuator;
- the actuator can produce large forces;
- small sized;
- easy to control.

The disadvantages of piezoelectric motors are the following:

- hysteresis behavior;
- drift in time;
- temperature dependence;

- limited stiffness.

In order to design a proper closed-loop controller, it is necessary to understand the open-loop characteristics of the nanopositioner. The expansion of a piezoelectric actuator is not exactly proportional to the electric field strength. This nonlinear behavior is shown in Figure 3.1.

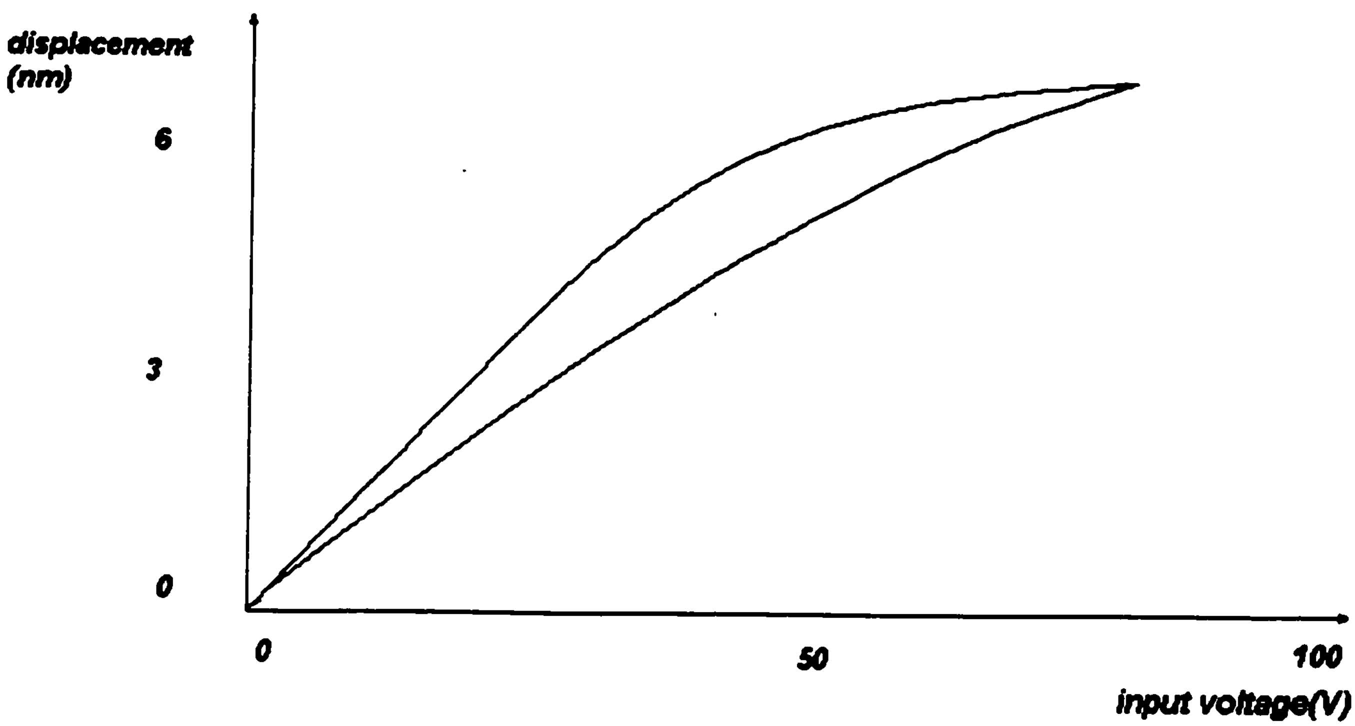

Figure 3.1: Hysteresis - voltage versus displacement

Experiments show that hysteresis depends on the voltage magnitude. For small input magnitude, hysteresis is small, and it increases with the input of voltage magnitude.

The goal of this thesis is to design a stiff nanoprecision linear piezoelectric device, which can be used in very precise motion applications in telecommunication industry. To this end, three piezoelectric actuators are integrated in a three axes position jig. In figure 3.2 (a): 1is cover s, 2 screws, 3 cover S and 4, 5 and 6 assembly flexure z, x respective y.

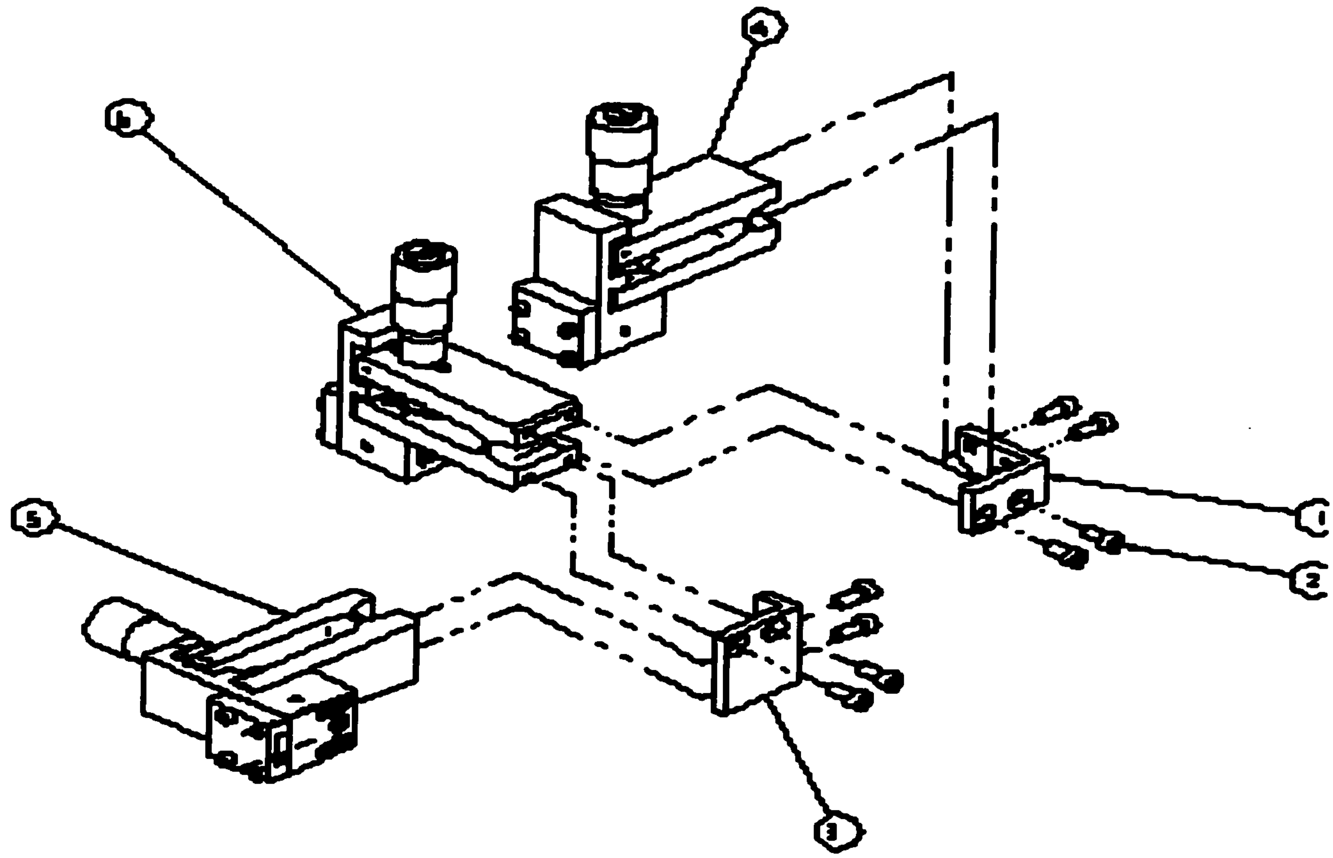

(a)

Figure 3.2 (a): Three-axis position jig (explode view)

Figure 3.2(a) shows the jig design. Practically, the operator, using the arm of the jig can achieve the desired trajectory. The micrometers can control precisely the distance between 3 mm and 5x 10^{-3} mm and the piezoelectric actuator takes over for the displacement under this lower limit. The second experiment shows that a controlled motion up to 1.8 x 10^{-4} mm can be achieved with a piezoelectric actuator. Where 1is cover s, 2 screws, 3 cover S and 4, 5 and 6 assembly flexure z, x respective y.

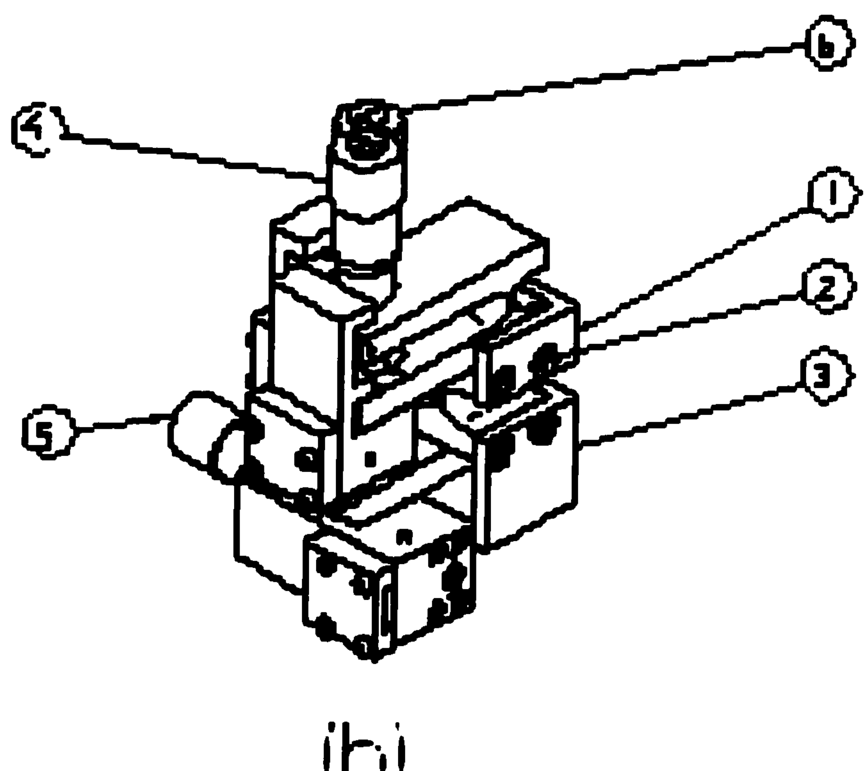

Figure 3.2 (b): Three-axis position jig (assembled)

The parts 1-6 hold the mechanism and help it to react properly to the operator input. On the following pages we will describe the parts, which compose this mechanism.

For this application is not needed to control motion over long distances. Using the piezoelectric actuators we succeed to create precise motion over a short distance without backlash and stick-slip process, which can otherwise influence negatively the accuracy.

On the other hand it is true that piezoelectric strains may cause a jerk in the motion of a linear piezomotor and the design must take into account the effects and the properties of piezoelectric materials. Jerk occurrence should be avoided as they may reduce the accuracy of a positioning system. In a particular design, the lateral or undesired deformation of a piezoelectric stack should be prevented from being transmitted to a motion mechanism.

Only the axial or the specified deformation should be allowed to contribute to the motion. Since mechanical interfaces usually have the lowest stiffness in a structural loop, it is not helpful to use them in a positioning system demanding high stiffness. However, if mechanical interference is unavoidable, the type of mechanical contacts has to be properly chosen. Surface contact yields the highest interface stiffness, compared to point or line contacts. Therefore, a surface contact and a large interface should be used to increase the stiffness of mechanical interface. High strength structures, high strength mechanical joints, and piezoelectric actuators with a large output force are necessary for obtaining a linear piezomotor with a large output force or precision motion.

A compact linear piezomotor is desirable in most applications, although it is relatively difficult to achieve compactness when high stiffness and a large output force are specified in addition to nanometer resolution over a large travel range.

In order to make the piezomotor compact and multifunctional it has to be designed using a limited number of components.

The flexure three axes positioner in Figure 3.3 holds the micrometer (1), but at the same time it has the property of being almost elastic. The motion over 5 microns is realized with the micrometer. The piezoceramic actuator has to be firm and to produce higher precision motion in the needed direction.

The exploded view from Figure 3.3 shows one micrometer-piezoelectric actuator axis position jig. The micrometer (1) is held in a flexure 3-axis tilt positioner (3) and is adjusted by screw (2). The flexure (3) axis positioner was designed in order to allow a displacement of its two arms; a spring (11) facilitates the displacement created by the micrometer (1). Piezoelectric actuator (12) produces the motion in the same direction as the micrometer (1). To avoid the damage of piezoelectric actuators by the micrometer, a disc (4) is inserted in between. The rest of the parts have the goal to hold the jig.

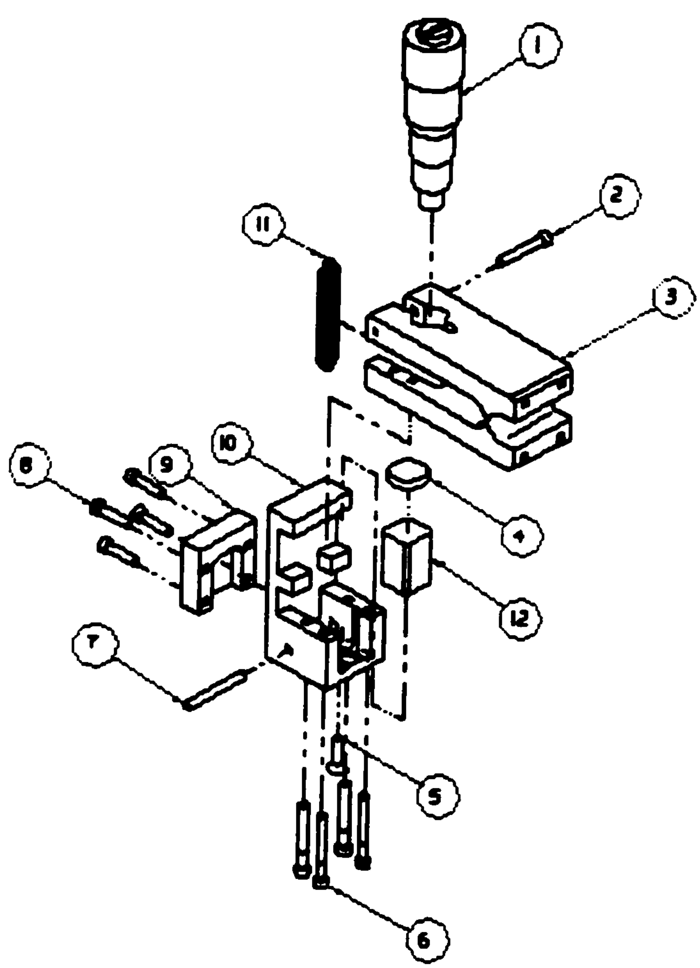

a

Figure 3.3 (a): Micrometer-piezoelectric actuator axis position jig (explode view)

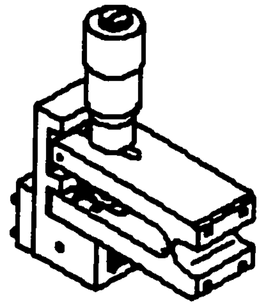

b

Figure 3.3 (b): Micrometer-piezoelectric actuator axis position jig (assembled)

The parts identified in Figure 3.3 (a) are the following:

Name	Quantity
1. Micrometer: MTI Resolution .005±. 00015	1
2. Screw	1
3. Flexure 3-axes tilt positioner	1
4. Disk	1
5. Screw	1
6. Screw	4
7. Pin spring	1
8. Screw	4
9. Cover 3-axes tilt positioner	1
10. Stopper 3-axes tilt positioner	1
11. Spring	1
12. Piezoelectric actuator	1

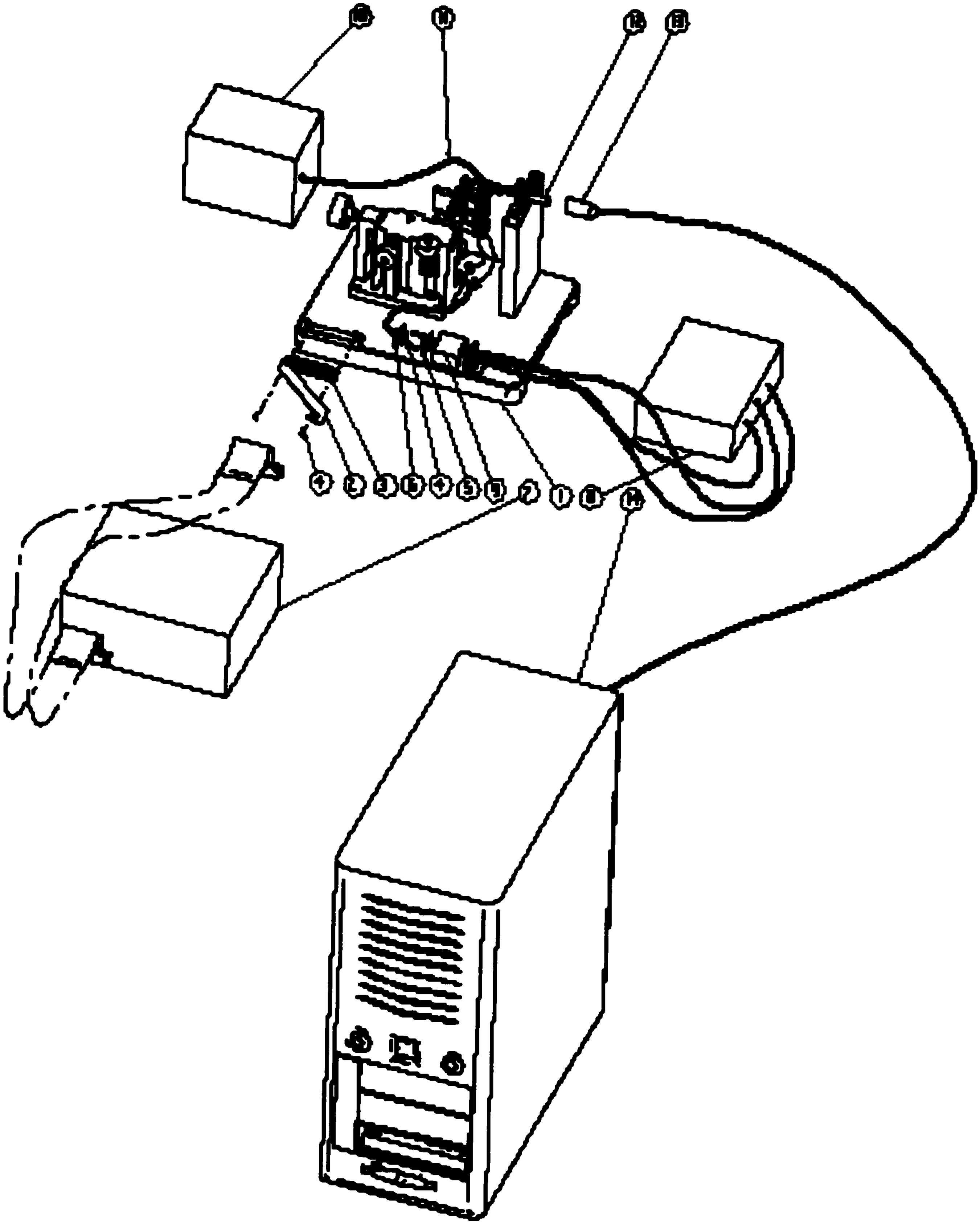

Figure 3.4: Experimental set up for piezoelectric actuator displacement

Figure 3.4 shows the first experimental set up using the jig. The flexure 3-axes belongs to a small mechanism, which comprises three "flexure 3-axis subsystem ", in order to actuate motion in x, y and z directions, shown in Figure 3.3. The small jig from Figure 3.2 is attached to a common mechanical three-axis position jig, which can produce controlled motion between 1mm and 4cm. The piezoelectric actuator is connected to the power supply through a controller (7) and (8). The controller can provide the voltage from 0 to 150 V, and can be switched in three different positions. Each position corresponds to a different piezoelectric actuator. The apparatus presented in this thesis can operate in three directions. When the light information from the power supply (10) is received through the glass fiber (11) from the collimator (12), the operator can control the position of the lens using the mechanical end electrical controllers. The quad-cell detector (13) receives the signal and transmits the analog information to the PC (14). The quad-cell detector is a photodiode, which is used as a position sensor. The operator can interpret and adjust the controller, in order to perform the operation.

The parts identified in Figure 3.4 are the following:

Name	Quantity
1. JIGASSY fiber tube to zoom lens active aligning	1
2. Cover connection	1
3. Cover connector	1
4. Screws	4
5. Connector	1
6. Connector	1
7. Controller of the heater	1

8. Controller of the piezoelectric element	1
9. Protection connector	1
10. Power supply	1
11. Fiber	1
12. Collimator	1
13. Quad–cell detector	1
14. PC	1

4. Analytical Modeling of Piezoelectric Actuators

The piezoelectric actuator (PEA) is a device used for producing extremely small displacements, in the range of 10 pm to 100 μm. This thesis presents a system with a piezo-actuated positioning mechanism. The actuator dynamic model is taken into consideration and is used to avoid the hysteresis effect. This PEA is a high precision actuator under direct human control.

The ratio of the input voltage to the output displacement is a very favorable property of the piezoelectric material for this purpose, but it has a highly nonlinear behavior. More specifically, a PEA shows hysteresis behavior and, for certain inputs, there is not a unique output because the output depends on the input history.

The focus of this thesis is on determining the positioning performance, taking into account the dynamic effects of the actuator.

A model of a PEA was published in 1987 by a standard committee of the IEEE [2]. This model consists of two linear constitutive relationships, but these relationships fail to account for the hysteresis nonlinearly and fail to describe the dynamic aspects of the actuator. In many other models, either only the linear dynamics or only the hysteresis nonlinearly is taken into account. Therefore, these models are not suitable for system design.

In 1997, Goldfarb and Celanovic proposed a model for the PEA that is based on physical principles [26]. This model is based on both electrical and a mechanical phenomena, as well as on their interactions.

In 2000, Han and al. [17] elaborated a more accurate and better applicable hysteresis and dynamical model.

From the first applications of piezoelectric materials as actuators, they are voltage controlled. In this section the basic principle of charge-control configuration, physical properties and an electromechanical model accounting for the hysteresis model are presented.

4.1. Introduction

Dielectric materials are insulators; their main property takes into account the relationship between electrical voltage and electrical charge. Piezoelectric materials are a special type of dielectric materials. For piezoelectric materials, an externally applied force induces an electrical charge (piezoelectric effect) and conversely, an applied electrical charge induces a force (inverse piezoelectric effect).

Besides the piezoelectric and inverse piezoelectric effect, there are other relationships: the electrical relationship between voltage and charge, the mechanical relationship between voltage and charge, and the mechanical relationship between force and elongation.

These effects are shown in Figure 4.1.

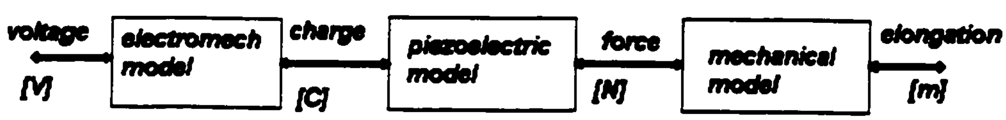

Figure 4.1: Block diagram of the different interactions in a PEA [17]

The piezoelectric effect is the basis of electromechanical actuators and represents the connection between the electrical and mechanical domains. Man-made piezoelectric polycrystalline ceramics are much more suitable for building actuators than natural materials, because the useful properties, such as maximum elongation, can be augmented by the proper mixture of ingredients. A disadvantage of man-made piezoelectric ceramics is that a hysteresis effect is still present in the interaction between electrical voltage and electrical charge. The piezo effect and the hysteresis play an important role in the dynamic behavior of these actuators.

Between charge and elongation no hysteresis effect is encountered because the effect is produced between voltage and charge. Voltage and charge steering can be realized by a voltage and charge source, respectively, which have an internal resistance zero and infinite, respectively, and which may be called the (galvanically) closed circuit and (galvanically) open circuit [17]. For drivers, a charge is induced on the electrodes of the PEA and, in the case of voltage driver; the hysteresis effect is present between voltage and charge. The electrical charge induces a force and results in an elongation of the ceramic material. This means that the piezo effect is present for both cases of electrical steering. The table below summarizes these phenomena:

	Closed circuit driver	Open circuit driver
Driver source	Voltage	Charge
Resistance of source	0	∞
Hysteresis effect	Yes	No
Piezo effect	Yes	Yes

4.2. Electromechanical Model

A typical PEA configuration is the stacked structure represented in Figure 4.2.

Such a PEA stack consists of a series connection of a number of piezo wafers with an electrode between every two wafers. The wafers are mechanically in series and electrically in parallel. This configuration strengthens the effect of the individual wafers. The piezo wafers have a thickness of

0.3-1 mm. For maximum elongation, ranging from 10 to 100 μm, the length of PEA ranges from approximately 40 mm to 120 mm. u_{pea} is the voltage over the total PEA.

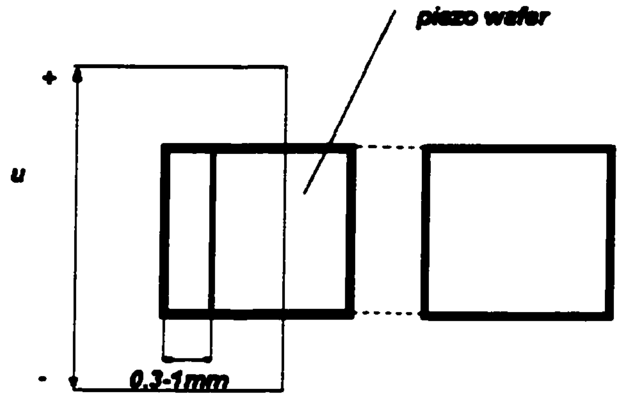

Figure 4.2: Schematic representation of the stacked configuration of a PEA

A fairly accurate overall electric and mechanical model of a PEA is given in Figure 4.3 [22].

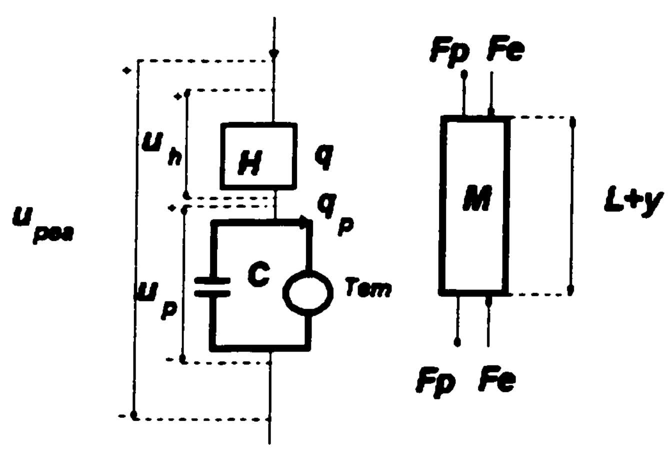

Figure 4.3: a) Electrical model b) Mechanical model

In Figure 4.3, the hysteresis and piezo effects are separated. H represents the hysteresis effect and U_h is the voltage due to this effect. The piezo effect is represented by T_{em}, which is an electromechanical transducer with the transformer ratio T_{em}. The capacitance C represents the sum of the capacitance of the individual wafers, which are electrically in parallel. The total charge q in the PEA. and q_p are the transduced charges for the mechanical side. The voltage u_p is due to the piezo effect.The total voltage over the PEA is U_{pea} in Figure 4.3 (b). The force F_p is the transduced force from the electrical side. The force Fe is externally applied, most often a pushing force. The resultant force F_p – Fe drives mechanically the piezo material. The resulting elongation of the PEA is denoted by y. The mechanical relationship between Fp and y is denoted by M. The piezo material has elasticity modulus E, viscosity η, and mass density ρ. The geometrical dimensions of the PEA are length L and cross-sectional aria A. Mass m_p, stiffness K_p, and damping coefficient C_p can be calculated from the material and geometrical propeties as follows :

$$m_p = \rho AL \qquad (1)$$

$$K_p = \frac{EA}{L} \qquad (2)$$

$$C_p = \frac{\eta A}{L} \qquad (3)$$

The electromechanical equations are :

$$u_{pea} = u_h + u_p \qquad (4)$$

$$q = H(u_h) \qquad (5)$$

$$q = Cu_p + q_p \qquad (6)$$

$$q_p = T_{wm} y \qquad (7)$$

$$F_p = T_{em} u_p \qquad (8)$$

$$Y = M(F_p - F_e) \qquad (9)$$

where H and M represent the hysteresis and mechanical operator.

Since in a PEA, the individual piezo wafers are mechanically in series, it is expected that the longitudinal dynamics play an important role in the mechanical operator. Because the individual piezo wafers are electrically in parallel, it is accurate to take the sum of the capacitance of the individual wafers as electrical model, resulting in the capacitance C.

The tranduced force F_p is, in fact, present in every piezo wafer. However, because every wafer tends to elongate, the internal forces at the connection of two wafers cancel out. Therefore, macroscopically there are only forces at the first and last electrodes.

4.3. Hysteresis Model

In this section we consider the operator H from equation (5) which is part of the total electromechanical model given by equations (4) to (9). By definition the hysteresis effect is dynamic, independent of the time scale, and nonlinear. A hysteresis loop is defined as the stationary loop in the input / output plane for a slowly quasi-static oscillating input.

The model is a first-order differential equation, proposed in (7). It has been developed to describe magnetic hysteresis but, at the same time, it has experimentally been verified that this equation is also suitable for describing electric hysteresis such as in a PEA.

The model for the hysteresis effect between u_h and q is given by the following nonlinear equation:

$$\dot{q} = \alpha \,/\, \dot{u}_h /(f(u_h) - q) + \dot{u}_h \, g(u_h) \qquad (10)$$

$f(u_h)$ and $g(u_h)$ are functions which can be parametrically adjusted to represent the shape of the hysteresis loop.

$$f(u_h) = au_h \tag{11}$$

$$g(u_h) = b$$

where a and b are constants

In practice, hysteresis loops are similar to the shape shown in Figure 4.4.

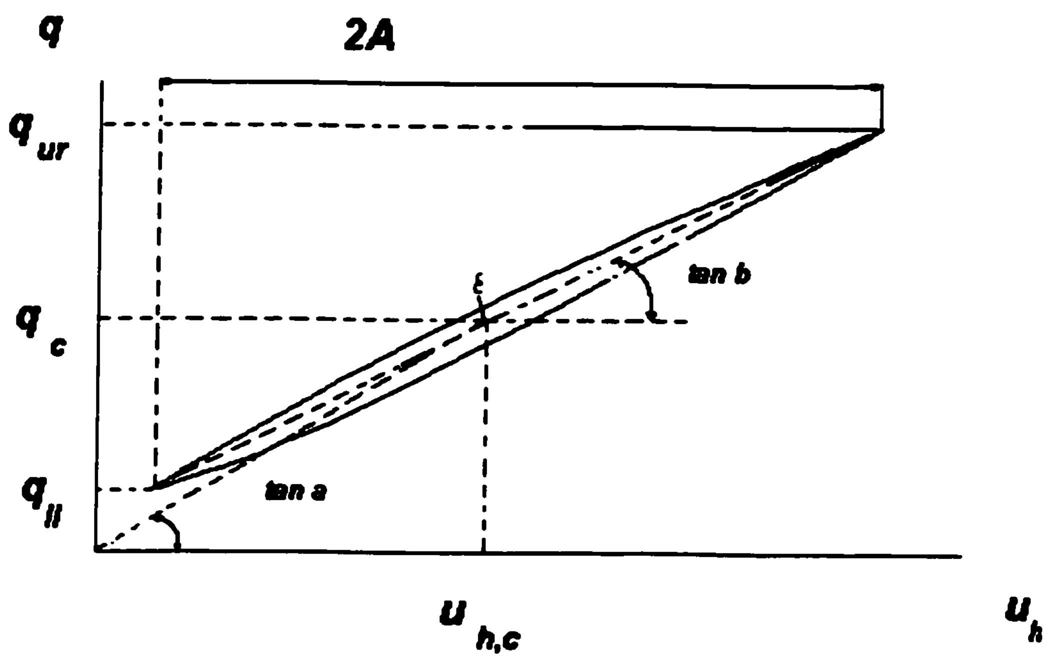

Figure 4.4: Typical hysteresis loop

A linear approximation can be obtained from Figure 4.4, where the tangent is equal with value of the angle and in this case we obtain the equations (12) and (13)

The linear equations for the center point and the average slope of a hysteresis loop are given by:

$$q_c = u_{h,c} \tan a \qquad (12)$$

$$q_{ur} - q_{ll} = 2A \tan b \qquad (13)$$

where q_{ur} and q_{ll} are the upper right and lower left side points of a hysteresis loop

In (10) and (11), there are three independent parameters, namely α , a, and b, refering to three independent characteristic quantities in a hysteresis loop. Besides the center points and the average slope in [28], a relationship can been derived from Figure 4.4 for the hysteresis area ε for relatively small amplitudes of the sinusoidal input:

$$\varepsilon = 4/3(a-b)\alpha A^3 \qquad (14)$$

If the parameters a and b are experimentally determined from center points and average slopes, the parameter α can be experimentally determined from hysteresis areas. For small deviations from a center point, the hysteresis nonlinearly is well approximated by its average slope:

$$\Delta q = \Delta u_h \tan b \qquad (15)$$

where Δ is used to indicate the deviation of the variable. This approximation allows for linear analysis for the total model. In [28], it has been proven that, for physically correct hysteresis, i.e., convergence to hysteresis loops and counterclockwise orientation and monotony of hysteresis loops, it is required that:

$$a\alpha > 0 \qquad 0 < (1/2)a \le b \le a \tag{16}$$

Inside of the hysteresis area for the same input different outputs result. In this thesis, the goal is to find out if it is possible to have precise and controlled motion with piezoelectric actuators, and, if the answer is positive, to understand the main advantage of using piezoelectric actuators for very precise motion.

5. Experiments

The purpose of this chapter is to demonstrate experimentally what was previously presented theoretically. The theory has shown the possibility to calculate the position of the center, the slope, and the aria of the hysteresis curve. It has been also acknowledged that different outputs are generated by the same input, and we expect to reach the outputs somewhere inside of the hysteresis curve. In the present chapter, we describe two experiments and their associated results.

5.1. Experimental Study of Piezoelectric Actuator

The purpose of the study is to determine the displacement performance of three ceramic actuators in order to reach a desired point in space. The displacement performances of individual actuators have to be taken into account in order to control the motion.

The experimental set up shown in Figure 5.1 contains the following elements:

- Power supply that produces the voltage necessary to achieve jig displacement and for the data acquisition and PC;
- Laser source that produces the light necessary for the experiment;
- Jig that is designed to hold the piezoelectric actuator;
- Quad cell detector, a photodiode that is used as a position sensor;
- Collimator, a fiber and lens combination that transforms the divergent beam coming out of the fiber into a parallel Gaussian beam.

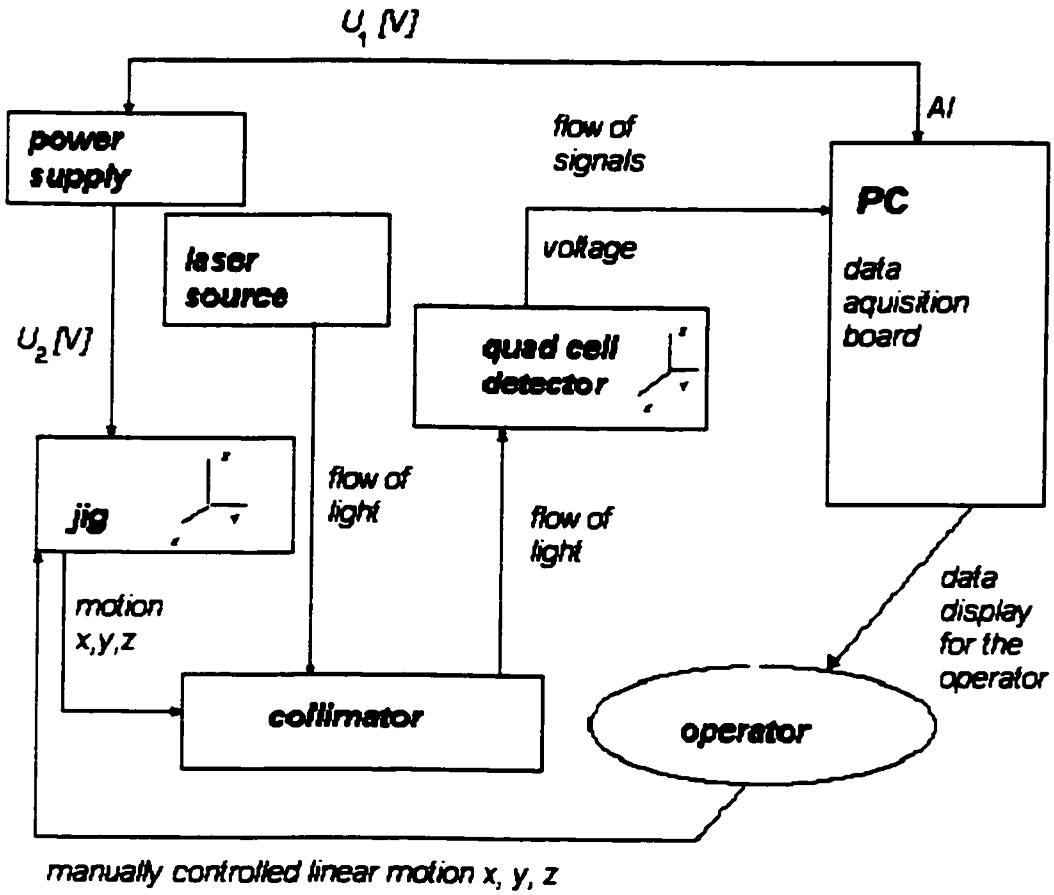

Figure 5.1: The block diagram of the experimental set up used in the first experiment

The collimator generates a beam with a width of about 700 microns, approximately equal to 3 ω, (ω is the Gaussian radius of the beam). The radius of the Gaussian beam is the distance from the centre of the beam to the point where the intensity of the beam decreases by $1/2.71^2$. The beam affects the quad cell spatial resolution. At this beam size, the quad cell spatial resolution is 0.5 microns. The 4 cells of the quad cell detector translate the optical power readings into voltage. The total intensity of the beam is set such as the quad cell operates in the linear range of its sensitivity curve. The data acquisition board receives the voltage output signals from the quad cell detector and transmits them to the PC. The PC analyses the voltage readings coming from the data acquisition board. Assuming a perfect Gaussian beam, when the beam is perfectly centred on the quad cell detector, the voltage signals coming from the four detector cells should be equal. The quad cell was oriented so that the lines separating the four cells of the detector were parallel with the x and y directions of movement of the jig holding the collimator. By this, when the collimator moved from the "centred position", the sum of the voltage readings coming from the two top detector cells should be higher than the sum of the voltage readings coming from the two bottom detector cells. A calibration measurement is used to translate the voltage reading into distance readings.

Quad – Cell Photodiode as Alignment and Measurement tool

The quad-cell photodiode is used as a position sensor [21]. Within the detector's linear response region, its differential output voltage is directly related to the shifting of beam position. The detector has a linear response region from -0.4ω to $+0.4\omega$ (ω is the Gaussian beam radius).

The quad-cell detector has a very good linearity of the differential output voltage to the beam shifting. The ability to measure the beam spot size by the quad-cell detector is explored in this experiment.

The quad-cell photodiode has been used as a position sensor in various applications. Differing from the conventional single-cell photodiode, the active area of the diode consists of four elements along the center, which can sense the incident beam separately. By subtracting the voltage signals from the opposite diode elements, the shifting of the incident beam can be obtained. The differential voltage signal versus the beam shifting is linear in a region depending on the beam size and the diode cutting grid width.

The cutting grid is the width of the four elements, which divide the four cells. We need a very small area of the cutting grid, and at the same time the beam size should be big enough for the measurement to be accurate.

The four elements of the detector are assumed to have a uniform response to the incident light beam. The diode cutting grid width is w. Figure.5.2 shows the schematic diagram of the quad-cell diode and the incident beam spot. The beam spot is off the center of the detector along X-axis by *xm*.

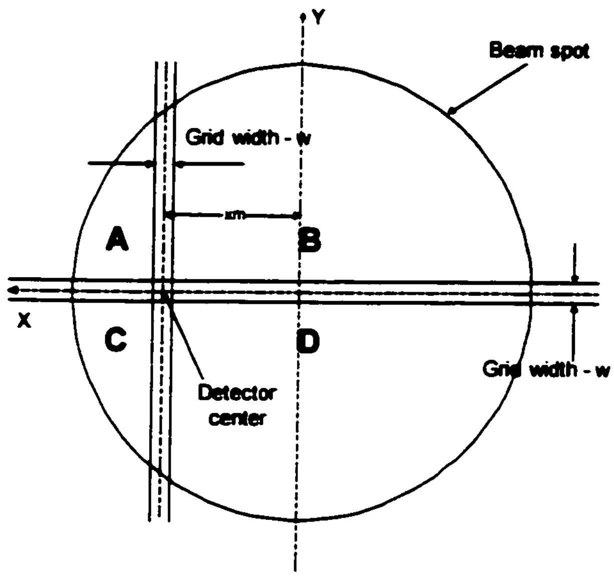

Figure 5.2: Schematic illustration of quad-cell photodiode front view

The detector registers the beam information; in the case shown in Figure 5.3 we assume a perfect Gaussian beam perfectly centred on the quad cell detector.

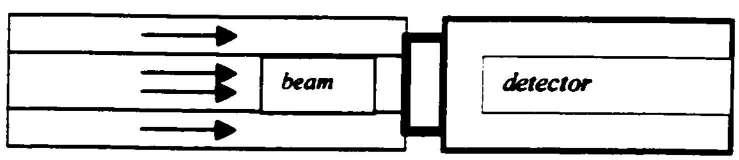

Figure.5.3: Schematic illustration of quad-cell photodiode side view

The incident laser beam on the detector plane is assumed to have an ideal Gaussian distribution, which has a unit radius and I_O is the intensity at the center of the beam (r =0).

$$I = I_O \exp\left\{\frac{2r^2}{r_\omega^2}\right\} \qquad (1)$$

where r_ω characterizes conventionally the beam spot size and r is the radius to the beam center.

The differential voltage is proportional to the power falling on the elements A and C minus power on B and D:

$$\Delta V \approx (P_A + P_c) - (P_B + P_D) \qquad (2)$$

The contribution from the diode cutting grids must be considered, since they are not responding to the light. [21]

$$\begin{aligned} P_A + P_C = & \int_{x_m}^{\infty} 2r \cdot Cos^{-1}(x_m / r) \cdot \exp[-2r^2]dr - \\ & \int_{-0.5a}^{+0.5a} \int_{x_m+0.5a}^{\infty} \exp[-2(x^2 + y^2)]dxdy - \\ & \int_{-\infty}^{+\infty} \int_{x_m}^{x_m+0.5a} \exp[-2(x^2 + y^2)]dxdy \end{aligned} \qquad (3)$$

Without the cutting grids, the total power of the incident beam is as follows: [21]

$$P_{total} = \int_0^{\infty} 2\pi r \cdot \exp[-2r^2]dr = \pi / 2 \qquad (4)$$

The beam power falling on the elements B and D can then be expressed as follows:

$$\begin{aligned} P_B + P_D = \pi / 2 - & \int_{x_m}^{\infty} 2r \cdot Cos^{-1}(x_m / r) \cdot \exp[-2r^2]dr - \\ & \int_{-0.5a}^{+0.5a} \int_{-\infty}^{x_m-0.5a} \exp[-2(x^2 + y^2)]dxdy - \\ & \int_{-\infty}^{+\infty} \int_{x_m-0.5a}^{x_m} \exp[-2(x^2 + y^2)]dxdy \end{aligned} \qquad (5)$$

Defining the normalized differential output as T, corresponding to the real quad-cell photodiode output voltage, the followings equation is obtained [21]:

$$T = \frac{(P_A + P_C) - (P_B + P_D)}{P_A + P_C + P_B + P_D} \qquad (6)$$

The differential output T is numerically calculated for different beam shifting positions and different diode cutting grid width w. The result is shown in Figure 5.4.

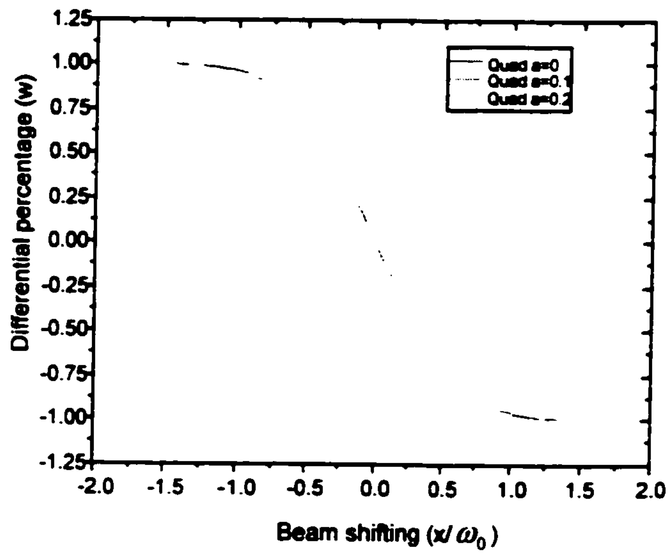

Figure 5.4: Quad-cell photodiode response (with grid width w considered)

When the contribution of the diode cutting grids is not considered (w = 0), the linear response region is –0.4ω~0.4ω (ω is the Gaussian beam radius) and the linear slope k is 1.4896. With the increase of the grid width w, the linear response region will decrease, and the linear slope will increase:

w = 0, k = 1.4896;

w = 0.1ω, k = 1.5859;

w = 0.2ω, k = 1.6813.

When the grid width w is 0.2ω, the linear response region is approximately –0.3ω ~0.3ω. In this sense, the quad-cell diode can be used to measure the beam shifting only if the shifting is within its linear response region, and the measurement sensitivity is depending on the linear response slope *k*:

$$\Delta V \approx k \cdot (x / \omega) \qquad (7)$$

where x is the beam shifting.

Since the linear slope *k* is a normalized quantity, the diode sensitivity will increase when the beam size ω_0 decreases. The trade off is that the effective linear response region will decrease with the beam size, and the beam spot cannot be too small due to the existence of the diode cutting grid width (normally 100~200μm).

However, due to the finite thickness of the diode cutting grid width w, the measured beam spot size will be smaller. Assuming the incident beam has a unit Gaussian radius (ω=1), the following simulation results are obtained:

When w = 0, measured ω = 1

When w = 0.1, measured ω = 0.937

When w = 0.2, measured ω = 0.879

When w = 0.4, measured ω = 0.776

If the grid width w is known, the beam spot size can then be obtained by fitting the experimental data.

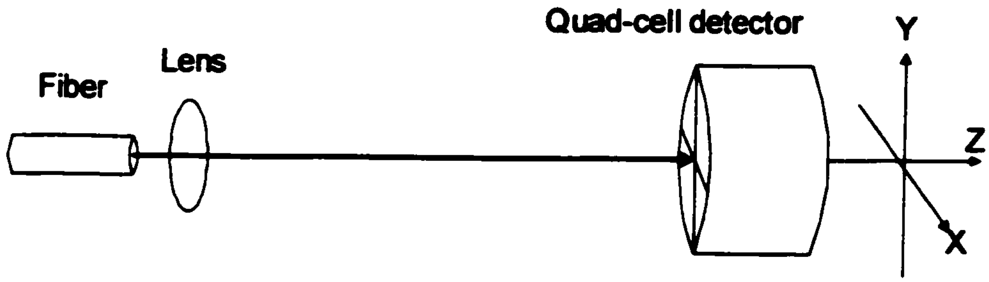

Figure 5.5: Illustration of quad-cell diode setup.

The differential output voltages along X- and Y- axis are manipulated as follows:

$$\Delta V_X = (V_A + V_C) - (V_B + V_D)$$
$$\Delta V_Y = (V_A + V_B) - (V_C + V_D) \quad (8)$$
$$V_{total} = (V_A + V_B + V_C + V_D)$$

where V_{total} is the total output for the incident beam. The beam shifting can be obtained by moving either the detector or the output beam along X and Y direction. The four diode-cells are aligned along X-axis and Y-axis such that the signal ΔV_Y does not change when the beam shifting is along the X-axis.

The ability to measure precisely the position is important for measurement and alignment tools.

5.2. Calibration of the Piezoelectric Actuator

The first operation required for the experiment is the calibration, including the direction and displacement of the piezoelectric actuator. The calibration establishes the correlation between the motion achieved with the micrometer and the quad-cell signal.

The accuracy of the correlation between displacement and the quad-cell signal increases with the number of measurements performed. The experiment is performed in six steps. The increment used for the experiment is 10 microns per step. At the end of each step, the average quad-cell signal is calculated. This value is necessary in order to correlate the piezoelectric displacement with the signal of the quad-cell.

The six steps of the calibration are presented as follows: (see Annex 1)

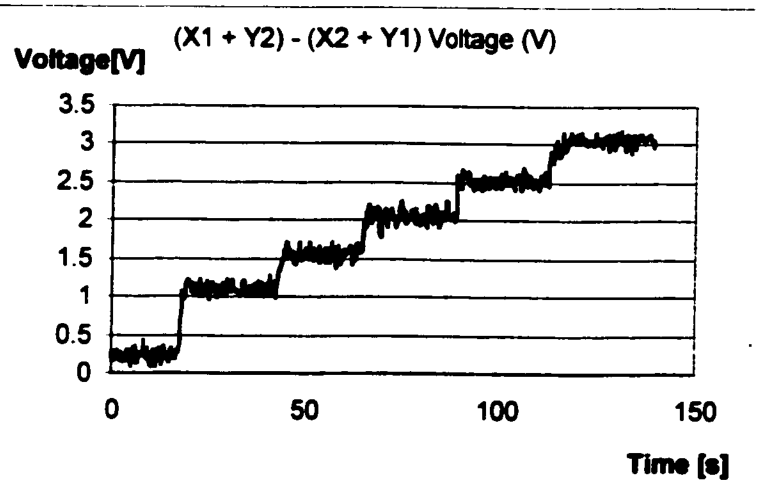

Figure 5.6: General graphic of the calibration

1st Step calibration, direction and displacement of the piezoelectric actuator

Average	0.227113

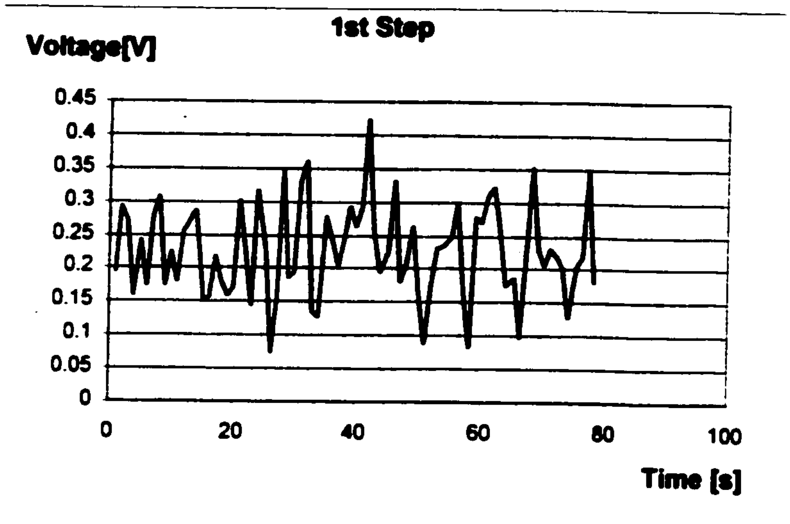

Figure 5.7: 1st Step calibration, direction and displacement of the piezoelectric actuator

2nd Step calibration, direction and displacement of the piezoelectric actuator

Average	1.098775

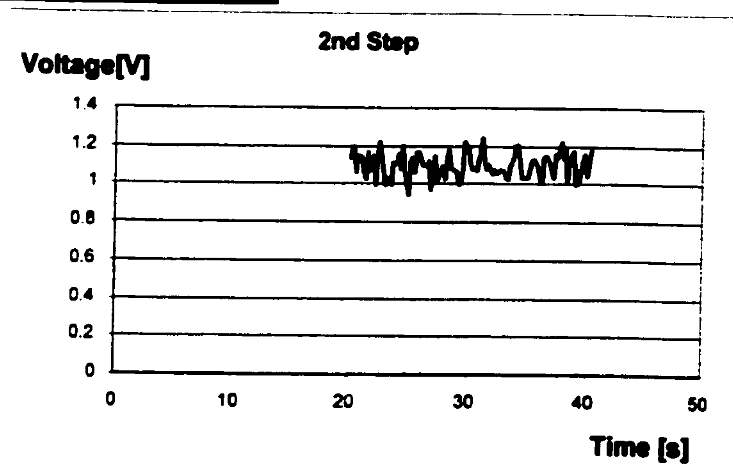

Figure 5.8: 2nd Step calibration, direction and displacement of the piezoelectric actuator

3rd Step calibration, direction and displacement of the piezoelectric actuator

Average	1.547948

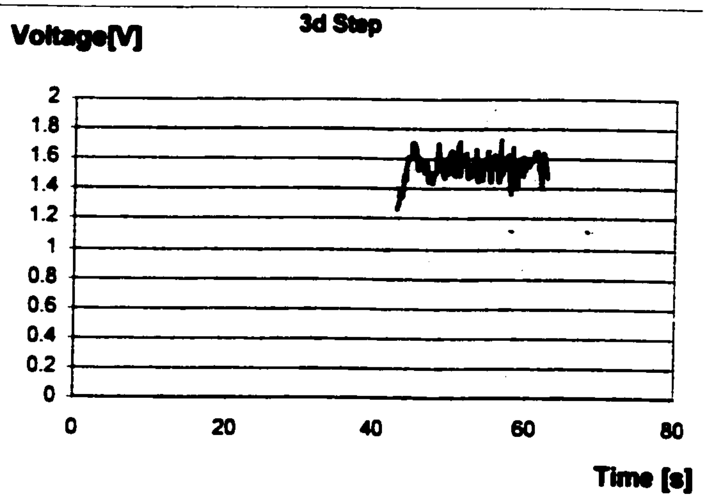

Figure 5.9: 3rd Step calibration, direction and displacement of the piezoelectric actuator

4th Step calibration, direction and displacement of the piezoelectric actuator

Average	2.057354

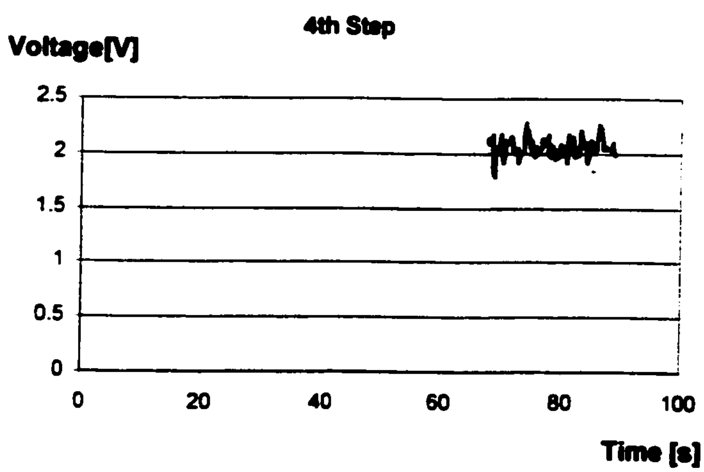

Figure 5.10: 4th Step calibration, direction and displacement of the piezoelectric actuator

5th Step calibration, direction and displacement of the piezoelectric actuator

Average	2.519199

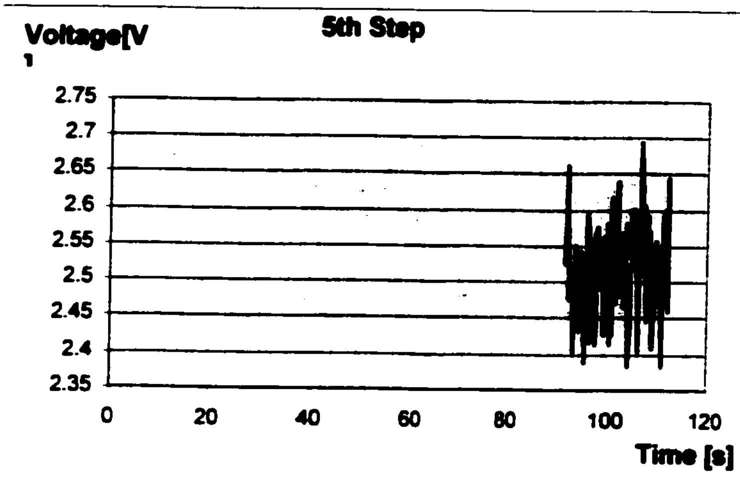

Figure 5.11: 5th Step calibration, direction and displacement of the piezoelectric actuator

6th Step calibration, direction and displacement of the piezoelectric actuator

Average	3.062394

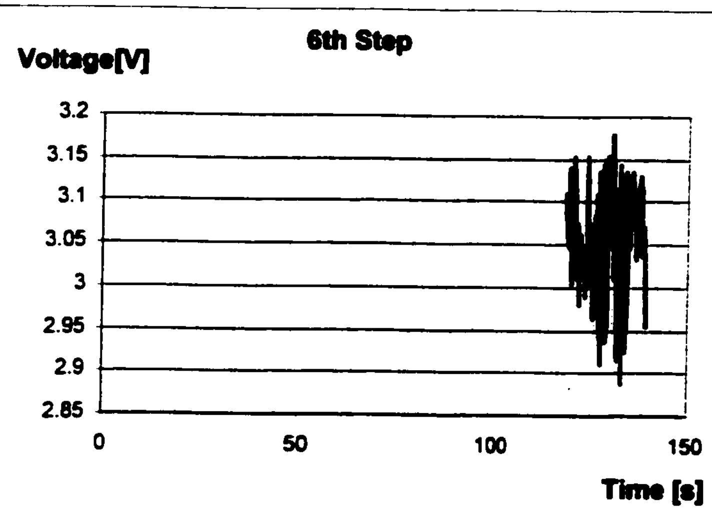

Figure 5.12: 6th Step calibration, direction and displacement of the piezoelectric actuator

The next table shows the corresponding values of the quad-cell voltage registered for each calibration step of the micrometer position. The micrometer displacement used for the experiment records 10 microns increment per step. For each increment, the quad-cell voltage deviation is calculated. Based on the calculation of the deviation for each increment, the mean deviation of the quad-cell voltage for the experiment is determined.

Calibration Step	Micrometer Displacement [microns]	Average Quad-Cell Voltage [volts]	Deviation [volts]
1st	10	0.227	-
2nd	20	1.099	0.872
3rd	30	1.548	0.449
4th	40	2.057	0.509
5th	50	2.519	0.462
6th	60	3.062	0.543
Mean Deviation			0.567

Table5.1: Table of calibration micrometer / quad-cell signal - mean deviation

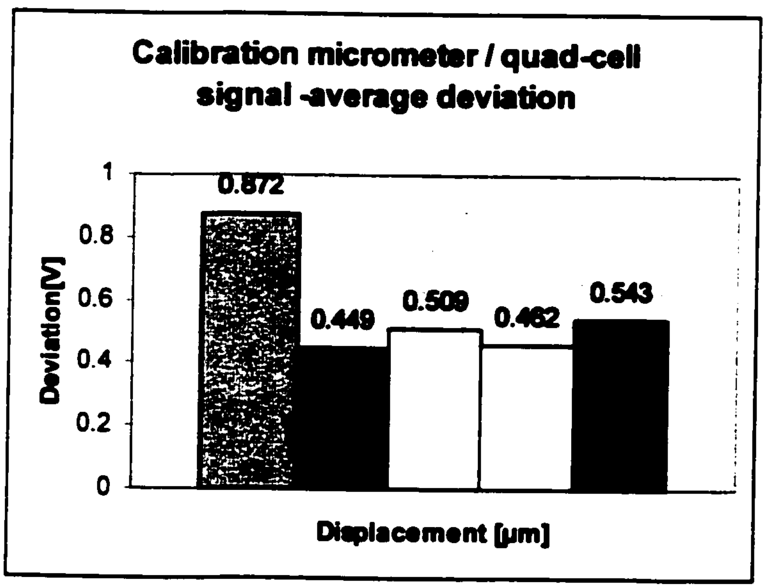

Figure 5.13: Graph of calibration micrometer / quad-cell signal - mean deviation

The results of the calibration establish that for each 10 micron increment, a mean deviation of 0.567 quad-cell voltage is recorded. Therefore, for each micron, a 0.0567 quad-cell voltage corresponds.

5.3. Experimental Results of Piezoelectric Actuator Displacement

The first part of the experiment established the correlation between the quad-cell voltage and the displacement. The second part of the experiment is targeted to explore the displacements generated this time with the piezoelectric actuator and to interpret the changes of piezoelectric

shape as result of voltage variation. In order to simplify the interpretation of data, three random values for the power supply at 30 V, 60 V, and 90 V were chosen. For each voltage, several measurements will be performed, in order to determine if piezoelectric materials are suitable to be used as actuators for automatic closed loop control applications.

For the first measurement at 30 V, the recorded result is 0.342627+/- 0.16 quad-cell voltage. (see Annex2.1)

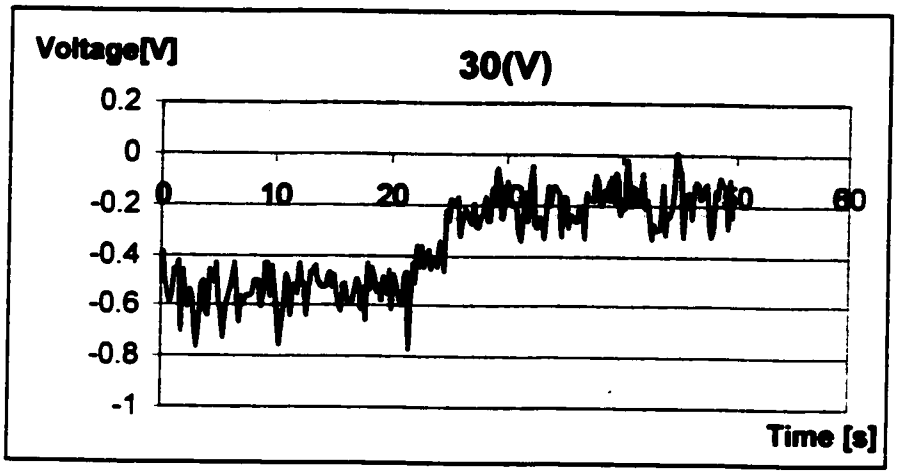

Figure 5.14: 1st Measurement at 30 V

For the second measurement at 30 V, the recorded result is 0.3258933+/- 0.16 quad-cell voltage. (see Annex2.1)

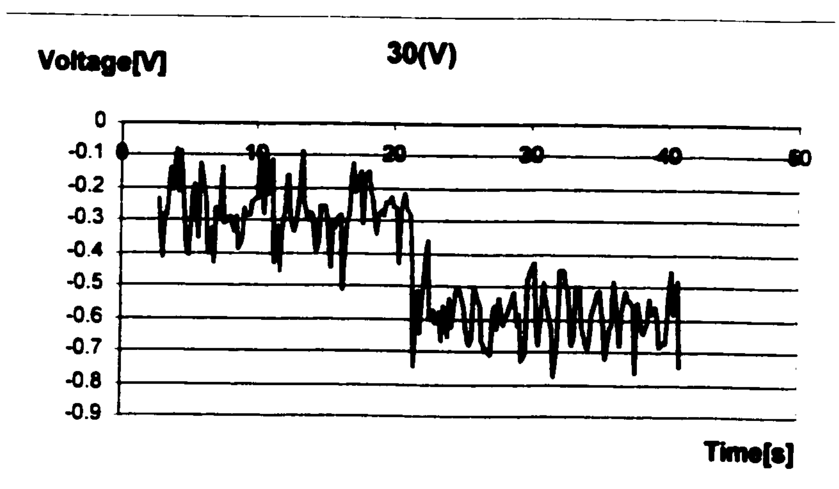

Figure 5.15: 2nd Measurement at 30V

For the third measurement at 30 V, the recorded result is 0.31189 +/- 0.16 quad-cell voltage. (see Annex2.1)

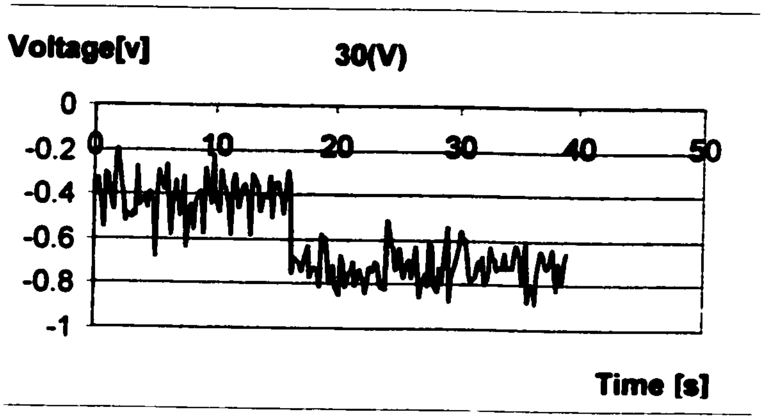

Figure 5.16: 3rd Measurement at 30V

For the fourth measurement at 30 V, the recorded result is 0.373517 +/- 0.16 quad-cell voltage. (see Annex2.1)

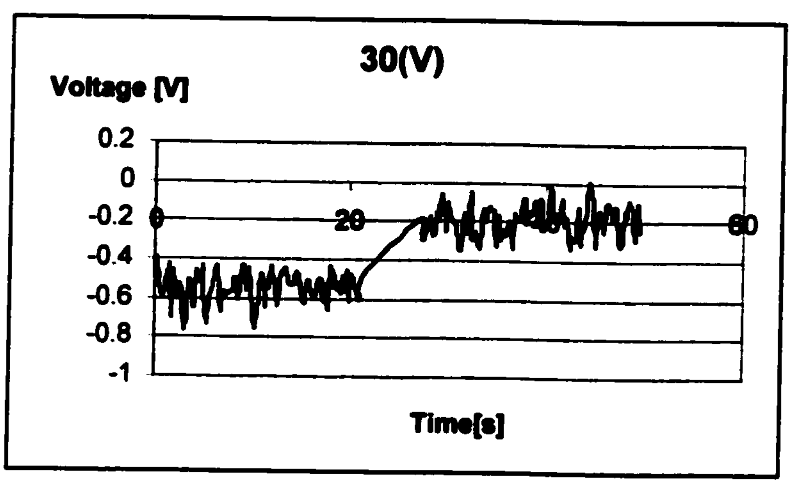

Figure 5.17: 4th Measurement at 30 V

For the first measurement at 60 V, the recorded result is 0.51446+/- 0.16 quad-cell voltage. (see Annex2.2)

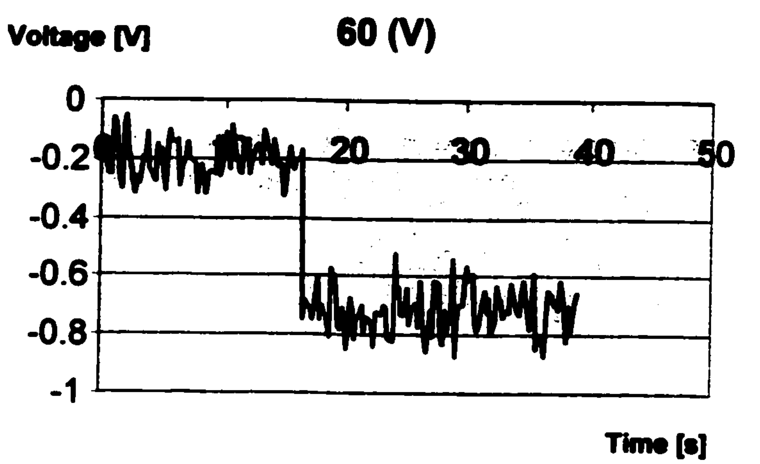

Figure 5.18: 1st Measurement at 60 V

For the second measurement at 60 V, the recorded result is 0.520235+/- 0.16 quad-cell voltage. (see Annex2.2)

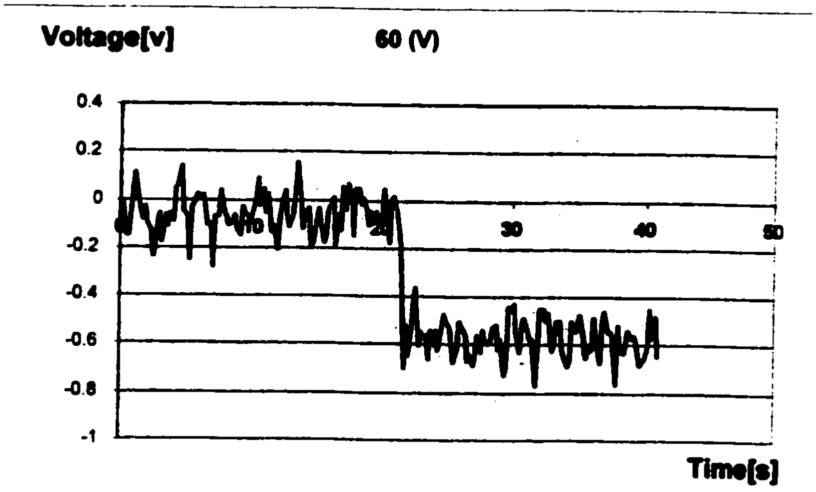

Figure 5.19: 2nd Measurement at 60 V

For the third measurement at 60 V, the recorded result is 0.604395+/- 0.16 quad-cell voltage. (see Annex2.2)

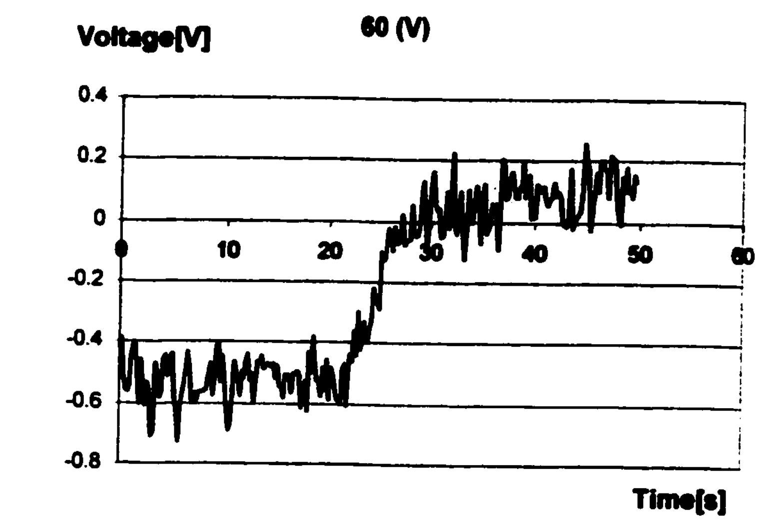

Figure 5.20: 3rd Measurement at 60 V

For the forth measurement at 60 V, the recorded result is 0.73335+/- 0.16 quad-cell voltage. (see Annex2.2)

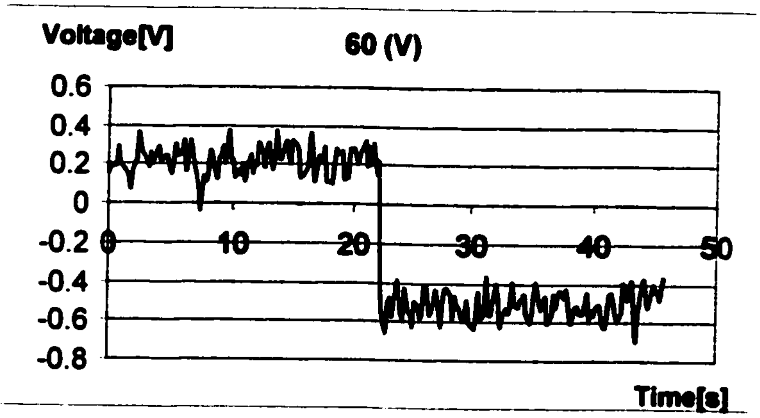

Figure 5.21: 4th Measurement at 60 V

For the first measurement at 90 V, the recorded result is 0.807862+/- 0.16 quad-cell voltage. (see Annex2.3)

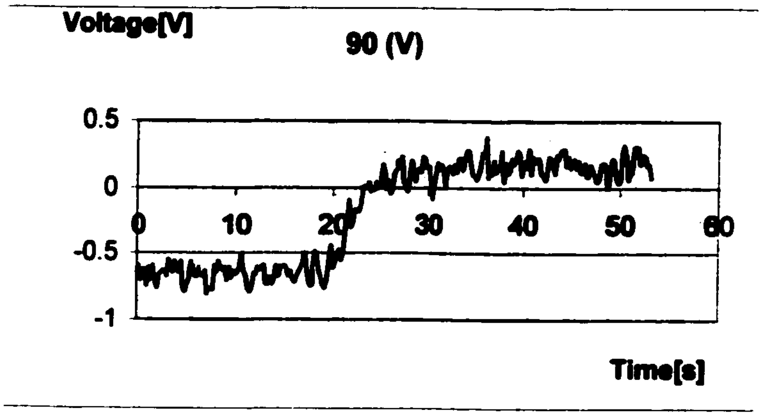

Figure 5.22: 1[st] Measurement at 90 V

For the second measurement at 90 V, the recorded result is 0.843076+/- 0.16 quad-cell voltage. (see Annex2.3)

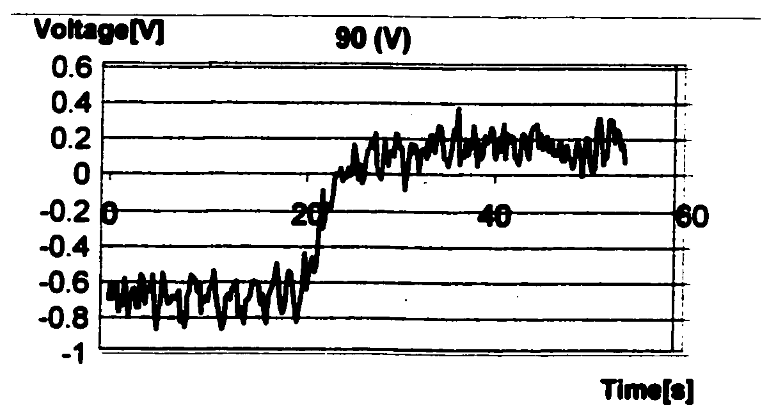

Figure 5.23: 2[nd] Measurement at 90 V

For the third measurement at 90 V, the recorded result is 0.820802+/- 0.16 quad-cell voltage. (see Annex2.3)

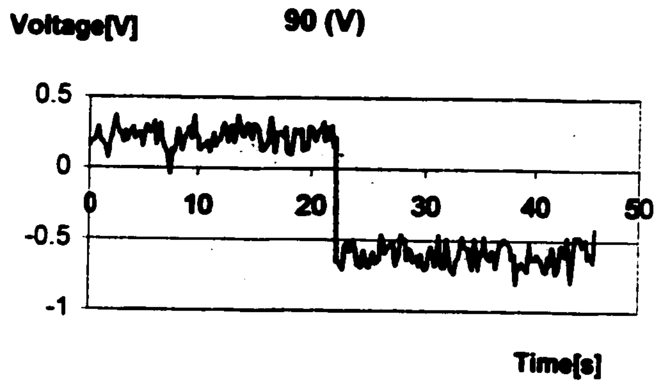

Figure 5.24: 3rd Measurement at 90 V

For the fourth measurement at 90 V, the recorded result is 0.967189+/- 0.16 quad-cell voltage. (see Annex2.3)

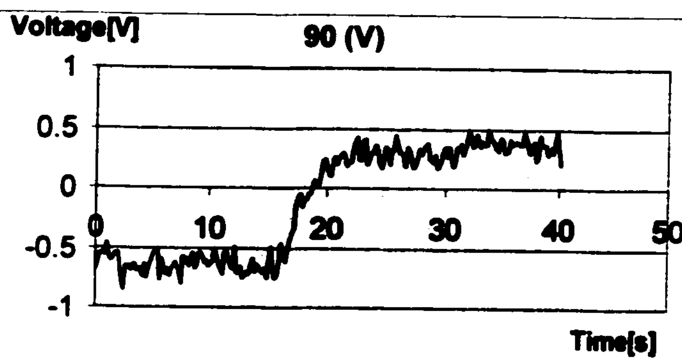

Figure 5.25: 4th Measurement at 90 V

In the next table the results of the measurements are summarized as follows:

Measurement	Power Supply (volts)	Quad-Cell (volts)
1st	30	0.34
2nd	30	0.32
3rd	30	0.31
4th	30	0.37
Average	30	0.34
1st	60	0.51
2nd	60	0.52
3rd	60	0.60
4th	60	0.73
Average	60	0.61
1st	90	0.81
2nd	90	0.84
3rd	90	0.82
4th	90	0.97
Average	90	0.86

Table5.2: Table of quad-cell signal at 30 V, 60 V, and 90 V

The table above supports with data the advantages of using piezoelectric actuators for small displacement applications. We can control the piezoelectric shape, or as in the present application the arm's motion, based on voltage changes.

The calibration experiments established that, for 0.06 quad-cell voltage corresponds one micron displacement. At 30 V, the average quad–cell signal voltage is 0.34 V, which will result in approximately 6μm displacement. At 60 V, the average quad–cell signal voltage is 0.61 V, which will result in approximately 10μm displacement. At 90 V, the average quad–cell signal voltage is 0.86 V, which will result in approximately 14μm displacement.

The following table and graph are illustrating the minimum and maximum result values from each series of 30 V, 60 V and respectively 90 V:

Power Supply (volts)	Minimum Quad-Cell (volts)	Maximum Quad-Cell (volts)
30	0.31	0.34
60	0.51	0.73
90	0.81	0.97

Table5.3: Table of quad-cell signal-hysteresis at 30 V, 60 V, and 90 V

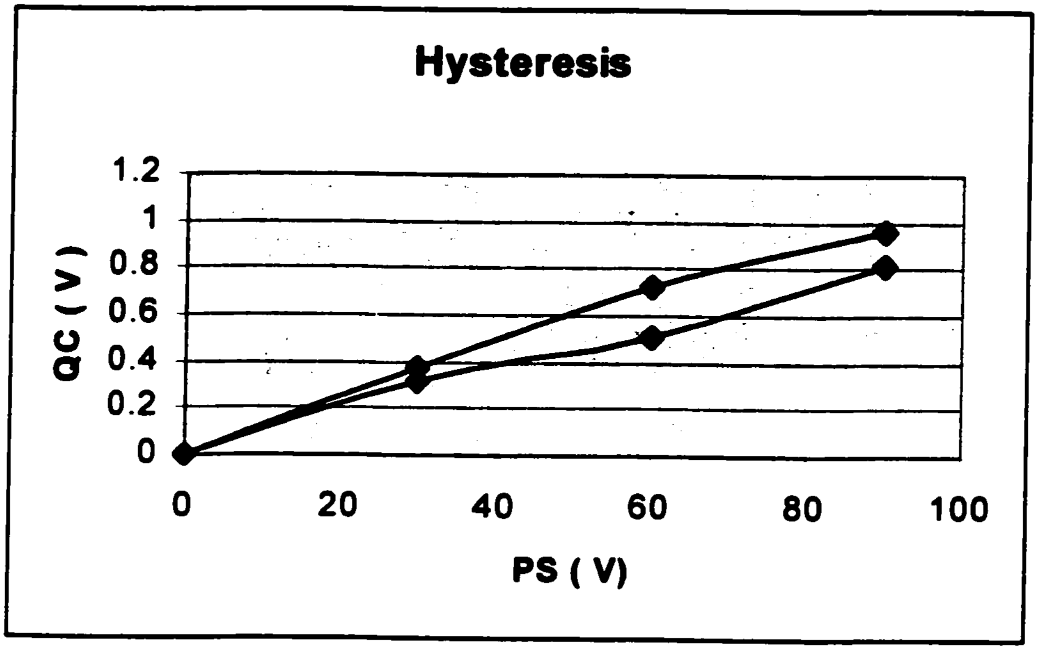

Figure 5.26: Graph of quad-cell signal-hysteresis at 30 V, 60 V, and 90 V

Figure 5.26 and Table 5.3are illustrations of the fact that the piezoelectric actuators, under automatic control for precise positioning, cannot be used in this configuration, given that for the same input different outputs are generated.

However, a very satisfactory result is achieved using the piezoelectric actuators for small displacements and controlled motion under operator control.

5.4. Evaluation of Motion Accuracy for Piezoceramic Positioning Device

The second experiment demonstrates the lack of adequacy of the classical micrometers for small displacement. The goal is to control the lens position with such level of precision, that increments smaller then 5×10^{-4} degrees will be achieved. If the increment is bigger than 5×10^{-4} degrees, the operator cannot find exactly the position for which the beam is split. The result of the second experiment demonstrates that piezoelectric actuators can generate displacements in smaller increments than the mechanical actuators.

This section will determine whether it is possible to use piezoelectric actuators for very small and precise motion in the fiber-optics industry, for which the classical devices, i.e. micrometers, lack the required level of positioning accuracy.

For the standard drive system in machine tools, such as a servo-ball-screw mechanism or other mechanical jigs, it is virtually impossible to obtain nanometric-positioning accuracy because the ball–screw mechanism positioning is affected by backlash and friction in the drive system.

A growing number of motion control applications require sub-micrometer positioning accuracy. In precision positioning systems, accuracy and range are key criteria.

Accuracy of a positioning device is normally defined as the difference between the desired position and the measured position during a controlled motion. The resolution is normally defined as the smallest change of a variable that can be measured by a detector.

In order to generate a beam split, the smallest position change of the lens relative to the sleeve is crucial. With the jig from the previous experiment, by using the controlled displacement of the piezoelectric actuators, our goal is to achieve the desired optical phenomena and to control it, until the cure process is mature and the position of the parts is stable.

Micro electro-mechanical system aligning jig

The experiment consists in incremental displacements with the jig, until the lens's position stabilizes in a very precise range.

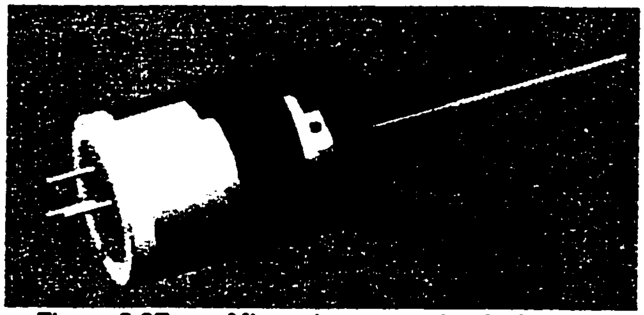

Figure 5.27: Micro electro-mechanical system

The light from the source traverses the lens and hits the mirror, under a very precise angle, such as the reflected beam is split, as shown in Figure 5.28. A special design allows the mirror to shift its position from POS1 to POS2 and vice versa.

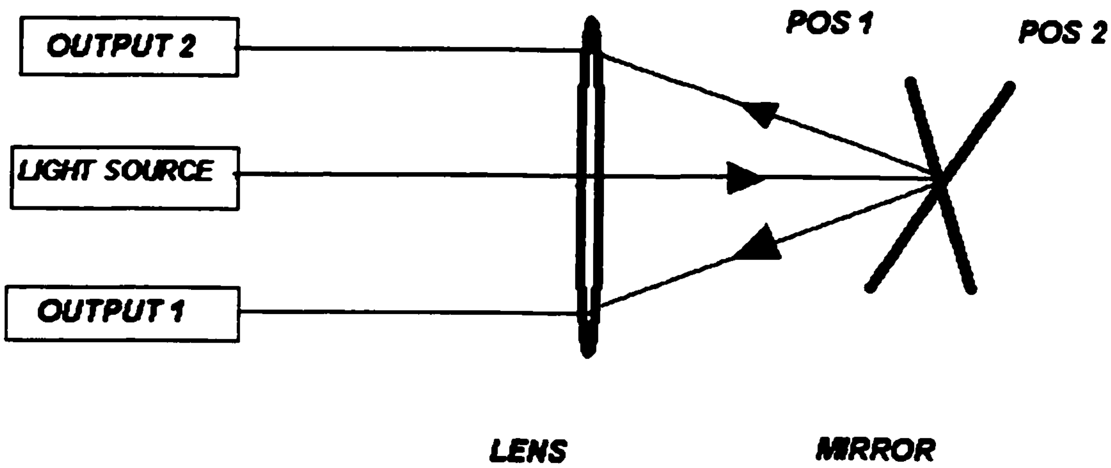

Figure 5.28: Micro electro-mechanical system - split beam

The basic principle is to combine a lens and a tilting mirror in order to split an input beam into two output fibers. The problem of the uncertainties in the rest angle of the mirror and the height of the main ray is solved by the use of a compound lens (a variable focal lens) such as it is shown in Figure 5.28.

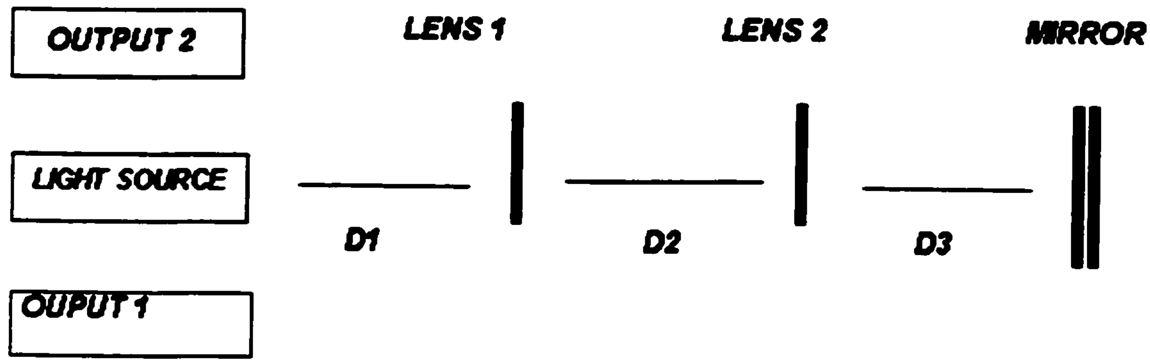

Figure 5.29: Micro electro-mechanical system - lenses & mirror position

The fundamental task is to achieve a very precise motion of a fiber tube, in order to create the exact angle for the beam to be split.

After the optical calculation, the results obtained are shown in Table 5.4: Table of requirements and tolerances for micro electro-mechanical system. The data from the table represent the maximum tolerance admissible, which is the maximum distance between two rotation points of the tube relative to the lens, and within which the beam can be split.

In other words, we have to produce a controlled motion using the jig's arm (using the piezoelectric actuator) to monitor the incremental displacement.

Using the mechanical three-axis position, it is impossible to perform a very precise controlled motion. The smallest controlled displacement that mechanical controlled micrometers are able to achieve ranges as low as $5x10^{-3}$ mm. [45]

The jig's arm has to control the motion of a fiber tube, both as a rotation and translation displacement.

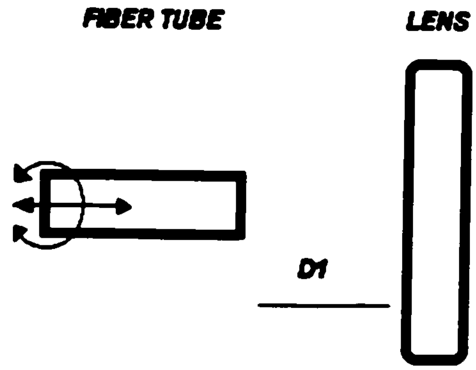

Figure 5.30: Micro electro-mechanical system - lens & fiber tube

Figure 5.30 shows how the fiber tube rotates or/and translates in different directions, in order to produce the beam split.

The jig's arm gives the operator the possibility to change the fiber tube position, based on the information displayed on the PC.

Specifications	
Overall Length	Max 15mm
D 1	0 mm to 1.2 mm with 0.05mm incr.
D 2	0 mm to 2.6 mm with 0.07mm incr.
D 3	1.4 mm +/-0.1mm
FiberTube movement	translation +/- 190 microns (vertically) +/-2deg rotation over X, Y- 0.0005deg incr.
Collimator Lens – Dimensions & Tolerances	Diameter: 3mm +0.005 –0.02mm; Length: 1.6mm +/-0.02

Table 5.4: Table of requirements and tolerances for micro electro-mechanical system

Figure 5.31 and Figure 5.32 present two different views of the micro electro-mechanical system.

The distance between the two lenses (D2) is adjusted by means of a double threaded sleeve; this pitch produces the specified 0.07mm increment.

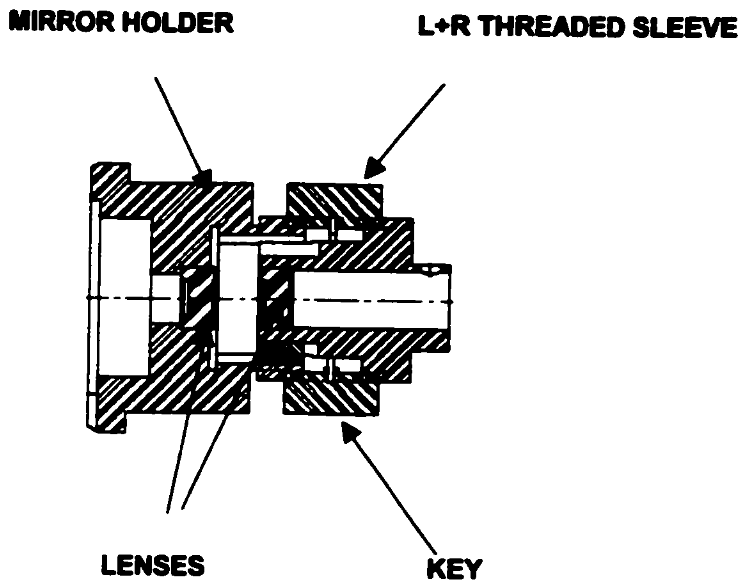

Figure 5.31: Micro electro-mechanical system (section)

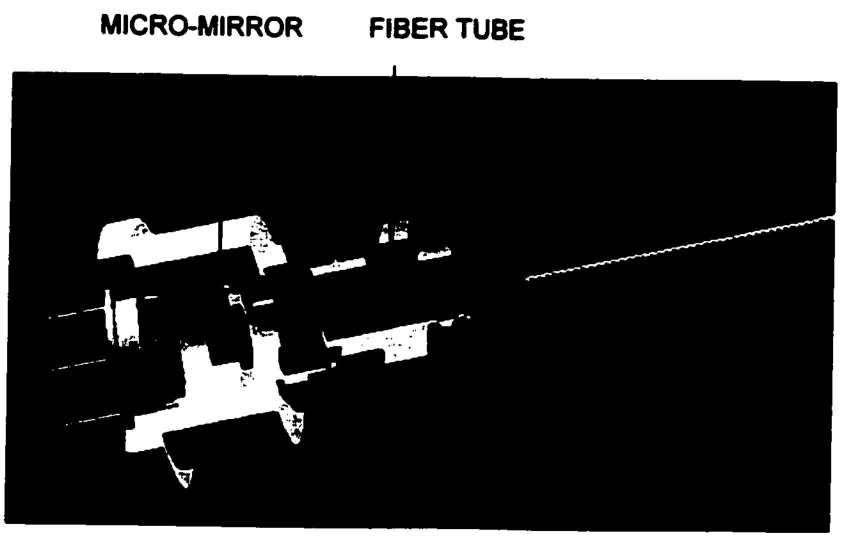

Figure 5.32: Micro electro-mechanical system (3D section)

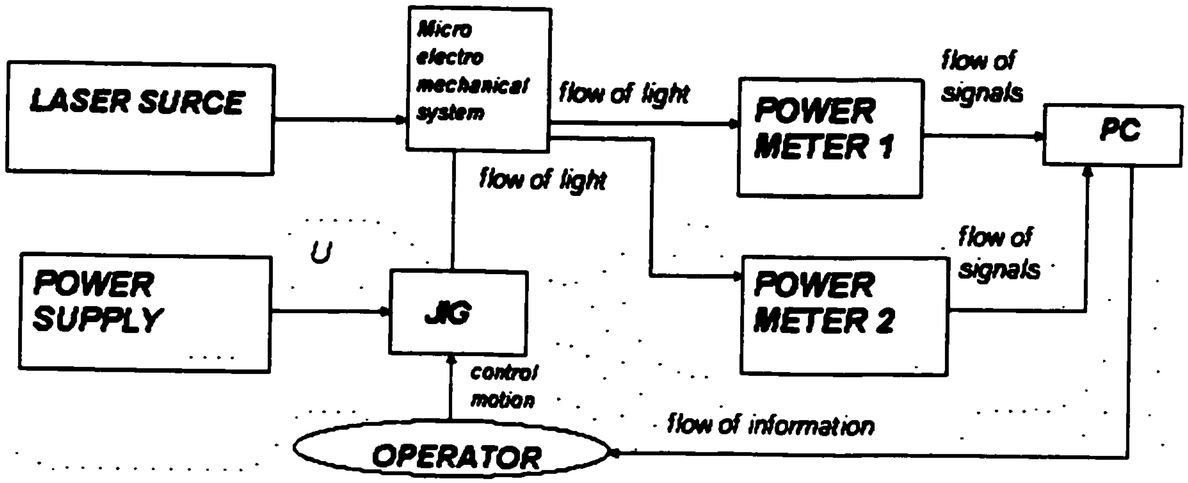

Figure 5.33: Micro electro-mechanical system – block diagram

Figure 5.33 shows the block diagram for the second experiment. The light comes from the laser source across the micro electro-mechanical system. Modifying the position of the lens, the beam is split. The power meter is basically a photo detector that transforms an intensity reading of the luminous signal in a voltage signal proportional with the intensity of the luminous signal. In general, the power meters are factory calibrated so one can read on the display directly the luminous intensity information. Usually, the power meters have an analogue voltage output, which can be transmitted directly to a data acquisition board. The beam traverses the micro electro-mechanical system, is detected by the power meter and the intensity is displayed by the PC. By changing the voltage of the power supply, the operator controls the motion of the piezoelectric actuator (jig's arm), and based on the rotation of the lens and the tube positioning the beam is split. The operator monitors and interprets the phenomena using the display of the displacement on PC monitor. This experiment demonstrates the fact that the jig with piezoelectric actuator shown in Figure 5.34 can be utilized successfully.

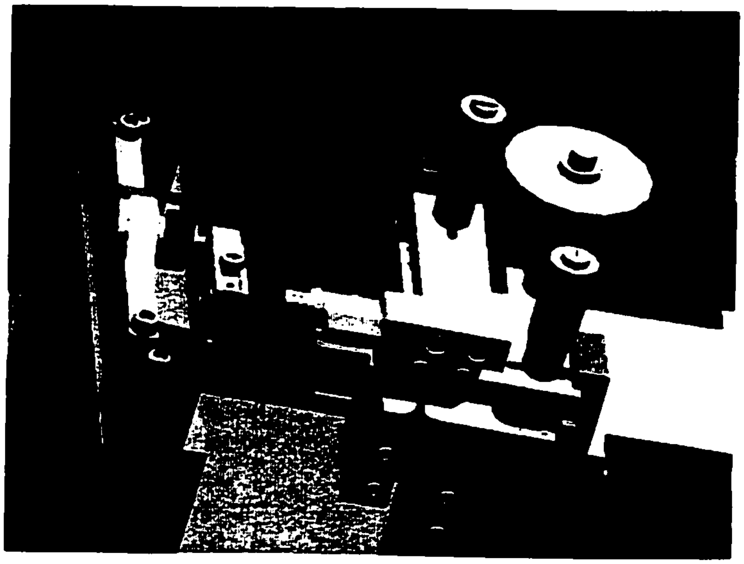

Figure 5.34: Micro electro-mechanical system and jig (3D)

The corresponding distance for each $\alpha = 0.0005^{\circ}$ degree increment is calculated as follows:

$$tg0.0005 = \frac{\Delta x}{21}$$

$$\Delta x = 1.8 \times 10^{-4}$$

The 21 mm is the rotation radius that represents the distance between the rotation point (end of the jig's arm) and the middle of the piezoelectric actuator, according to the drawing specification. The 0.0005 degree increment is the maximum admissible value to achieve the beam split.

The experiment demonstrates that very precise, controlled displacement can be generated, up to the $\Delta x = 1.8 \times 10^{-4}$ mm range.

6. Conclusions

The standard drive system in machine tools (as a servo-ball screw mechanism or other mechanical jigs) cannot achieve nanometric-positioning accuracy when using ball-screw mechanisms, due to the presence of backlash and friction in the drive system.

This thesis demonstrates the possibility of successfully using piezoelectric actuators in fiber optic positioning. Using an operator to control the operation, the piezoelectric actuators can achieve accurate motion for very small displacements.

The motion can be controlled with a piezoelectric actuator much more precisely than with mechanical actuators only. The micrometer resolution ranges from $5\text{x } 10^{-3} \pm 0.0015$mm, while the piezoelectric actuator achieves $1.8\text{x}10^{-4}$mm. A twenty five times resolution improvement is expected, when a piezoelectric actuator is used instead of a micrometer (i.e. $5x10^{-3}/1.8x10^{-4} \cong 25$ times).

However, piezoelectric materials are not suitable to be used as actuators for automatic closed loop control because the hysteresis results in different outputs for identical inputs.

7. References

1. Youseti-Koma A, Sasiadek J.Z, Vukovich G., LQC Control of Flexible Structures Using Piezo Elements, American Institute of Aeronautics and Astronautics, GNC Conference, 1994
2. An American National Standard on Piezoelectricity, ANSI/IEEE Standard pp176-177, 1987
3. Faria Vaz Anthony, Active Vibration Damping in Large Flexible Space Structures, Canadian Space Agency Report, June 1991
4. Faria Vaz Anthony, Composite Modeling of Flexible Structures with Bonded Piezoelectric Film Actuators and Sensors, Ph.D. Thesis, Department of Mechanical and Aerospace Engineering at McMaster University, 2001
5. Faria Vaz Anthony, Modeling of Piezoelectric Behavior for Actuators and Sensor Applications, Canadian Space Agency Report, February 25th, 2001
6. Faria Vaz Anthony, Trip Report on the First Join U.S. Japan, Conference on Adaptive Structures, Maui, Hawaii, Nov. 13-15, 1990
7. Coleman B.D. and. Hodgdon M.L, A Constitutive Relationship for Rate-Independent Hysteresis in Ferromagnetically Soft Materials, Int J. Eng. Sci., Vol.24, pp 897-919, 1986
8. Bousquet A, Labert M., Quittet A.M. and Guinier A., Acta Crystallog. 16 (1963) 989
9. Newcomb C.V and Flinn I, Improving the Linearity of Piezoelectric Ceramic Actuators, Electron. Lett, Vol.18, pp 442-444, 1982
10. Design of a Linear Piezomotor, www.physicinstrument.com, 2001
11. Necsulescu D, Mechatronics MCG4136 course, University of Ottawa, 2000
12. Jun Ni and Zhu Zhenqi, Design, Fabrication, and Real-Time Neural Network Control, IEEE ASME Transaction on Mechatronics, Vol.5, No.3, pp 441-444, September 2000
13. Digital Instruments Vertical Engagement Scanners –Support Note 223 Rev C, 1990

14. Lagoudas Dimitris and Iradjg Tadjbakhsh, Active Flexible Rods with Embedded SMA Fibers, Rev.Sci.Instrum., March 1992, pp13-15

15. Furuhata H and Toriyama K., Appli. Phys. Lett 23, pp 361, 1973

16. G. L. Pearson and W.L. Feldman, J. Phys. Chem. Solids 9 pp28,1958

17. Han J.M.T.A. Adrians, Willem L. de Koning, and Banning Reinder, Modeling Piezoelectric Actuators, IEEE ASME Transactions on Mechanism, Vol.5, No. 4,pp331-335, Dec 2000

18. Piezoelectric Actuators. University of Maryland,http://www.glue.umd.edu/~gmkamath/er.html , 2001

19. Hooton J. A. and Merz W.J. Phys. Rev 98, pp 409-411, 1955

20. Hatano J., Suda F., and Futama F, Jpn. J. Applied. Physics 12 1644. 1973

21. A. Zhao, Quad Cell Detector Photodiode as Alignment and Measurement Tool, Report JDS Uniphase(unpublished), March 2001

22. Junjitani, Toshiyuki Takagi and Jinhao Qiu, Intelligent Material Systems: Application of Functional Materials, ASME Reprint no. AMR253, Appl Mech Rev. Vol.51, No.8, pp505-540, August 1998

23. Yoshino K., Taniguchi H. Ozaki, Ferroelectrics 91, pp 267,1989

24. Shahinpoor M., Micro-Electro and Mechanics of Ionic Polymeric Gels as Electrically Controllable Artificial Muscles, Precision Eng, Vol.17, pp221-216, 1995.

25. Shahinpoor M., Cohen Y Bar, Simpson J.O. and Smith J., Ionic Polymer–metal Composites (IPMC's) as Biomimetic Sensors, Actuators and Artificial Muscles, in Proc.IFAC Motion Control, pp 37-42, 1996

26. GoldfarbM and Celanovic N, Modeling Piezoelectric Stack Actuators for Control Manipulation, IEEE Contr. Syst.Mag. Vol.17, pp 69-79,1997

27. Shahinpoor M, Micro-Electro-Mechanics of Ionic Polymeric Gels As Electrically Controllable Artificial Muscles, Journal of Intelligent Material Systems and Structures, Vol.6, pp425-443 May 1995

28. Nellya N. Rogacheva, The Theory of Piezoelectric Shells and Plates, CRC Press, 1994

29. Nonlinear Constitutive Relationships for Piezoceramic Materials, Smart Mater. Struct.1 Center for Composition Materials, University of Texas at Arlington, USA, December 6, 1991

30. Pierangelo Masarati, Ghiringhelli Gian Luca, On Local Solutions for Piezoelectric Laminates, Elsevier Science Ltd. Computational Fluid and Solid Mechanics, 2001.

31. Banning R, Chen B , Lee T, Robust controller design for piezoelectric actuator with hysteresis, IEEE Transaction Contr. Syst. Technol., Vol.40, pp160-174, Mar 1999

32. .Comsteck R.H, Charge Control of Piezoelectric Actuators to Reduce the Hysteresis Effects, U.S. Patent 4 2263527, 1981

33. Rao S and Sunar M, Piezoelectricity and its use in disturbance, Appl Mech Rev vol 47, no 4, pp 113-118, April 1994

34. Clark R.L, Flemming M.R., C.R. Fuller, Piezoelectric Actuators for Distributed Vibration Excitations of Thin Plates: A Comparison Between Theory and Experiment, Journal of Vibration and Acoustics, Vol.115, July 1993

35. Nakajima S. and Cetinkunt S., Design , fabrication and real-time network control of a piezoelectric actuated tool post, ASME Dynamic System and Control , IMECE-95 vol 57, pp 767-772, 1995

36. Sang-Soon Ku, Ge P. and Jounaneh M, Modeling hysteresis in piezoceramics actuators, Precision Eng., vol 17, pp 211-221, 1995

37. Miller Scott E., Dr. Hubbard James ,Smart Components for Structural Vibration Control, Appl. Mech Rev Vol.51, No.8, August 1998

38. Madill TD.R and Wang D, Modeling and L2-Stability of a Shape Memory Alloy Position Control System, IEEE Trans. Contr. Syst. Technol. Vol.6, pp 473-481, July 1998

39. Shrout R. Thomas , Relaxor Based Ferroelectric Single Crystals for Electro-Mechanical Actuators, Springer-Verlag, 1997

40. Merz W.J., Pozzi M, Dynamic characteristic of piezoelectric multilayer actuators, Recent Advances Mechatron Conf., pp461-466, 1999

41. Furuhata Y. and Toriyama K., Applied Physics Lett 23, pp 361-363, 1973

42. Yuhuan Xu, Ferroelectric Materials and Their Applications, University of California Los Angeles, CA, USA, 1991

43. Piezo.System inc. Cambridge MA 02139. Design and prototyping tools, Product Catalog, 2002

44. Institut Mitutoyo de Métrologie France, Catalogue Micrometres . 2002

ANNEX 1

Calibration of the Piezoelectric Actuator

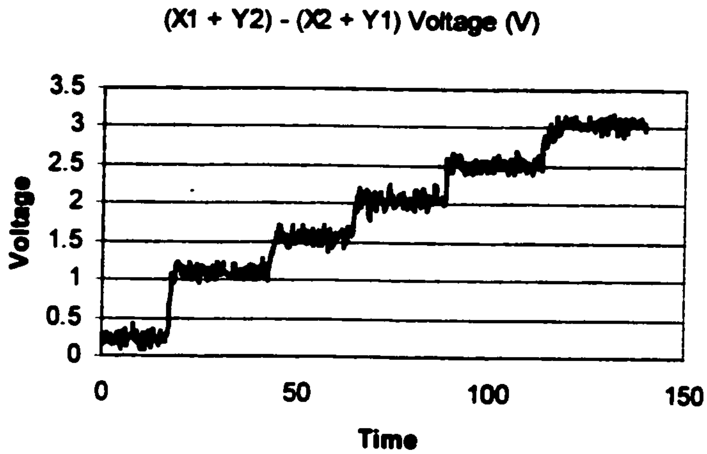

1st Step calibration, direction and displacement of the piezoelectric actuator

Time (s)	Voltage (V)
0.2	0.292969
0.397	0.273438
0.597	0.161133
0.799	0.244141
1.001	0.175781
1.201	0.27832
1.401	0.307617
1.599	0.175781
1.801	0.224609
2.001	0.180664
2.201	0.253906
2.4	0.268555
2.598	0.288086
2.798	0.151367
2.997	0.15625
3.195	0.219727
3.394	0.180664

3.592	0.161133
3.792	0.170898
3.991	0.302734
4.19	0.224609
4.39	0.146484
4.588	0.317383
4.786	0.229492
4.984	0.073242
5.183	0.15625
5.381	0.34668
5.58	0.185547
5.778	0.195313
5.978	0.327148
6.177	0.361328
6.377	0.136719
6.575	0.126953
6.773	0.27832
6.973	0.244141
7.172	0.205078
7.37	0.244141
7.569	0.292969
7.766	0.263672
7.965	0.292969
8.164	0.424805
8.361	0.258789
8.597	0.195313
8.795	0.224609
8.994	0.332031
9.193	0.180664
9.39	0.209961
9.589	0.263672
9.787	0.161133
9.984	0.087891
10.184	0.175781
10.382	0.229492
10.58	0.234375
10.781	0.249023
10.981	0.297852
11.184	0.166016
11.386	0.083008
11.588	0.27832
11.789	0.268555
11.99	0.307617
12.193	0.322266
12.394	0.253906
12.596	0.175781
12.797	0.185547
13	0.097656
13.203	0.224609
13.401	0.351563

13.602	0.229492
13.803	0.205078
14.004	0.229492
14.206	0.219727
14.408	0.200195
14.611	0.126953
14.812	0.205078
15.013	0.219727
15.214	0.34668
15.414	0.180664
Average	0.227113

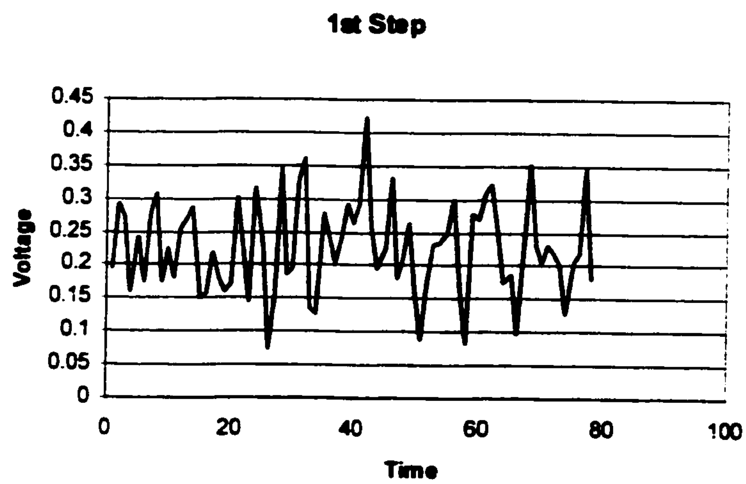

1st Step calibration, direction and displacement of the piezoelectric actuator

2nd Step calibration, direction and displacement of the piezoelectric actuator

Time (s)	Voltage (V)
20.232	1.196289
20.431	1.196289
20.628	1.054688
20.827	1.152344
21.026	1.142578
21.224	1.064453
21.424	1.025391
21.624	1.166992
21.822	1.069336
22.022	1.152344
22.221	0.996094
22.421	1.142578
22.618	1.225586
22.817	1.147461
23.016	0.996094
23.214	1.030273
23.414	1.030273
23.611	0.991211
23.809	1.113281
24.008	1.108398
24.206	1.162109
24.405	1.079102
24.605	1.210938
24.802	1.069336
25	0.942383
25.2	1.113281
25.399	1.142578
25.597	1.05957
25.795	1.171875
25.993	1.171875
26.192	1.098633
26.391	1.098633
26.589	1.098633
26.789	1.12793
26.986	0.966797
27.186	1.147461
27.43	1.010742
27.627	1.044922
27.824	1.09375
28.024	1.025391
28.222	1.123047
28.421	1.186523
28.619	1.088867
28.817	1.079102
29.015	1.064453
29.213	0.996094
29.413	1.000977

29.613	1.064453
29.81	1.225586
30.007	1.191406
30.206	1.108398
30.404	1.079102
30.602	1.088867
30.8	1.064453
30.998	1.176758
31.195	1.245117
31.394	1.123047
31.594	1.079102
31.795	1.103516
31.998	1.049805
32.2	1.074219
32.402	1.054688
32.602	1.054688
32.803	1.079102
33.004	1.064453
33.205	1.030273
33.406	1.020508
33.608	1.09375
33.808	1.137695
34.009	1.210938
34.21	1.206055
34.41	1.123047
34.613	1.030273
34.814	1.030273
35.015	1.035156
35.216	1.083984
35.418	1.123047
35.618	1.132813
35.817	1.09375
36.018	1.040039
36.219	1.000977
36.42	1.137695
36.62	1.147461
36.819	1.113281
37.021	1.064453
37.223	1.030273
37.422	1.157227
37.62	1.137695
37.825	1.220703
38.021	1.132813
38.216	1.196289
38.414	1.015625
38.609	1.12793
38.806	1.181641
39.003	0.996094
39.199	1.079102
39.395	1.010742

39.594	1.079102
39.791	1.157227
39.989	1.040039
40.186	1.12793
40.383	1.191406
Average	1.098775

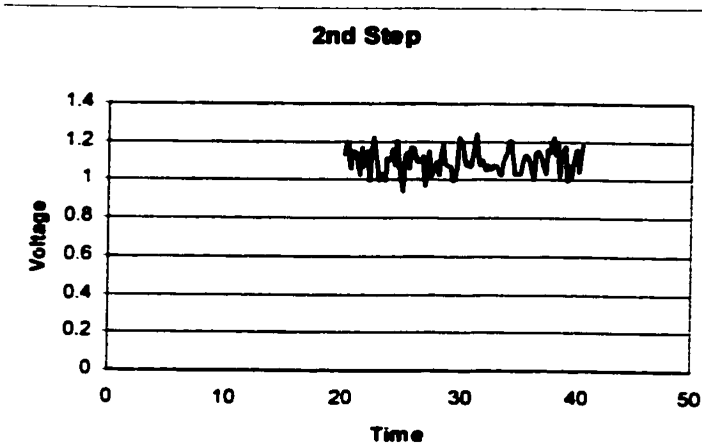

2nd Step calibration, direction and displacement of the piezoelectric actuator

3rd Step calibration, direction and displacement of the piezoelectric actuator

Time (s)	Voltage (V)
43.141	1.279297
43.339	1.376953
43.536	1.342773
43.733	1.352539
43.93	1.494141
44.129	1.455078
44.328	1.552734
44.524	1.611328
44.724	1.601563
44.921	1.616211
45.119	1.713867
45.318	1.708984
45.516	1.669922
45.715	1.523438
45.914	1.621094
46.114	1.577148
46.314	1.5625
46.513	1.503906
46.712	1.572266
46.91	1.586914
47.112	1.450195
47.313	1.508789
47.511	1.513672
47.71	1.425781
47.908	1.508789
48.109	1.52832
48.309	1.508789
48.507	1.713867
48.703	1.542969
48.899	1.542969
49.097	1.52832
49.294	1.464844
49.491	1.59668
49.689	1.513672
49.886	1.494141
50.082	1.640625
50.279	1.655273
50.477	1.503906
50.672	1.494141
50.87	1.489258
51.066	1.650391
51.263	1.71875
51.46	1.489258
51.656	1.59668
51.852	1.625977
52.049	1.557617
52.248	1.640625

52.445	1.474609
52.641	1.538086
52.837	1.52832
53.034	1.484375
53.23	1.586914
53.428	1.577148
53.624	1.665039
53.82	1.450195
54.017	1.518555
54.213	1.572266
54.41	1.455078
54.608	1.591797
54.805	1.572266
55.001	1.557617
55.198	1.650391
55.395	1.44043
55.591	1.616211
55.788	1.601563
55.983	1.630859
56.18	1.611328
56.377	1.44043
56.574	1.733398
56.771	1.489258
56.967	1.508789
57.166	1.601563
57.364	1.547852
57.561	1.616211
57.757	1.635742
57.953	1.367188
58.151	1.68457
58.348	1.547852
58.544	1.572266
58.741	1.503906
58.937	1.40625
59.134	1.591797
59.331	1.508789
59.527	1.479492
59.726	1.611328
59.922	1.523438
60.118	1.59668
60.315	1.577148
60.512	1.552734
60.71	1.606445
60.907	1.586914
61.106	1.630859
61.305	1.645508
61.504	1.660156
61.703	1.533203
61.902	1.484375
62.102	1.40625

62.3	1.640625
62.5	1.577148
62.699	1.469727
Average	1.547948

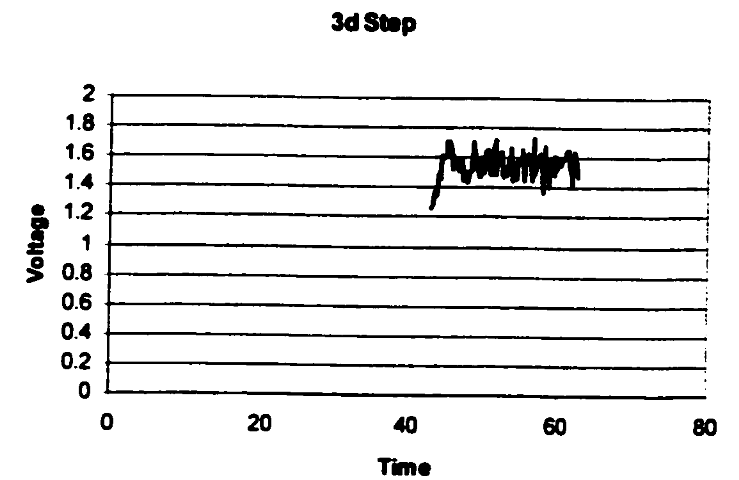

3rd Step calibration, direction and displacement of the piezoelectric actuator

4[th] Step calibration, direction and displacement of the piezoelectric actuator

Time (s)	Voltage (V)
68.257	2.084961
68.456	2.084961
68.654	2.167969
68.852	1.831055
69.051	1.777344
69.251	2.03125
69.45	2.06543
69.649	2.016602
69.848	1.99707
70.046	2.172852
70.246	2.172852
70.446	1.904297
70.644	1.992188
70.843	2.119141
71.041	2.089844
71.241	2.084961
71.445	2.109375
71.643	2.15332
71.842	2.133789
72.04	2.016602
72.241	2.050781
72.441	2.016602
72.639	2.055664
72.838	1.914063
73.036	1.987305
73.236	2.011719
73.435	1.992188
73.633	2.016602
73.832	2.138672
74.03	2.275391
74.23	2.15332
74.43	2.207031
74.631	2.050781
74.829	2.114258
75.028	2.104492
75.227	2.021484
75.427	1.958008
75.626	1.987305
75.825	2.06543
76.025	2.001953
76.224	2.016602
76.423	2.03125
76.622	2.084961
76.82	2.138672
77.019	2.06543
77.22	2.114258
77.42	2.099609

77.618	2.167969
77.817	1.992188
78.016	1.967773
78.215	2.094727
78.414	2.060547
78.612	1.972656
78.811	1.938477
79.008	2.03125
79.208	1.958008
79.407	1.958008
79.607	2.060547
79.804	2.080078
80.002	1.987305
80.202	2.050781
80.4	2.06543
80.599	1.967773
80.797	1.904297
80.995	2.182617
81.193	2.177734
81.392	2.041016
81.591	2.06543
81.79	2.15332
81.987	2.03125
82.188	1.967773
82.387	1.977539
82.584	1.992188
82.781	1.987305
82.98	2.128906
83.177	2.211914
83.377	2.099609
83.575	2.055664
83.773	2.109375
83.971	2.084961
84.17	1.904297
84.37	1.972656
84.572	2.114258
84.774	2.070313
84.974	2.104492
85.174	2.094727
85.375	2.016602
85.576	2.026367
85.777	2.099609
85.977	2.216797
86.178	2.270508
86.38	2.231445
86.581	2.070313
86.782	2.041016
86.981	2.041016
87.184	2.070313
87.386	2.026367

87.628	2.045898
87.826	2.041016
88.027	2.026367
88.231	2.104492
88.429	2.055664
88.629	1.982422
Average	2.057354

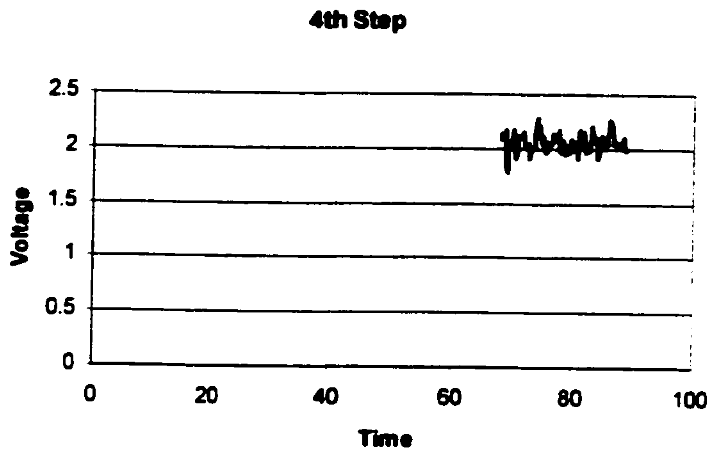

Figure 5.7: 4th Step calibration, direction and displacement of the piezoelectric actuator

5th Step calibration, direction and displacement of the piezoelectric actuator

Time (s)	Voltage (V)
92.218	2.661133
92.417	2.602539
92.614	2.509766
92.811	2.475586
93.008	2.5
93.207	2.490234
93.405	2.480469
93.602	2.402344
93.8	2.553711
93.997	2.475586
94.194	2.543945
94.394	2.519531
94.591	2.431641
94.789	2.431641
94.985	2.543945
95.182	2.490234
95.38	2.539063
95.578	2.539063
95.775	2.387695
95.972	2.485352
96.169	2.524414
96.368	2.597656
96.565	2.558594
96.763	2.416992
96.959	2.495117
97.158	2.529297
97.356	2.548828
97.554	2.495117
97.751	2.568359
97.948	2.412109
98.145	2.578125
98.343	2.558594
98.541	2.504883
98.737	2.543945
98.935	2.490234
99.131	2.519531
99.329	2.563477
99.527	2.426758
99.724	2.46582
99.92	2.519531
100.117	2.529297
100.315	2.583008
100.512	2.451172
100.71	2.412109
100.906	2.617188
101.102	2.426758
101.3	2.602539

101.498	2.563477
101.695	2.470703
101.891	2.573242
102.087	2.641602
102.286	2.480469
102.484	2.5
102.68	2.480469
102.877	2.509766
103.074	2.568359
103.272	2.46582
103.471	2.46582
103.667	2.583008
103.865	2.509766
104.061	2.514648
104.258	2.382813
104.456	2.446289
104.654	2.524414
104.852	2.519531
105.048	2.602539
105.244	2.602539
105.443	2.543945
105.639	2.509766
105.837	2.592773
106.033	2.402344
106.23	2.509766
106.428	2.53418
106.625	2.695313
106.822	2.626953
107.017	2.509766
107.214	2.573242
107.412	2.607422
107.608	2.446289
107.803	2.514648
107.998	2.592773
108.194	2.553711
108.393	2.573242
108.592	2.53418
108.791	2.460938
108.99	2.407227
109.189	2.524414
109.387	2.451172
109.585	2.529297
109.785	2.558594
109.984	2.519531
110.183	2.480469
110.382	2.509766
110.58	2.504883
110.776	2.382813
110.974	2.519531
111.172	2.592773

111.37	2.573242
111.569	2.602539
111.763	2.5
111.96	2.460938
112.158	2.646484
Average	2.519199

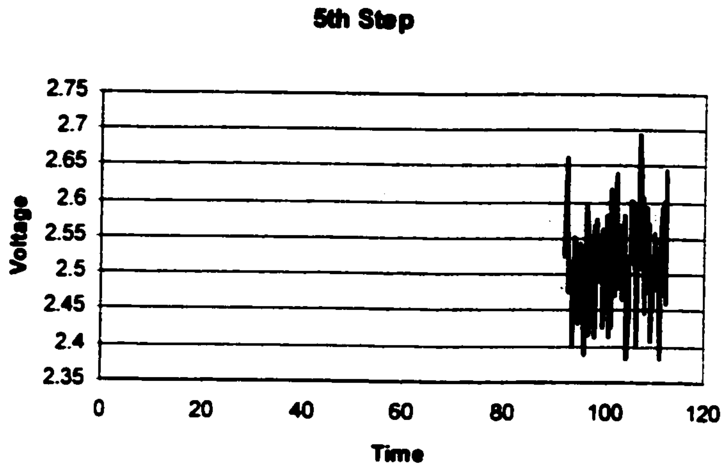

5^{th} Step calibration, direction and displacement of the piezoelectric actuator

6th Step calibration, direction and displacement of the piezoelectric actuator

Time (s)	Voltage (V)
119.362	3.110352
119.562	3.061523
119.762	3.061523
119.962	3.046875
120.161	3.066406
120.361	3.139648
120.561	3.115234
120.761	3.00293
120.96	3.144531
121.161	3.125
121.36	3.154297
121.561	3.110352
121.761	3.081055
121.961	3.066406
122.163	3.007813
122.364	3.076172
122.564	3.056641
122.764	2.978516
122.964	3.037109
123.164	3.061523
123.364	3.046875
123.566	3.017578
123.766	3.032227
123.966	3.017578
124.166	3.046875
124.367	2.988281
124.568	3.051758
124.769	3.056641
124.97	3.154297
125.169	3.00293
125.369	3.007813
125.571	3.012695
125.77	3.076172
125.971	3.051758
126.171	3.037109
126.372	2.963867
126.573	3.085938
126.774	3.085938
126.974	3.056641
127.176	3.095703
127.377	3.110352
127.578	3.071289
127.778	3.134766
127.979	2.96875
128.179	2.910156
128.38	3.022461
128.582	3.041992

128.782	3.144531
128.982	3.100586
129.183	3.022461
129.383	2.93457
129.585	2.958984
129.787	3.115234
129.987	3.154297
130.187	3.061523
130.388	3.061523
130.589	3.046875
130.788	3.061523
130.987	3.178711
131.186	3.09082
131.385	3.007813
131.586	3.032227
131.785	3.041992
131.984	3.115234
132.184	2.915039
132.381	3.041992
132.581	3.144531
132.778	3.071289
132.975	3.120117
133.172	3.120117
133.37	2.885742
133.574	3.061523
133.773	2.993164
133.974	3.115234
134.174	3.134766
134.379	3.041992
134.585	2.924805
134.788	3.017578
134.987	3.110352
135.19	3.110352
135.393	3.046875
135.597	3.129883
135.8	3.085938
136.002	3.134766
136.202	3.071289
136.403	3.076172
136.607	3.100586
136.807	3.051758
137.008	3.032227
137.211	3.081055
137.414	3.085938
137.616	3.115234
137.816	3.125
138.016	3.129883
138.217	3.100586
138.421	3.115234
138.62	3.037109

138.819	3.071289
139.022	3.056641
139.227	2.954102
Average	3.062394

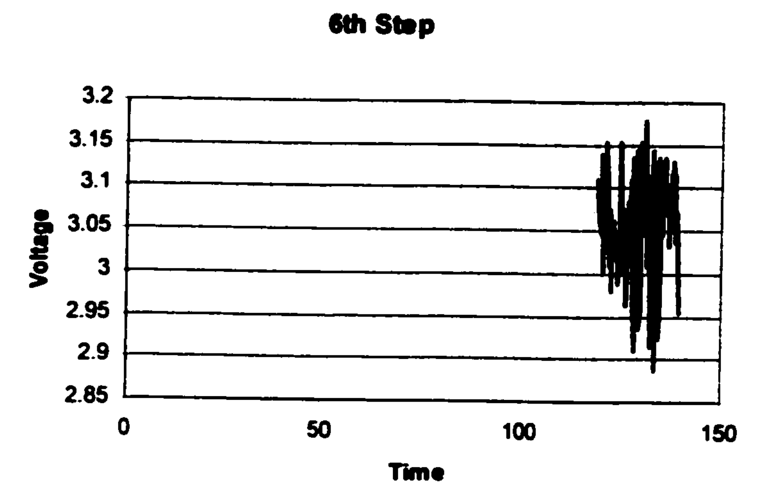

6th Step calibration, direction and displacement of the piezoelectric actuator

ANNEX 2.1

Measurement at 30 V

For the first measurement at 30 V, the recorded result is 0.342627+/- 0.16 quad-cell voltage.

:

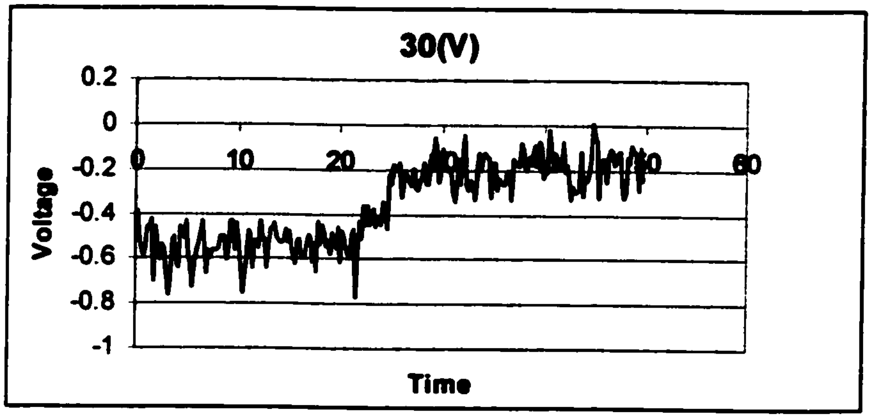

1[st] Measurement at 30 V

(X1 + Y1) - (X2 + Y2)

Time (s)	Voltage (V)
0.001	-0.41992
0.2	-0.38574
0.399	-0.50781
0.6	-0.55664
0.802	-0.59082
1.003	-0.54688
1.203	-0.45898
1.405	-0.4541
1.606	-0.4248
1.808	-0.69824
2.011	-0.4541
2.213	-0.55176
2.415	-0.60547
2.618	-0.53223
2.821	-0.56152
3.024	-0.7666
3.226	-0.68848

3.427	-0.51758
3.632	-0.50293
3.834	-0.62012
4.036	-0.64453
4.237	-0.4541
4.438	-0.49316
4.642	-0.5127
4.844	-0.43457
5.044	-0.58594
5.246	-0.625
5.448	-0.73242
5.651	-0.61035
5.854	-0.57129
6.056	-0.53711
6.258	-0.48828
6.459	-0.42969
6.661	-0.54688
6.863	-0.66406
7.065	-0.56152
7.266	-0.5957
7.465	-0.56641
7.668	-0.56641
7.87	-0.56152
8.073	-0.55176
8.274	-0.50293
8.475	-0.49805
8.679	-0.60547
8.883	-0.55664
9.083	-0.42969
9.283	-0.42969
9.485	-0.56152
9.685	-0.43945
9.888	-0.54199
10.089	-0.63477
10.289	-0.75684
10.492	-0.66406
10.694	-0.60059
10.898	-0.47852
11.101	-0.49805
11.304	-0.64453
11.505	-0.52246
11.706	-0.51758
11.908	-0.55176
12.111	-0.43457
12.312	-0.52246
12.514	-0.50781
12.717	-0.63965
12.922	-0.53711
13.123	-0.46387
13.324	-0.46875

13.525	-0.43945
13.728	-0.49805
13.931	-0.52734
14.133	-0.52734
14.336	-0.52246
14.536	-0.46875
14.737	-0.52734
14.939	-0.47363
15.14	-0.54688
15.343	-0.5957
15.545	-0.62012
15.749	-0.51758
15.954	-0.50781
16.155	-0.57617
16.358	-0.59082
16.559	-0.59082
16.762	-0.53711
16.964	-0.49316
17.165	-0.50781
17.364	-0.61523
17.565	-0.52734
17.767	-0.6543
17.97	-0.42969
18.173	-0.53711
18.372	-0.44922
18.574	-0.4834
18.775	-0.54688
18.977	-0.52246
19.177	-0.57617
19.38	-0.4834
19.582	-0.55664
19.783	-0.4541
19.986	-0.61035
20.188	-0.47852
20.389	-0.50781
20.589	-0.55176
20.79	-0.58105
20.991	-0.60059
21.193	-0.48828
21.396	-0.46875
21.598	-0.77148
21.797	-0.55664
21.996	-0.43457
22.195	-0.5127
22.394	-0.35645
22.593	-0.44434
22.792	-0.36133
22.994	-0.44434
23.192	-0.40039
23.39	-0.37598

23.589	-0.45898
23.79	-0.41016
23.991	-0.41016
24.19	-0.44434
24.388	-0.34668
24.588	-0.37598
24.79	-0.46387
24.994	-0.22461
25.193	-0.26367
25.393	-0.18066
25.592	-0.20508
25.793	-0.20508
25.994	-0.16602
26.191	-0.32227
26.39	-0.25879
26.589	-0.20996
26.787	-0.25879
26.987	-0.27344
27.186	-0.19043
27.385	-0.2832
27.584	-0.28809
27.783	-0.24414
27.983	-0.23438
28.184	-0.1709
28.383	-0.26855
28.583	-0.26367
28.784	-0.15137
28.983	-0.19531
29.184	-0.05371
29.384	-0.10742
29.582	-0.25391
29.782	-0.2002
29.983	-0.10254
30.184	-0.16602
30.381	-0.2002
30.578	-0.19531
30.775	-0.21973
30.976	-0.30762
31.174	-0.34668
31.374	-0.25879
31.572	-0.15137
31.77	-0.26367
31.968	-0.1416
32.167	-0.04883
32.365	-0.26855
32.563	-0.29297
32.76	-0.24902
32.961	-0.26855
33.161	-0.33691
33.36	-0.22949

33.559	-0.12695
33.757	-0.2002
33.958	-0.13672
34.157	-0.12207
34.356	-0.1416
34.555	-0.14648
34.753	-0.32715
34.954	-0.1709
35.153	-0.16602
35.352	-0.29297
35.551	-0.23926
35.749	-0.26855
35.949	-0.26367
36.15	-0.20996
36.351	-0.2002
36.549	-0.33691
36.747	-0.15137
36.946	-0.18066
37.146	-0.18066
37.346	-0.18555
37.545	-0.07813
37.744	-0.10254
37.945	-0.19043
38.145	-0.20508
38.345	-0.1416
38.543	-0.16113
38.742	-0.12695
38.943	-0.08789
39.144	-0.18555
39.343	-0.07324
39.543	-0.09766
39.742	-0.23438
39.942	-0.20996
40.143	-0.21484
40.343	-0.01953
40.542	-0.1123
40.741	-0.16602
40.942	-0.19043
41.145	-0.19043
41.346	-0.15137
41.545	-0.19043
41.745	-0.07324
41.947	-0.21484
42.149	-0.17578
42.35	-0.24414
42.551	-0.33203
42.75	-0.27344
42.951	-0.29785
43.153	-0.29297
43.353	-0.11719

43.552	-0.3125
43.751	-0.22949
43.955	-0.24414
44.157	-0.21484
44.358	-0.14648
44.558	0.004883
44.759	-0.04883
44.959	-0.07324
45.159	-0.32227
45.359	-0.1709
45.561	-0.14648
45.762	-0.15137
45.965	-0.25391
46.168	-0.13672
46.372	-0.10254
46.574	-0.11719
46.776	-0.18066
46.98	-0.1709
47.183	-0.12207
47.387	-0.11719
47.589	-0.26855
47.792	-0.32715
47.994	-0.30273
48.198	-0.1416
48.397	-0.1709
48.598	-0.09277
48.799	-0.12207
49.003	-0.13184
49.203	-0.29297
49.405	-0.09766
49.608	-0.24902

Column1	
Mean	-0.53301
Standard Error	0.007589
Median	-0.52734
Mode	-0.50781
Standard Deviation	0.082437
Sample Variance	0.006796
Kurtosis	0.510605
Skewness	-0.51138
Range	0.415039
Minimum	-0.77148
Maximum	-0.35645
Sum	-62.8955
Count	118

Column2	
Mean	-0.19039
Standard Error	0.00741
Median	-0.18555
Mode	-0.1709
Standard Deviation	0.078071
Sample Variance	0.006095
Kurtosis	-0.58726
Skewness	-0.00362
Range	0.351563
Minimum	-0.34668
Maximum	0.004883
Sum	-21.1328
Count	111

0.342627 (+/-.016)

For the second measurement at 30 V, the recorded result is 0.3258933+/- 0.16 quad-cell voltage.

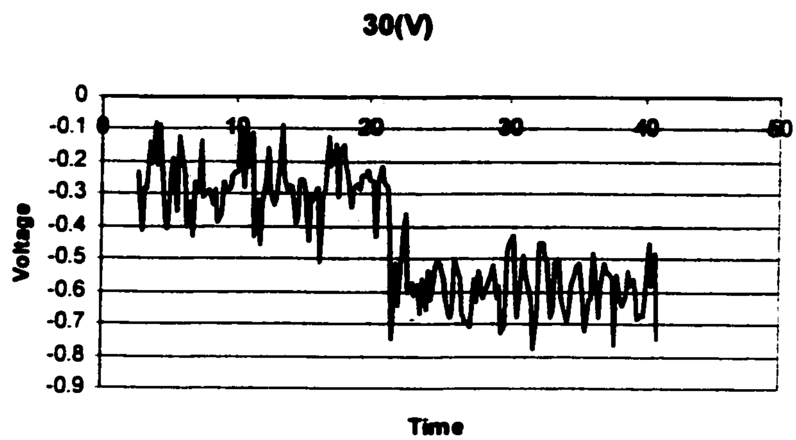

2nd Measurement at 30V

(X1 + Y1) - (X2 + Y2)

Time (s)	Voltage (V)
0.001	-0.3125
0.201	-0.25391
0.399	-0.31738
0.598	-0.39551
0.802	-0.26855
1.003	-0.13672
1.203	-0.15625
1.403	-0.24902
1.602	-0.34668
1.804	-0.24902
2.008	-0.27344
2.211	-0.33203
2.414	-0.39063
2.618	-0.24414
2.821	-0.22949
3.025	-0.41504
3.228	-0.27832
3.431	-0.28809
3.634	-0.1416
3.835	-0.20508

4.036	-0.07813
4.236	-0.21484
4.439	-0.08789
4.641	-0.28809
4.842	-0.38086
5.043	-0.40527
5.244	-0.22949
5.445	-0.18555
5.645	-0.35156
5.848	-0.12207
6.051	-0.16602
6.253	-0.24414
6.453	-0.40039
6.656	-0.32227
6.858	-0.42969
7.061	-0.26367
7.261	-0.2832
7.462	-0.13672
7.664	-0.30762
7.866	-0.29297
8.066	-0.2832
8.267	-0.33691
8.467	-0.28809
8.668	-0.39063
8.87	-0.36133
9.071	-0.25879
9.271	-0.28809
9.472	-0.2832
9.673	-0.24414
9.873	-0.22949
10.076	-0.22949
10.276	-0.09277
10.476	-0.27832
10.676	-0.09766
10.876	-0.21973
11.079	-0.1123
11.28	-0.42969
11.481	-0.31738
11.683	-0.4541
11.884	-0.32715
12.087	-0.24902
12.288	-0.16113
12.487	-0.2832
12.687	-0.33691
12.886	-0.30762
13.087	-0.2002
13.288	-0.08789
13.488	-0.24902
13.685	-0.29297
13.884	-0.27344

14.084	-0.27832
14.283	-0.39551
14.484	-0.37109
14.685	-0.25391
14.883	-0.25391
15.083	-0.2832
15.281	-0.44434
15.483	-0.30273
15.683	-0.32227
15.884	-0.2832
16.084	-0.27832
16.284	-0.5127
16.486	-0.29785
16.686	-0.2832
16.887	-0.12207
17.092	-0.21484
17.29	-0.2002
17.489	-0.14648
17.688	-0.3125
17.887	-0.16602
18.089	-0.14648
18.293	-0.20996
18.492	-0.23438
18.692	-0.3418
18.893	-0.27832
19.093	-0.26855
19.294	-0.28809
19.492	-0.24414
19.689	-0.24414
19.889	-0.22461
20.088	-0.25391
20.287	-0.25879
20.483	-0.43457
20.683	-0.26855
20.883	-0.21484
21.084	-0.25879
21.285	-0.27832
21.484	-0.41992
21.684	-0.74707
21.882	-0.5127
22.082	-0.64453
22.28	-0.55176
22.478	-0.40527
22.676	-0.36133
22.875	-0.60059
23.074	-0.57129
23.274	-0.61523
23.472	-0.57617
23.671	-0.66895
23.869	-0.55664

24.069	-0.6543
24.267	-0.53711
24.466	-0.625
24.666	-0.52246
24.864	-0.50293
25.063	-0.50781
25.262	-0.55664
25.461	-0.625
25.659	-0.67871
25.856	-0.6543
26.054	-0.49805
26.252	-0.54199
26.451	-0.55664
26.649	-0.66895
26.845	-0.69824
27.045	-0.69336
27.244	-0.71289
27.442	-0.55664
27.639	-0.63477
27.836	-0.53711
28.035	-0.62012
28.233	-0.5957
28.43	-0.58594
28.628	-0.54688
28.825	-0.51758
29.023	-0.62012
29.221	-0.58594
29.419	-0.72754
29.618	-0.70801
29.815	-0.47852
30.012	-0.4541
30.211	-0.4248
30.409	-0.57617
30.606	-0.68359
30.802	-0.55176
31	-0.48828
31.199	-0.54688
31.398	-0.60059
31.594	-0.63477
31.791	-0.77637
31.99	-0.66406
32.189	-0.44922
32.386	-0.44922
32.584	-0.49805
32.781	-0.50293
32.98	-0.68359
33.179	-0.65918
33.376	-0.50781
33.574	-0.50293
33.771	-0.62012

33.969	-0.64453
34.168	-0.69336
34.366	-0.66406
34.565	-0.58105
34.762	-0.54199
34.96	-0.51758
35.158	-0.5127
35.356	-0.63477
35.552	-0.72266
35.748	-0.625
35.946	-0.62012
36.146	-0.4834
36.343	-0.60059
36.541	-0.67871
36.738	-0.57617
36.935	-0.50781
37.136	-0.54199
37.333	-0.54199
37.53	-0.56152
37.726	-0.7666
37.923	-0.54688
38.125	-0.625
38.324	-0.64453
38.524	-0.61035
38.723	-0.53711
38.923	-0.58594
39.124	-0.56152
39.324	-0.60059
39.524	-0.68848
39.726	-0.66895
39.927	-0.67383
40.131	-0.60547
40.335	-0.44922
40.537	-0.58105
40.737	-0.47852
40.94	-0.74707

Column1	
Mean	-0.26885
Standard Error	0.009007
Median	-0.27832
Mode	-0.2832
Standard Deviation	0.089622
Sample Variance	0.008032
Kurtosis	0.005901
Skewness	0.002996
Range	0.43457
Minimum	-0.5127
Maximum	-0.07813
Sum	-26.6162
Count	99

Column1	
Mean	-0.59416
Standard Error	0.009279
Median	-0.5957
Mode	-0.54199
Standard Deviation	0.082478
Sample Variance	0.006803
Kurtosis	-0.69819
Skewness	-0.0509
Range	0.351563
Minimum	-0.77637
Maximum	-0.4248
Sum	-46.9385
Count	79

-0.268264619

-0.59416 0.3258933

For the third measurement at 30 V, the recorded result is 0.31189 +/- 0.16 quad-cell voltage.

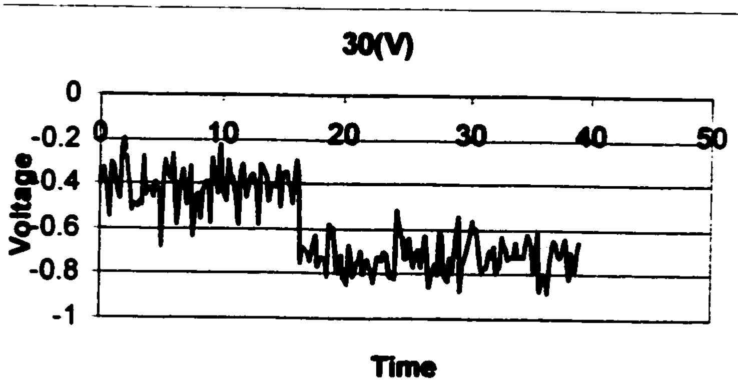

3rd Measurement at 30V

(X1 + Y1) - (X2 + Y2)

Time (s)	Voltage (V)
0	-0.41016
0.2	-0.34668
0.398	-0.32715
0.6	-0.44434
0.801	-0.54688
1	-0.30273
1.199	-0.32227
1.398	-0.42969
1.599	-0.46875
1.798	-0.23926
1.999	-0.19531
2.199	-0.34668
2.399	-0.41992
2.602	-0.52246
2.803	-0.48828
3.004	-0.50293
3.204	-0.47852
3.405	-0.49316
3.607	-0.27344
3.808	-0.4541
4.011	-0.41992
4.214	-0.41992
4.419	-0.46387
4.625	-0.38574
4.828	-0.42969
5.03	-0.67871
5.235	-0.39551
5.438	-0.28809
5.644	-0.36621
5.847	-0.38086
6.05	-0.26855
6.254	-0.58105
6.458	-0.45898
6.663	-0.40039
6.866	-0.33691
7.071	-0.49805
7.276	-0.41504
7.479	-0.31738
7.684	-0.63477
7.89	-0.44922
8.094	-0.44434
8.298	-0.55664
8.501	-0.42969
8.706	-0.39063
8.909	-0.39063
9.113	-0.57129
9.317	-0.2832

9.522	-0.38574
9.727	-0.44434
9.93	-0.22461
10.133	-0.41504
10.336	-0.47363
10.541	-0.28809
10.744	-0.36133
10.947	-0.37598
11.148	-0.45898
11.351	-0.58594
11.556	-0.3418
11.759	-0.3125
11.965	-0.46387
12.165	-0.41016
12.37	-0.37109
12.574	-0.35645
12.777	-0.41992
12.979	-0.58105
13.184	-0.3125
13.387	-0.32715
13.591	-0.37109
13.793	-0.47852
13.997	-0.4248
14.2	-0.40039
14.402	-0.41992
14.605	-0.32227
14.809	-0.50293
15.011	-0.35156
15.213	-0.3418
15.415	-0.40039
15.617	-0.41504
15.819	-0.4834
16.023	-0.28809
16.224	-0.35645
16.422	-0.75195
16.623	-0.68359
16.825	-0.70313
17.028	-0.70801
17.229	-0.74707
17.43	-0.69824
17.631	-0.625
17.833	-0.7666
18.034	-0.74707
18.237	-0.72266
18.437	-0.73242
18.638	-0.81055
18.839	-0.57129
19.038	-0.5957
19.237	-0.5957
19.435	-0.78613

19.635	-0.80078
19.835	-0.71289
20.035	-0.81055
20.233	-0.84961
20.432	-0.67383
20.63	-0.71289
20.83	-0.81543
21.029	-0.75195
21.262	-0.74219
21.461	-0.69824
21.659	-0.80566
21.859	-0.7373
22.059	-0.77148
22.257	-0.77637
22.455	-0.83984
22.653	-0.72266
22.855	-0.72266
23.053	-0.74219
23.251	-0.69824
23.451	-0.70801
23.649	-0.81055
23.848	-0.81543
24.045	-0.8252
24.243	-0.51758
24.44	-0.62988
24.64	-0.63965
24.836	-0.73242
25.03	-0.72754
25.225	-0.63477
25.422	-0.7666
25.62	-0.73242
25.819	-0.70313
26.017	-0.68848
26.215	-0.77148
26.412	-0.62988
26.61	-0.74707
26.808	-0.85449
27.008	-0.80078
27.206	-0.75195
27.403	-0.80566
27.6	-0.61035
27.8	-0.625
27.998	-0.80078
28.195	-0.83008
28.394	-0.72754
28.591	-0.79102
28.79	-0.71289
28.987	-0.54199
29.184	-0.87402
29.381	-0.76172

29.58	-0.7373
29.777	-0.69824
29.976	-0.62012
30.175	-0.56152
30.376	-0.61035
30.577	-0.59082
30.779	-0.75195
30.98	-0.79102
31.18	-0.7666
31.38	-0.77148
31.581	-0.68848
31.783	-0.72266
31.986	-0.66895
32.186	-0.80078
32.387	-0.75684
32.587	-0.62988
32.79	-0.67383
32.991	-0.68359
33.189	-0.7373
33.388	-0.71777
33.588	-0.72266
33.788	-0.65918
33.988	-0.72266
34.187	-0.71289
34.385	-0.72754
34.586	-0.66895
34.786	-0.61523
34.985	-0.67383
35.184	-0.79102
35.383	-0.69336
35.581	-0.61035
35.781	-0.87402
35.982	-0.7959
36.181	-0.80566
36.381	-0.88379
36.579	-0.74707
36.777	-0.64453
36.975	-0.66406
37.175	-0.69824
37.372	-0.72266
37.57	-0.71777
37.771	-0.63965
37.974	-0.71777
38.173	-0.82031
38.373	-0.69824
38.573	-0.78613
38.773	-0.68848
38.972	-0.65918

Column1	
Mean	-0.41127
Standard Error	0.010457
Median	-0.41504
Mode	-0.41992
Standard Deviation	0.092948
Sample Variance	0.008639
Kurtosis	0.361069
Skewness	-0.32273
Range	0.483398
Minimum	-0.67871
Maximum	-0.19531
Sum	-32.4902
Count	79

Column2	
Mean	-0.72316
Standard Error	0.007443
Median	-0.72266
Mode	-0.72266
Standard Deviation	0.076631
Sample Variance	0.005872
Kurtosis	-0.22541
Skewness	0.280339
Range	0.366211
Minimum	-0.88379
Maximum	-0.51758
Sum	-76.6553
Count	106

-0.31189 (+/-.16)

For the fourth measurement at 30 V, the recorded result is 0.373517 +/- 0.16 quad-cell voltage.

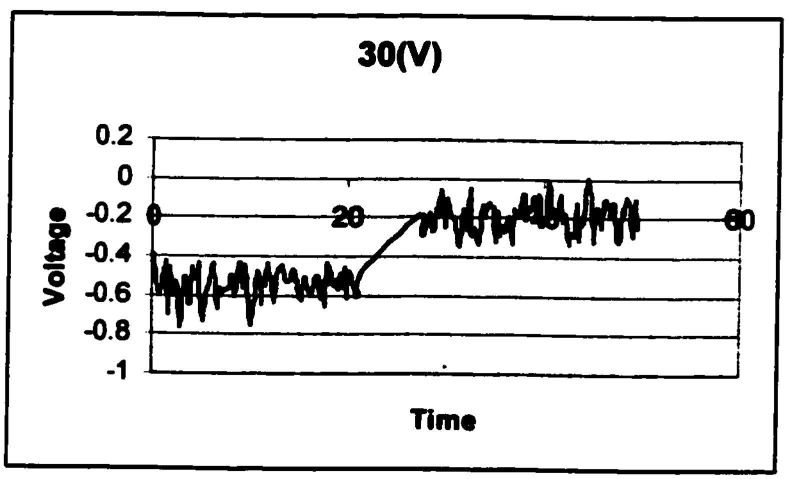

4th Measurement at 30 V

(X1 + Y1) - (X2 + Y2)

Time (s)	Voltage (V)
0.001	-0.41992
0.2	-0.38574
0.399	-0.50781
0.6	-0.55664
0.802	-0.59082
1.003	-0.54688
1.203	-0.45898
1.405	-0.4541
1.606	-0.4248
1.808	-0.69824
2.011	-0.4541
2.213	-0.55176
2.415	-0.60547
2.618	-0.53223
2.821	-0.56152
3.024	-0.7666
3.226	-0.68848
3.427	-0.51758
3.632	-0.50293
3.834	-0.62012
4.036	-0.64453
4.237	-0.4541
4.438	-0.49316
4.642	-0.5127
4.844	-0.43457
5.044	-0.58594
5.246	-0.625
5.448	-0.73242
5.651	-0.61035
5.854	-0.57129
6.056	-0.53711
6.258	-0.48828
6.459	-0.42969
6.661	-0.54688
6.863	-0.66406
7.065	-0.56152
7.266	-0.5957
7.465	-0.56641
7.668	-0.56641
7.87	-0.56152
8.073	-0.55176
8.274	-0.50293
8.475	-0.49805
8.679	-0.60547
8.883	-0.55664
9.083	-0.42969
9.283	-0.42969

9.485	-0.56152
9.685	-0.43945
9.888	-0.54199
10.089	-0.63477
10.289	-0.75684
10.492	-0.66406
10.694	-0.60059
10.898	-0.47852
11.101	-0.49805
11.304	-0.64453
11.505	-0.52246
11.706	-0.51758
11.908	-0.55176
12.111	-0.43457
12.312	-0.52246
12.514	-0.50781
12.717	-0.63965
12.922	-0.53711
13.123	-0.46387
13.324	-0.46875
13.525	-0.43945
13.728	-0.49805
13.931	-0.52734
14.133	-0.52734
14.336	-0.52246
14.536	-0.46875
14.737	-0.52734
14.939	-0.47363
15.14	-0.54688
15.343	-0.5957
15.545	-0.62012
15.749	-0.51758
15.954	-0.50781
16.155	-0.57617
16.358	-0.59082
16.559	-0.59082
16.762	-0.53711
16.964	-0.49316
17.165	-0.50781
17.364	-0.61523
17.565	-0.52734
17.767	-0.6543
17.97	-0.42969
18.173	-0.53711
18.372	-0.44922
18.574	-0.4834
18.775	-0.54688
18.977	-0.52246
19.177	-0.57617
19.38	-0.4834

19.582	-0.55664
19.783	-0.4541
19.986	-0.61035
20.188	-0.47852
20.389	-0.50781
20.589	-0.55176
20.79	-0.58105
20.991	-0.60059
21.193	-0.48828
27.186	-0.19043
27.385	-0.2832
27.584	-0.28809
27.783	-0.24414
27.983	-0.23438
28.184	-0.1709
28.383	-0.26855
28.583	-0.26367
28.784	-0.15137
28.983	-0.19531
29.184	-0.05371
29.384	-0.10742
29.582	-0.25391
29.782	-0.2002
29.983	-0.10254
30.184	-0.16602
30.381	-0.2002
30.578	-0.19531
30.775	-0.21973
30.976	-0.30762
31.174	-0.34668
31.374	-0.25879
31.572	-0.15137
31.77	-0.26367
31.968	-0.1416
32.167	-0.04883
32.365	-0.26855
32.563	-0.29297
32.76	-0.24902
32.961	-0.26855
33.161	-0.33691
33.36	-0.22949
33.559	-0.12695
33.757	-0.2002
33.958	-0.13672
34.157	-0.12207
34.356	-0.1416
34.555	-0.14648
34.753	-0.32715
34.954	-0.1709
35.153	-0.16602

35.352	-0.29297
35.551	-0.23926
35.749	-0.26855
35.949	-0.26367
36.15	-0.20996
36.351	-0.2002
36.549	-0.33691
36.747	-0.15137
36.946	-0.18066
37.146	-0.18066
37.346	-0.18555
37.545	-0.07813
37.744	-0.10254
37.945	-0.19043
38.145	-0.20508
38.345	-0.1416
38.543	-0.16113
38.742	-0.12695
38.943	-0.08789
39.144	-0.18555
39.343	-0.07324
39.543	-0.09766
39.742	-0.23438
39.942	-0.20996
40.143	-0.21484
40.343	-0.01953
40.542	-0.1123
40.741	-0.16602
40.942	-0.19043
41.145	-0.19043
41.346	-0.15137
41.545	-0.19043
41.745	-0.07324
41.947	-0.21484
42.149	-0.17578
42.35	-0.24414
42.551	-0.33203
42.75	-0.27344
42.951	-0.29785
43.153	-0.29297
43.353	-0.11719
43.552	-0.3125
43.751	-0.22949
43.955	-0.24414
44.157	-0.21484
44.358	-0.14648
44.558	0.004883
44.759	-0.04883
44.959	-0.07324
45.159	-0.32227

45.359	-0.1709
45.561	-0.14648
45.762	-0.15137
45.965	-0.25391
46.168	-0.13672
46.372	-0.10254
46.574	-0.11719
46.776	-0.18066
46.98	-0.1709
47.183	-0.12207
47.387	-0.11719
47.589	-0.26855
47.792	-0.32715
47.994	-0.30273
48.198	-0.1416
48.397	-0.1709
48.598	-0.09277
48.799	-0.12207
49.003	-0.13184
49.203	-0.29297
49.405	-0.09766
49.608	-0.24902

ANNEX 2.2

Measurement at 60 V

For the first measurement at 60 V, the recorded result is 0.51446+/- 0.16 quad-cell voltage.

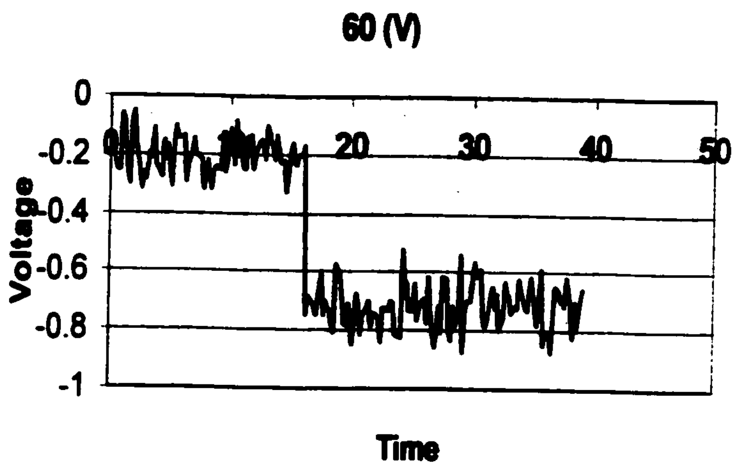

1st Measurement at 60 V

(X1 + Y2) - (X2 + Y1)

Time (s)	Voltage (V)
0	-0.20508
0.2	-0.13184
0.398	-0.2002
0.6	-0.24902
0.801	-0.25391
1	-0.05859
1.199	-0.08789
1.398	-0.26367
1.599	-0.30273
1.798	-0.08301
1.999	-0.04883
2.199	-0.1709
2.399	-0.26367
2.602	-0.31738
2.803	-0.26367
3.004	-0.28809
3.204	-0.19531
3.405	-0.20996

3.607	-0.10742
3.808	-0.23926
4.011	-0.24414
4.214	-0.27344
4.419	-0.15137
4.625	-0.21973
4.828	-0.16602
5.03	-0.30762
5.235	-0.1709
5.438	-0.10254
5.644	-0.1416
5.847	-0.14648
6.05	-0.13184
6.254	-0.29785
6.458	-0.23438
6.663	-0.19531
6.866	-0.1416
7.071	-0.20508
7.276	-0.2002
7.479	-0.21973
7.684	-0.32227
7.89	-0.26367
8.094	-0.21973
8.298	-0.32227
8.501	-0.26367
8.706	-0.24414
8.909	-0.24414
9.113	-0.24902
9.317	-0.12695
9.522	-0.25879
9.727	-0.22949
9.93	-0.10742
10.133	-0.15137
10.336	-0.23926
10.541	-0.08301
10.744	-0.18555
10.947	-0.2002
11.148	-0.24414
11.351	-0.25391
11.556	-0.14648
11.759	-0.13672
11.965	-0.24902
12.165	-0.20508
12.37	-0.17578
12.574	-0.15137
12.777	-0.16602
12.979	-0.21973
13.184	-0.09766
13.387	-0.16113
13.591	-0.17578

13.793	-0.21484
13.997	-0.13184
14.2	-0.22461
14.402	-0.22461
14.605	-0.21484
14.809	-0.32715
15.011	-0.20508
15.213	-0.15625
15.415	-0.22461
15.617	-0.23926
15.819	-0.2002
16.023	-0.2002
16.224	-0.1709
16.422	-0.75195
16.623	-0.68359
16.825	-0.70313
17.028	-0.70801
17.229	-0.74707
17.43	-0.69824
17.631	-0.5957
17.833	-0.74707
18.034	-0.69824
18.237	-0.72266
18.437	-0.73242
18.638	-0.81055
18.839	-0.57129
19.038	-0.5957
19.237	-0.5957
19.435	-0.77637
19.635	-0.78125
19.835	-0.70313
20.035	-0.74219
20.233	-0.84961
20.432	-0.67383
20.63	-0.71289
20.83	-0.81543
21.029	-0.75195
21.262	-0.72266
21.461	-0.69824
21.659	-0.78613
21.859	-0.7373
22.059	-0.75195
22.257	-0.77637
22.455	-0.83984
22.653	-0.72266
22.855	-0.72266
23.053	-0.73242
23.251	-0.69824
23.451	-0.70801
23.649	-0.81055

23.848	-0.81543
24.045	-0.8252
24.243	-0.51758
24.44	-0.62988
24.64	-0.63965
24.836	-0.73242
25.03	-0.72754
25.225	-0.63477
25.422	-0.7666
25.62	-0.73242
25.819	-0.70313
26.017	-0.68848
26.215	-0.77148
26.412	-0.61035
26.61	-0.74707
26.808	-0.85449
27.008	-0.80078
27.206	-0.71289
27.403	-0.80566
27.6	-0.61035
27.8	-0.625
27.998	-0.80078
28.195	-0.83008
28.394	-0.71777
28.591	-0.79102
28.79	-0.71289
28.987	-0.54199
29.184	-0.87402
29.381	-0.74219
29.58	-0.69824
29.777	-0.69824
29.976	-0.62012
30.175	-0.56152
30.376	-0.61035
30.577	-0.59082
30.779	-0.75195
30.98	-0.79102
31.18	-0.7666
31.38	-0.72266
31.581	-0.64941
31.783	-0.72266
31.986	-0.66895
32.186	-0.80078
32.387	-0.75684
32.587	-0.62988
32.79	-0.67383
32.991	-0.68359
33.189	-0.7373
33.388	-0.71777
33.588	-0.72266

33.788	-0.62012
33.988	-0.66406
34.187	-0.71289
34.385	-0.72754
34.586	-0.66895
34.786	-0.61523
34.985	-0.67383
35.184	-0.78125
35.383	-0.68359
35.581	-0.59082
35.781	-0.84473
35.982	-0.7959
36.181	-0.80566
36.381	-0.87402
36.579	-0.74707
36.777	-0.64453
36.975	-0.66406
37.175	-0.69824
37.372	-0.68359
37.57	-0.71777
37.771	-0.61035
37.974	-0.71777
38.173	-0.82031
38.373	-0.69824
38.573	-0.78613
38.773	-0.68848
38.972	-0.65918

Column1	
Mean	-0.20146
Standard Error	0.007161
Median	-0.20508
Mode	-0.2002
Standard Deviation	0.064449
Sample Variance	0.004154
Kurtosis	-0.39863
Skewness	0.210357
Range	0.27832
Minimum	-0.32715
Maximum	-0.04883
Sum	-16.3184
Count	81

Column2	
Mean	-0.71593
Standard Error	0.007174
Median	-0.71777
Mode	-0.69824
Standard Deviation	0.075581
Sample Variance	0.005713
Kurtosis	-0.29535
Skewness	0.201135
Range	0.356445
Minimum	-0.87402
Maximum	-0.51758
Sum	-79.4678
Count	111

-0.51446 (+/-.15)

For the second measurement at 60 V, the recorded result is 0.520235+/- 0.16 quad-cell voltage.

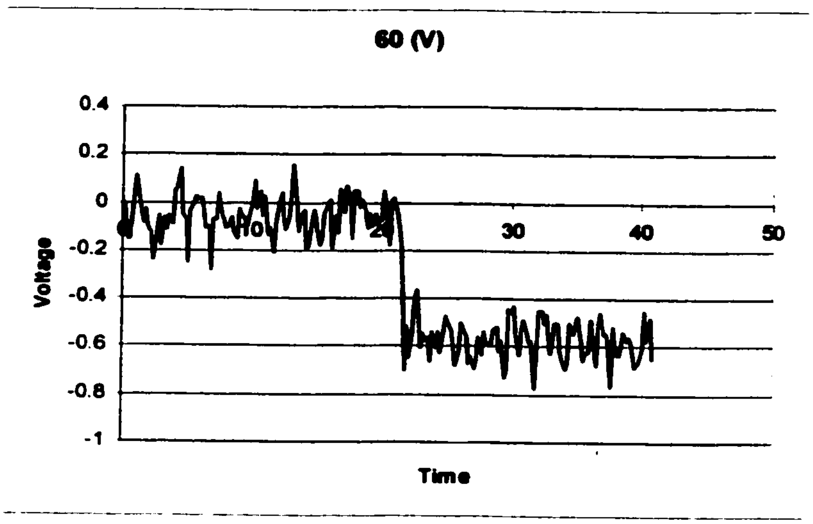

2nd Measurement at 60 V

(X1 + Y2) - (X2 + Y1)

Time (s)	Voltage (V)
0.001	-0.078125
0.201	0
0.399	-0.151367188
0.598	-0.151367188
0.802	-0.063476563
1.003	0.1171875

1.203	0.05859375
1.403	-0.004882813
1.602	-0.083007813
1.804	-0.024414063
2.008	-0.09765625
2.211	-0.126953125
2.414	-0.234375
2.618	-0.1171875
2.821	-0.053710938
3.025	-0.180664063
3.228	-0.063476563
3.431	-0.112304688
3.634	-0.053710938
3.835	-0.087890625
4.036	0.048828125
4.236	0.05859375
4.439	0.146484375
4.641	-0.043945313
4.842	-0.068359375
5.043	-0.249023438
5.244	-0.034179688
5.445	0
5.645	0.029296875
5.848	0.014648438
6.051	0.01953125
6.253	-0.029296875
6.453	-0.107421875
6.656	-0.09765625
6.858	-0.283203125
7.061	-0.068359375
7.261	-0.068359375
7.462	0.0390625
7.664	-0.053710938
7.866	-0.068359375
8.066	-0.107421875
8.267	-0.092773438
8.467	-0.063476563
8.668	-0.1171875
8.87	-0.146484375
9.071	-0.024414063
9.271	-0.053710938
9.472	-0.068359375
9.673	-0.09765625
9.873	-0.053710938
10.076	0.004882813
10.276	0.092773438
10.476	-0.024414063
10.676	0.048828125
10.876	-0.053710938
11.079	0.024414063

11.28	-0.13671875
11.481	-0.102539063
11.683	-0.209960938
11.884	-0.083007813
12.087	-0.034179688
12.288	0.043945313
12.487	-0.068359375
12.687	-0.112304688
12.886	-0.063476563
13.087	0.024414063
13.288	0.15625
13.488	-0.004882813
13.685	-0.1171875
13.884	-0.068359375
14.084	-0.034179688
14.283	-0.190429688
14.484	-0.185546875
14.685	-0.078125
14.883	-0.029296875
15.083	-0.09765625
15.281	-0.180664063
15.483	-0.146484375
15.683	-0.048828125
15.884	-0.009765625
16.084	0.014648438
16.284	-0.190429688
16.486	-0.053710938
16.686	-0.126953125
16.887	0.053710938
17.092	-0.0390625
17.29	0.073242188
17.489	0.01953125
17.688	-0.146484375
17.887	0.048828125
18.089	0.048828125
18.293	-0.014648438
18.492	0.009765625
18.692	-0.0390625
18.893	-0.102539063
19.093	-0.043945313
19.294	-0.092773438
19.492	-0.048828125
19.689	-0.068359375
19.889	-0.078125
20.088	0.048828125
20.287	-0.014648438
20.483	-0.180664063
20.683	0.004882813
20.883	0.01953125
21.084	-0.043945313

21.285	-0.102539063
21.484	-0.185546875
21.684	-0.698242188
21.882	-0.512695313
22.082	-0.64453125
22.28	-0.532226563
22.478	-0.405273438
22.676	-0.361328125
22.875	-0.600585938
23.074	-0.541992188
23.274	-0.576171875
23.472	-0.556640625
23.671	-0.659179688
23.869	-0.537109375
24.069	-0.60546875
24.267	-0.537109375
24.466	-0.625
24.666	-0.522460938
24.864	-0.473632813
25.063	-0.498046875
25.262	-0.52734375
25.461	-0.595703125
25.659	-0.678710938
25.856	-0.615234375
26.054	-0.498046875
26.252	-0.522460938
26.451	-0.556640625
26.649	-0.668945313
26.845	-0.639648438
27.045	-0.693359375
27.244	-0.654296875
27.442	-0.556640625
27.639	-0.634765625
27.836	-0.537109375
28.035	-0.581054688
28.233	-0.5859375
28.43	-0.5859375
28.628	-0.52734375
28.825	-0.517578125
29.023	-0.620117188
29.221	-0.576171875
29.419	-0.727539063
29.618	-0.698242188
29.815	-0.439453125
30.012	-0.454101563
30.211	-0.424804688
30.409	-0.546875
30.606	-0.634765625
30.802	-0.532226563
31	-0.48828125

31.199	-0.546875
31.398	-0.581054688
31.594	-0.576171875
31.791	-0.776367188
31.99	-0.615234375
32.189	-0.44921875
32.386	-0.44921875
32.584	-0.498046875
32.781	-0.463867188
32.98	-0.625
33.179	-0.590820313
33.376	-0.498046875
33.574	-0.502929688
33.771	-0.620117188
33.969	-0.64453125
34.168	-0.693359375
34.366	-0.6640625
34.565	-0.502929688
34.762	-0.541992188
34.96	-0.517578125
35.158	-0.473632813
35.356	-0.576171875
35.552	-0.654296875
35.748	-0.625
35.946	-0.620117188
36.146	-0.483398438
36.343	-0.551757813
36.541	-0.678710938
36.738	-0.5078125
36.935	-0.458984375
37.136	-0.541992188
37.333	-0.541992188
37.53	-0.561523438
37.726	-0.766601563
37.923	-0.517578125
38.125	-0.625
38.324	-0.634765625
38.524	-0.590820313
38.723	-0.537109375
38.923	-0.576171875
39.124	-0.561523438
39.324	-0.581054688
39.524	-0.688476563
39.726	-0.668945313
39.927	-0.6640625
40.131	-0.60546875
40.335	-0.44921875
40.537	-0.571289063
40.737	-0.478515625
40.94	-0.649414063

Column1	
Mean	-0.05449403
Standard Error	0.007905104
Median	-0.053710938
Mode	-0.068359375
Standard Deviation	0.08138803
Sample Variance	0.006624011
Kurtosis	0.338363551
Skewness	-0.100253989
Range	0.439453125
Minimum	-0.283203125
Maximum	0.15625
Sum	-5.776367188
Count	106

-0.05449403

Column2	
Mean	-0.574729226
Standard Error	0.00829036
Median	-0.576171875
Mode	-0.537109375
Standard Deviation	0.077770469
Sample Variance	0.006048246
Kurtosis	-0.416813512
Skewness	-0.249625166
Range	0.3515625
Minimum	-0.776367188
Maximum	-0.424804688
Sum	-50.57617188
Count	88

-0.574729226

For the third measurement at 60 V, the recorded result is 0.604395+/- 0.16 quad-cell voltage.

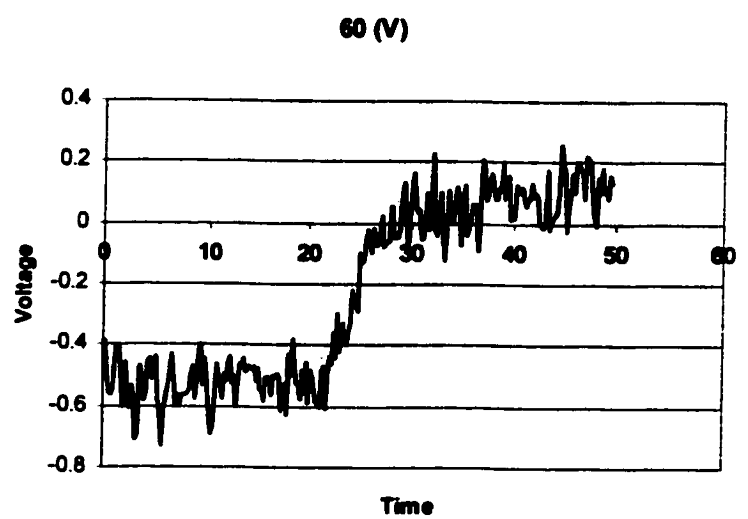

3rd Measurement at 60 V

(X1 + Y2) - (X2 + Y1)

Time (s)	Voltage (V)
0.001	-0.41992
0.2	-0.38574
0.399	-0.50781
0.6	-0.55664
0.802	-0.56152
1.003	-0.54688
1.203	-0.43945
1.405	-0.40527
1.606	-0.40527
1.808	-0.60059
2.011	-0.4541
2.213	-0.54199
2.415	-0.60547
2.618	-0.53223
2.821	-0.56152
3.024	-0.70801
3.226	-0.68848
3.427	-0.46875
3.632	-0.50293
3.834	-0.58105
4.036	-0.56641
4.237	-0.4541
4.438	-0.44434
4.642	-0.5127
4.844	-0.43457
5.044	-0.58594
5.246	-0.625
5.448	-0.73242
5.651	-0.61035
5.854	-0.57129
6.056	-0.53711
6.258	-0.48828
6.459	-0.42969
6.661	-0.50781
6.863	-0.5957
7.065	-0.56152
7.266	-0.5957
7.465	-0.56641
7.668	-0.56641
7.87	-0.56152
8.073	-0.55176
8.274	-0.50293
8.475	-0.46875
8.679	-0.57617
8.883	-0.51758
9.083	-0.41992
9.283	-0.40039

9.485	-0.53223
9.685	-0.43945
9.888	-0.52246
10.089	-0.61523
10.289	-0.68848
10.492	-0.66406
10.694	-0.56152
10.898	-0.45898
11.101	-0.49805
11.304	-0.57617
11.505	-0.49316
11.706	-0.51758
11.908	-0.46387
12.111	-0.43457
12.312	-0.52246
12.514	-0.49805
12.717	-0.60059
12.922	-0.52734
13.123	-0.46387
13.324	-0.46875
13.525	-0.43945
13.728	-0.48828
13.931	-0.47852
14.133	-0.46875
14.336	-0.4834
14.536	-0.46875
14.737	-0.51758
14.939	-0.47363
15.14	-0.54688
15.343	-0.54688
15.545	-0.58105
15.749	-0.50781
15.954	-0.50781
16.155	-0.50781
16.358	-0.56152
16.559	-0.50293
16.762	-0.50781
16.964	-0.49316
17.165	-0.50781
17.364	-0.61523
17.565	-0.52734
17.767	-0.625
17.97	-0.42969
18.173	-0.49805
18.372	-0.38086
18.574	-0.4834
18.775	-0.52734
18.977	-0.52246
19.177	-0.57617
19.38	-0.4834

19.582	-0.55664
19.783	-0.4541
19.986	-0.59082
20.188	-0.47852
20.389	-0.50781
20.589	-0.55176
20.79	-0.58105
20.991	-0.60059
21.193	-0.48828
21.396	-0.46875
21.598	-0.60547
21.797	-0.48828
21.996	-0.43457
22.195	-0.46387
22.394	-0.35645
22.593	-0.44434
22.792	-0.29297
22.994	-0.4248
23.192	-0.40039
23.39	-0.32715
23.589	-0.37109
23.79	-0.40039
23.991	-0.35156
24.19	-0.32715
24.388	-0.21973
24.588	-0.24902
24.79	-0.28809
24.994	-0.09766
25.193	-0.12695
25.393	-0.12207
25.592	-0.07813
25.793	-0.01953
25.994	-0.04883
26.191	-0.09766
26.39	-0.01465
26.589	-0.07324
26.787	-0.07324
26.987	-0.04883
27.186	0.024414
27.385	-0.07813
27.584	-0.06348
27.783	-0.05859
27.983	-0.05859
28.184	0.053711
28.383	-0.04395
28.583	-0.04883
28.784	-0.02441
28.983	0.058594
29.184	0.131836
29.384	0.048828

29.582	-0.09766
29.782	0.014648
29.983	0.102539
30.184	0.166016
30.381	0.053711
30.578	0.039063
30.775	0.043945
30.976	-0.05371
31.174	-0.04395
31.374	0.004883
31.572	0.102539
31.77	-0.01953
31.968	0.092773
32.167	0.224609
32.365	-0.02441
32.563	-0.03906
32.76	0.102539
32.961	-0.02441
33.161	-0.12207
33.36	-0.01465
33.559	0.107422
33.757	0.004883
33.958	0
34.157	0.053711
34.356	0.12207
34.555	0.087891
34.753	-0.07324
34.954	0.073242
35.153	0.126953
35.352	-0.03906
35.551	-0.02441
35.749	-0.00488
35.949	0.058594
36.15	0.03418
36.351	0.063477
36.549	-0.09277
36.747	0.209961
36.946	0.180664
37.146	0.073242
37.346	0.087891
37.545	0.146484
37.744	0.161133
37.945	0.12207
38.145	0.078125
38.345	0.083008
38.543	0.12207
38.742	0.107422
38.943	0.205078
39.144	0.078125
39.343	0.131836

39.543	0.15625
39.742	0.009766
39.942	0.014648
40.143	0.019531
40.343	0.126953
40.542	0.102539
40.741	0.117188
40.942	0.083008
41.145	0.053711
41.346	0.083008
41.545	0.083008
41.745	0.131836
41.947	0.087891
42.149	0.097656
42.35	0.078125
42.551	0
42.75	-0.00977
42.951	-0.01465
43.153	0.019531
43.353	0.175781
43.552	-0.01953
43.751	0.004883
43.955	0.019531
44.157	0.039063
44.358	0.097656
44.558	0.258789
44.759	0.195313
44.959	0.170898
45.159	-0.0293
45.359	0.053711
45.561	0.097656
45.762	0.161133
45.965	0.097656
46.168	0.205078
46.372	0.200195
46.574	0.175781
46.776	0.170898
46.98	0.083008
47.183	0.219727
47.387	0.205078
47.589	0.083008
47.994	-0.00977
48.198	0.151367
48.397	0.102539
48.598	0.180664
48.799	0.102539
49.003	0.112305
49.203	0.078125
49.405	0.15625
49.608	0.131836

Column1	
Mean	-0.52231
Standard Error	0.007216
Median	-0.51758
Mode	-0.50781
Standard Deviation	0.071065
Sample Variance	0.00505
Kurtosis	0.353135
Skewness	-0.479
Range	0.351563
Minimum	-0.73242
Maximum	-0.38086
Sum	-50.6641
Count	97

Column1	
Mean	0.082086
Standard Error	0.008375
Median	0.085449
Mode	0.083008
Standard Deviation	0.079454
Sample Variance	0.006313
Kurtosis	-0.43644
Skewness	-0.1434
Range	0.380859
Minimum	-0.12207
Maximum	0.258789
Sum	7.387695
Count	90

0.604395 .+/-.16

For the forth measurement at 60 V, the recorded result is 0.73335+/- 0.16 quad-cell voltage.

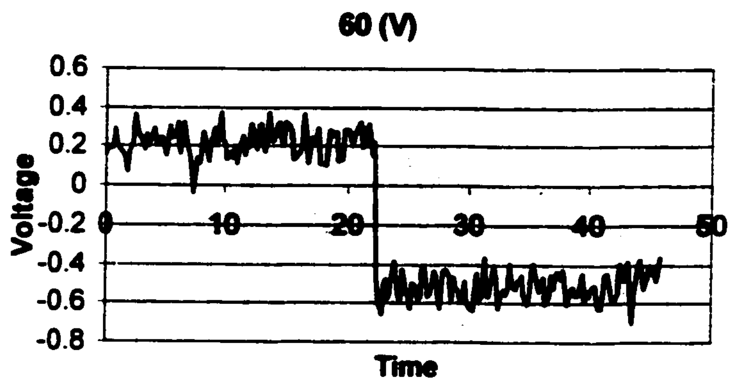

4th Measurement at 60 V

(X1 + Y2) - (X2 + Y1)

Time (s)	Voltage (V)
0.001	0.15625
0.201	0.185547
0.401	0.195313
0.602	0.19043
0.805	0.297852
1.006	0.200195
1.209	0.19043
1.41	0.161133
1.61	0.146484
1.813	0.068359
2.013	0.175781
2.214	0.219727
2.414	0.371094
2.614	0.297852
2.816	0.253906
3.017	0.244141
3.217	0.185547
3.417	0.263672
3.615	0.200195
3.817	0.239258
4.018	0.297852
4.219	0.209961
4.42	0.224609
4.619	0.249023
4.823	0.244141
5.023	0.15625
5.223	0.219727
5.421	0.302734
5.622	0.244141
5.822	0.258789

6.021	0.327148
6.221	0.166016
6.421	0.239258
6.622	0.322266
6.824	0.195313
7.025	0.151367
7.225	0.092773
7.423	-0.04395
7.624	0.141602
7.826	0.112305
8.024	0.166016
8.224	0.27832
8.424	0.219727
8.622	0.126953
8.821	0.234375
9.02	0.249023
9.219	0.292969
9.419	0.205078
9.617	0.380859
9.819	0.219727
10.019	0.224609
10.216	0.131836
10.416	0.170898
10.614	0.146484
10.813	0.200195
11.012	0.112305
11.212	0.185547
11.411	0.253906
11.611	0.15625
11.813	0.214844
12.01	0.19043
12.208	0.317383
12.407	0.268555
12.605	0.180664
12.802	0.27832
13.004	0.3125
13.202	0.175781
13.398	0.229492
13.598	0.380859
13.797	0.239258
13.996	0.219727
14.195	0.292969
14.396	0.322266
14.594	0.249023
14.792	0.205078
14.992	0.322266
15.193	0.302734
15.391	0.273438
15.588	0.131836
15.787	0.141602

15.985	0.170898
16.183	0.195313
16.381	0.366211
16.577	0.263672
16.775	0.117188
16.977	0.244141
17.174	0.244141
17.369	0.219727
17.565	0.297852
17.762	0.117188
17.961	0.112305
18.159	0.102539
18.359	0.214844
18.554	0.283203
18.751	0.253906
18.952	0.273438
19.151	0.126953
19.348	0.136719
19.546	0.136719
19.742	0.288086
19.941	0.288086
20.142	0.258789
20.336	0.200195
20.531	0.253906
20.73	0.273438
20.929	0.327148
21.129	0.19043
21.325	0.292969
21.523	0.205078
21.719	0.3125
21.919	0.15625
22.115	0.224609
22.31	-0.44434
22.508	-0.58105
22.705	-0.6543
22.904	-0.50781
23.104	-0.47852
23.302	-0.58105
23.501	-0.50781
23.699	-0.38086
23.898	-0.47363
24.098	-0.55664
24.297	-0.59082
24.497	-0.41992
24.695	-0.54688
24.894	-0.56152
25.095	-0.62988
25.294	-0.49805
25.493	-0.5127
25.692	-0.59082

25.891	-0.56641
26.092	-0.41504
26.291	-0.41504
26.49	-0.57129
26.688	-0.54199
26.888	-0.50781
27.09	-0.43457
27.289	-0.46875
27.489	-0.625
27.687	-0.4834
27.887	-0.43945
28.087	-0.42969
28.287	-0.46387
28.486	-0.58594
28.685	-0.46387
28.884	-0.52734
29.085	-0.52246
29.284	-0.5957
29.484	-0.56152
29.683	-0.4834
29.882	-0.60059
30.084	-0.625
30.282	-0.63965
30.482	-0.56641
30.679	-0.44434
30.878	-0.58594
31.078	-0.55664
31.276	-0.36621
31.474	-0.56152
31.672	-0.56641
31.871	-0.50293
32.075	-0.40039
32.274	-0.4834
32.472	-0.62988
32.67	-0.57617
32.869	-0.52246
33.068	-0.55176
33.267	-0.52734
33.465	-0.39551
33.663	-0.50781
33.861	-0.52246
34.061	-0.4834
34.26	-0.48828
34.465	-0.45898
34.664	-0.55664
34.862	-0.61035
35.062	-0.55664
35.26	-0.4541
35.461	-0.39063
35.659	-0.49316

35.858	-0.53223
36.058	-0.49316
36.257	-0.46387
36.456	-0.61035
36.654	-0.57129
36.851	-0.45898
37.053	-0.52246
37.252	-0.46875
37.45	-0.43457
37.649	-0.47852
37.848	-0.4248
38.047	-0.51758
38.246	-0.60547
38.445	-0.52734
38.644	-0.51758
38.843	-0.55176
39.044	-0.55176
39.243	-0.56152
39.444	-0.44434
39.643	-0.59082
39.843	-0.53223
40.044	-0.57129
40.243	-0.52734
40.443	-0.50293
40.643	-0.58105
40.843	-0.62988
41.044	-0.62988
41.243	-0.45898
41.443	-0.44922
41.641	-0.49805
41.841	-0.55176
42.042	-0.5957
42.245	-0.54688
42.447	-0.39551
42.648	-0.46387
42.849	-0.4834
43.053	-0.38086
43.255	-0.53711
43.456	-0.70313
43.653	-0.54688
43.853	-0.40039
44.053	-0.37109
44.252	-0.44434
44.454	-0.52734
44.654	-0.48828
44.854	-0.40039
45.058	-0.44434
45.26	-0.41992
45.463	-0.4834
45.665	-0.36621

Column1	
Mean	0.220562
Standard Error	0.006894
Median	0.219727
Mode	0.219727
Standard Deviation	0.072633
Sample Variance	0.005275
Kurtosis	0.621143
Skewness	-0.2728
Range	0.424805
Minimum	-0.04395
Maximum	0.380859
Sum	24.48242
Count	111

Column2	
Mean	-0.51278
Standard Error	0.006867
Median	-0.52246
Mode	-0.4834
Standard Deviation	0.071698
Sample Variance	0.005141
Kurtosis	-0.56694
Skewness	0.055921
Range	0.336914
Minimum	-0.70313
Maximum	-0.36621
Sum	-55.8936
Count	109

-0.73335 (+/-.14)

ANNEX 2.3

Measurement at 90 V

For the first measurement at 90 V, the recorded result is 0.807862+/- 0.16 quad-cell voltage.

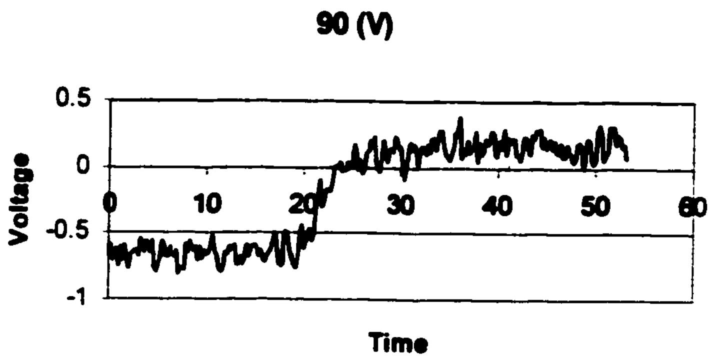

1st Measurement at 90 V

(X1 + Y2) - (X2 + Y1)

Time (s)	Voltage (V)
0.001	-0.64453
0.203	-0.58594
0.403	-0.69824
0.605	-0.62988
0.808	-0.61035
1.013	-0.75195
1.216	-0.60547
1.417	-0.70801
1.619	-0.58105
1.822	-0.69336
2.023	-0.75684
2.224	-0.65918
2.424	-0.64453
2.625	-0.62988
2.828	-0.625
3.03	-0.67383
3.233	-0.53711
3.434	-0.58105

3.638	-0.64453
3.842	-0.55176
4.044	-0.60059
4.246	-0.64941
4.448	-0.55664
4.649	-0.75684
4.852	-0.78613
5.054	-0.7373
5.257	-0.68359
5.458	-0.55176
5.661	-0.60059
5.863	-0.67871
6.067	-0.67383
6.268	-0.5957
6.469	-0.63965
6.67	-0.66406
6.871	-0.67383
7.075	-0.625
7.277	-0.80566
7.479	-0.75684
7.681	-0.76172
7.884	-0.77148
8.084	-0.59082
8.286	-0.63965
8.487	-0.56152
8.717	-0.5957
8.919	-0.625
9.119	-0.60547
9.32	-0.69824
9.521	-0.60059
9.723	-0.68359
9.925	-0.625
10.126	-0.65918
10.325	-0.63965
10.527	-0.60059
10.728	-0.5127
10.933	-0.63477
11.135	-0.67383
11.335	-0.75684
11.535	-0.79102
11.736	-0.76172
11.939	-0.64941
12.138	-0.66406
12.339	-0.60059
12.542	-0.63477
12.744	-0.60059
12.945	-0.58105
13.147	-0.73242
13.347	-0.73242
13.548	-0.67383

13.75	-0.72754
13.953	-0.68848
14.153	-0.58594
14.355	-0.66895
14.556	-0.60547
14.757	-0.5957
14.958	-0.59082
15.159	-0.61035
15.361	-0.67383
15.561	-0.62988
15.761	-0.68359
15.963	-0.71289
16.167	-0.67383
16.367	-0.64453
16.567	-0.62012
16.768	-0.56641
16.97	-0.49316
17.172	-0.61035
17.373	-0.71777
17.574	-0.74219
17.776	-0.72266
17.977	-0.59082
18.18	-0.4834
18.382	-0.50781
18.585	-0.62988
18.787	-0.67871
18.989	-0.73242
19.192	-0.75684
19.393	-0.69336
19.594	-0.55664
19.797	-0.43945
20.001	-0.62012
20.204	-0.57129
20.405	-0.50781
20.605	-0.46387
20.803	-0.55176
21.005	-0.49805
21.207	-0.30762
21.409	-0.26367
21.608	-0.08789
21.807	-0.30273
22.006	-0.25391
22.206	-0.16602
22.404	-0.1709
22.603	-0.19043
22.801	-0.11719
22.999	-0.00977
23.199	0.004883
23.4	-0.00488
23.599	0.039063

23.8	-0.03906
24.001	-0.00488
24.202	-0.01465
24.403	0.039063
24.602	-0.00977
24.799	0.004883
24.999	0.166016
25.202	0.107422
25.402	-0.02441
25.603	0.058594
25.803	-0.05371
26.005	-0.01953
26.208	0.092773
26.409	0.131836
26.61	0.146484
26.81	0.200195
27.012	0.151367
27.215	0.234375
27.416	0.043945
27.617	-0.00488
27.82	-0.0293
28.022	0.063477
28.224	0.200195
28.426	0.107422
28.628	0.043945
28.83	0.12207
29.033	0.136719
29.235	0.107422
29.437	0.239258
29.638	0.224609
29.84	0.146484
30.043	0.15625
30.244	0.039063
30.446	-0.08789
30.648	0.004883
30.848	0.117188
31.051	0.185547
31.255	0.12207
31.456	0.170898
31.656	0.12207
31.857	0.009766
32.06	0.126953
32.262	0.151367
32.463	0.141602
32.664	0.097656
32.863	0.180664
33.067	0.117188
33.268	0.224609
33.47	0.219727
33.67	0.126953

33.875	0.209961
34.077	0.27832
34.279	0.273438
34.481	0.175781
34.683	0.092773
34.883	0.087891
35.086	0.048828
35.288	0.102539
35.49	0.161133
35.691	0.258789
35.893	0.249023
36.095	0.380859
36.298	0.063477
36.5	0.12207
36.701	0.102539
36.901	0.200195
37.104	0.112305
37.306	0.146484
37.507	0.161133
37.708	0.283203
37.91	0.195313
38.113	0.043945
38.315	0.185547
38.515	0.097656
38.717	0.126953
38.92	0.224609
39.122	0.180664
39.322	0.205078
39.521	0.273438
39.719	0.244141
39.917	0.087891
40.115	0.141602
40.312	0.209961
40.511	0.141602
40.708	0.292969
40.905	0.092773
41.106	0.239258
41.307	0.185547
41.505	0.224609
41.703	0.214844
41.901	0.102539
42.1	0.092773
42.304	0.058594
42.507	0.131836
42.709	0.239258
42.913	0.219727
43.116	0.136719
43.318	0.092773
43.52	0.244141
43.719	0.224609

43.922	0.273438
44.123	0.283203
44.323	0.288086
44.524	0.161133
44.723	0.234375
44.924	0.146484
45.127	0.166016
45.325	0.224609
45.525	0.141602
45.726	0.205078
45.928	0.112305
46.129	0.136719
46.331	0.112305
46.529	0.195313
46.728	0.083008
46.929	0.078125
47.132	0.166016
47.329	0.107422
47.529	0.092773
47.728	0.039063
47.928	0.068359
48.128	0.180664
48.331	0.185547
48.532	0.151367
48.729	-0.00488
48.932	0.131836
49.13	0.214844
49.331	0.200195
49.531	0.073242
49.731	0.019531
49.932	0.048828
50.134	0.263672
50.334	0.327148
50.534	0.234375
50.733	0.058594
50.934	0.102539
51.134	0.107422
51.335	0.3125
51.537	0.3125
51.737	0.302734
51.943	0.175781
52.149	0.253906
52.363	0.239258
52.565	0.151367
52.766	0.180664
52.967	0.068359

Column1	
Mean	-0.6518
Standard Error	0.007065
Median	-0.64453
Mode	-0.67383
Standard Deviation	0.067027
Sample Variance	0.004493
Kurtosis	-0.42036
Skewness	-0.24638
Range	0.3125
Minimum	-0.80566
Maximum	-0.49316
Sum	-58.6621
Count	90

Column2	
Mean	0.156061
Standard Error	0.007341
Median	0.151367
Mode	0.224609
Standard Deviation	0.083378
Sample Variance	0.006952
Kurtosis	-0.12274
Skewness	-0.03457
Range	0.46875
Minimum	-0.08789
Maximum	0.380859
Sum	20.13184
Count	129

0.807862 (+/-.15)

For the second measurement at 90 V, the recorded result is 0.843076+/- 0.16 quad-cell voltage.

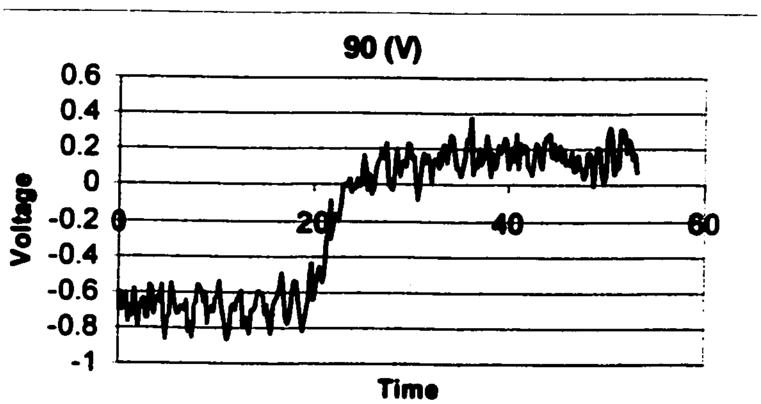

2nd Measurement at 90 V

(X1 + Y1) - (X2 + Y2)

Time (s)	Voltage (V)
0.001	-0.70313
0.203	-0.60547
0.403	-0.69824
0.605	-0.65918
0.808	-0.61035
1.013	-0.77148
1.216	-0.68359
1.417	-0.7373
1.619	-0.58105
1.822	-0.69336
2.023	-0.78613
2.224	-0.67871
2.424	-0.64453
2.625	-0.63965
2.828	-0.74219
3.03	-0.74219
3.233	-0.55664
3.434	-0.58105
3.638	-0.72266
3.842	-0.63965
4.044	-0.62988
4.246	-0.65918
4.448	-0.55664
4.649	-0.7666
4.852	-0.86426
5.054	-0.74707
5.257	-0.72266
5.458	-0.55176
5.661	-0.60059
5.863	-0.67871
6.067	-0.72266
6.268	-0.71289
6.469	-0.67871
6.67	-0.68359
6.871	-0.70313
7.075	-0.64453
7.277	-0.8252
7.479	-0.7666
7.681	-0.85938
7.884	-0.77148
8.084	-0.67871

8.286	-0.65918
8.487	-0.56152
8.717	-0.5957
8.919	-0.6543
9.119	-0.60547
9.32	-0.77637
9.521	-0.70801
9.723	-0.71289
9.925	-0.68359
10.126	-0.71777
10.325	-0.63965
10.527	-0.62988
10.728	-0.53223
10.933	-0.67383
11.135	-0.73242
11.335	-0.78613
11.535	-0.86914
11.736	-0.83984
11.939	-0.68848
12.138	-0.66406
12.339	-0.69824
12.542	-0.63477
12.744	-0.62988
12.945	-0.59082
13.147	-0.79102
13.347	-0.74219
13.548	-0.74219
13.75	-0.83496
13.953	-0.69824
14.153	-0.70313
14.355	-0.67871
14.556	-0.60547
14.757	-0.5957
14.958	-0.61035
15.159	-0.61035
15.361	-0.72266
15.561	-0.66895
15.761	-0.77148
15.963	-0.83008
16.167	-0.68359
16.367	-0.64453
16.567	-0.62012
16.768	-0.58594
16.97	-0.49316
17.172	-0.61035
17.373	-0.7373
17.574	-0.78125
17.776	-0.73242
17.977	-0.61035
18.18	-0.53223

18.382	-0.54688
18.585	-0.65918
18.787	-0.7373
18.989	-0.82031
19.192	-0.75684
19.393	-0.69336
19.594	-0.625
19.797	-0.43945
20.001	-0.64941
20.204	-0.57129
20.405	-0.50781
20.605	-0.46387
20.803	-0.55176
21.005	-0.49805
21.207	-0.30762
21.409	-0.26367
21.608	-0.08789
21.807	-0.30273
22.006	-0.25391
22.206	-0.16602
22.404	-0.1709
22.603	-0.19043
22.801	-0.11719
22.999	-0.00977
23.199	0.004883
23.4	-0.00488
23.599	0.039063
23.8	-0.03906
24.001	-0.00488
24.202	-0.01465
24.403	0.039063
24.602	-0.00977
24.799	0.004883
24.999	0.166016
25.202	0.107422
25.402	-0.02441
25.603	0.058594
25.803	-0.05371
26.005	-0.01953
26.208	0.092773
26.409	0.131836
26.61	0.146484
26.81	0.200195
27.012	0.151367
27.215	0.234375
27.416	0.043945
27.617	-0.00488
27.82	-0.0293
28.022	0.063477
28.224	0.200195

28.426	0.107422
28.628	0.043945
28.83	0.12207
29.033	0.136719
29.235	0.107422
29.437	0.239258
29.638	0.224609
29.84	0.146484
30.043	0.15625
30.244	0.039063
30.446	-0.08789
30.648	0.004883
30.848	0.117188
31.051	0.185547
31.255	0.12207
31.456	0.170898
31.656	0.12207
31.857	0.009766
32.06	0.126953
32.262	0.151367
32.463	0.141602
32.664	0.097656
32.863	0.180664
33.067	0.117188
33.268	0.224609
33.47	0.219727
33.67	0.126953
33.875	0.209961
34.077	0.27832
34.279	0.273438
34.481	0.175781
34.683	0.092773
34.883	0.087891
35.086	0.048828
35.288	0.102539
35.49	0.161133
35.691	0.258789
35.893	0.249023
36.095	0.380859
36.298	0.063477
36.5	0.12207
36.701	0.102539
36.901	0.200195
37.104	0.112305
37.306	0.146484
37.507	0.161133
37.708	0.283203
37.91	0.195313
38.113	0.043945
38.315	0.185547

38.515	0.097656
38.717	0.126953
38.92	0.224609
39.122	0.180664
39.322	0.205078
39.521	0.273438
39.719	0.244141
39.917	0.087891
40.115	0.141602
40.312	0.209961
40.511	0.141602
40.708	0.292969
40.905	0.092773
41.106	0.239258
41.307	0.185547
41.505	0.224609
41.703	0.214844
41.901	0.102539
42.1	0.092773
42.304	0.058594
42.507	0.131836
42.709	0.239258
42.913	0.219727
43.116	0.136719
43.318	0.092773
43.52	0.244141
43.719	0.224609
43.922	0.273438
44.123	0.283203
44.323	0.288086
44.524	0.161133
44.723	0.234375
44.924	0.146484
45.127	0.166016
45.325	0.224609
45.525	0.141602
45.726	0.205078
45.928	0.112305
46.129	0.136719
46.331	0.112305
46.529	0.195313
46.728	0.083008
46.929	0.078125
47.132	0.166016
47.329	0.107422
47.529	0.092773
47.728	0.039063
47.928	0.068359
48.128	0.180664
48.331	0.185547

48.532	0.151367
48.729	-0.00488
48.932	0.131836
49.13	0.214844
49.331	0.200195
49.531	0.073242
49.731	0.019531
49.932	0.048828
50.134	0.263672
50.334	0.327148
50.534	0.234375
50.733	0.058594
50.934	0.102539
51.134	0.107422
51.335	0.3125
51.537	0.3125
51.737	0.302734
51.943	0.175781
52.149	0.253906
52.363	0.239258
52.565	0.151367
52.766	0.180664
52.967	0.068359

Column1	
Mean	-0.68182
Standard Error	0.008527
Median	-0.68359
Mode	-0.61035
Standard Deviation	0.084844
Sample Variance	0.007199
Kurtosis	-0.02799
Skewness	0.030698
Range	0.429688
Minimum	-0.86914
Maximum	-0.43945
Sum	-67.5
Count	99

Column2	
Mean	0.161258
Standard Error	0.007539
Median	0.15625
Mode	0.224609
Standard Deviation	0.08155
Sample Variance	0.00665
Kurtosis	-0.00733
Skewness	-0.0208
Range	0.46875
Minimum	-0.08789
Maximum	0.380859
Sum	18.86719
Count	117

0.843076 (+/-.16)

For the third measurement at 90 V, the recorded result is 0.820802+/- 0.16 quad-cell voltage.

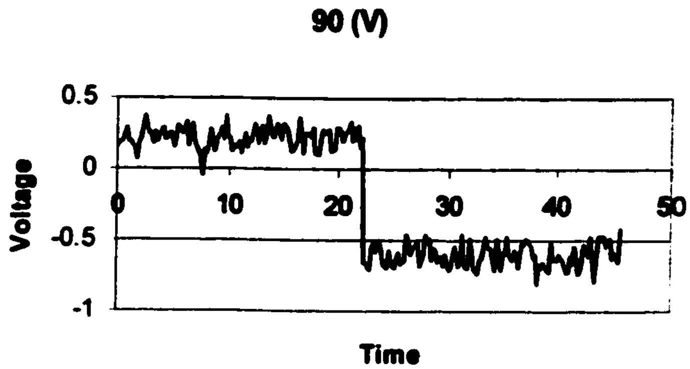

3rd Measurement at 90 V

(X1 + Y1) - (X2 + Y2)

Time (s)	Voltage (V)
0.001	0.15625
0.201	0.185547
0.401	0.195313
0.602	0.19043
0.805	0.297852
1.006	0.200195
1.209	0.19043
1.41	0.161133
1.61	0.146484
1.813	0.068359
2.013	0.175781
2.214	0.219727
2.414	0.371094
2.614	0.297852
2.816	0.253906

3.017	0.244141
3.217	0.185547
3.417	0.263672
3.615	0.200195
3.817	0.239258
4.018	0.297852
4.219	0.209961
4.42	0.224609
4.619	0.249023
4.823	0.244141
5.023	0.15625
5.223	0.219727
5.421	0.302734
5.622	0.244141
5.822	0.258789
6.021	0.327148
6.221	0.166016
6.421	0.239258
6.622	0.322266
6.824	0.195313
7.025	0.151367
7.225	0.092773
7.423	-0.04395
7.624	0.141602
7.826	0.112305
8.024	0.166016
8.224	0.27832
8.424	0.219727
8.622	0.126953
8.821	0.234375
9.02	0.249023
9.219	0.292969
9.419	0.205078
9.617	0.380859
9.819	0.219727
10.019	0.224609
10.216	0.131836
10.416	0.170898
10.614	0.146484
10.813	0.200195
11.012	0.112305
11.212	0.185547
11.411	0.253906
11.611	0.15625
11.813	0.214844
12.01	0.19043
12.208	0.317383
12.407	0.268555
12.605	0.180664
12.802	0.27832

13.004	0.3125
13.202	0.175781
13.398	0.229492
13.598	0.380859
13.797	0.239258
13.996	0.219727
14.195	0.292969
14.396	0.322266
14.594	0.249023
14.792	0.205078
14.992	0.322266
15.193	0.302734
15.391	0.273438
15.588	0.131836
15.787	0.141602
15.985	0.170898
16.183	0.195313
16.381	0.366211
16.577	0.263672
16.775	0.117188
16.977	0.244141
17.174	0.244141
17.369	0.219727
17.565	0.297852
17.762	0.117188
17.961	0.112305
18.159	0.102539
18.359	0.214844
18.554	0.283203
18.751	0.253906
18.952	0.273438
19.151	0.126953
19.348	0.136719
19.546	0.136719
19.742	0.288086
19.941	0.288086
20.142	0.258789
20.336	0.200195
20.531	0.253906
20.73	0.273438
20.929	0.327148
21.129	0.19043
21.325	0.292969
21.523	0.205078
21.719	0.3125
21.919	0.15625
22.115	0.224609
22.31	-0.65918
22.508	-0.65918
22.705	-0.70313

22.904	-0.55664
23.104	-0.51758
23.302	-0.58105
23.501	-0.54688
23.699	-0.49805
23.898	-0.57129
24.098	-0.66406
24.297	-0.69824
24.497	-0.56641
24.695	-0.64453
24.894	-0.67871
25.095	-0.68848
25.294	-0.625
25.493	-0.58105
25.692	-0.66895
25.891	-0.63477
26.092	-0.46387
26.291	-0.49316
26.49	-0.59082
26.688	-0.55176
26.888	-0.54688
27.09	-0.53223
27.289	-0.51758
27.489	-0.67383
27.687	-0.59082
27.887	-0.45898
28.087	-0.51758
28.287	-0.4834
28.486	-0.64453
28.685	-0.55176
28.884	-0.56641
29.085	-0.64941
29.284	-0.60547
29.484	-0.67871
29.683	-0.60059
29.882	-0.66895
30.084	-0.70313
30.282	-0.68848
30.482	-0.61523
30.679	-0.54199
30.878	-0.67383
31.078	-0.64453
31.276	-0.46387
31.474	-0.64941
31.672	-0.69336
31.871	-0.68848
32.075	-0.48828
32.274	-0.57129
32.472	-0.68848
32.67	-0.73242

32.869	-0.63965
33.068	-0.62988
33.267	-0.55664
33.465	-0.47363
33.663	-0.54688
33.861	-0.55176
34.061	-0.56152
34.26	-0.71289
34.465	-0.48828
34.664	-0.58594
34.862	-0.70801
35.062	-0.58594
35.26	-0.60059
35.461	-0.47852
35.659	-0.60059
35.858	-0.63965
36.058	-0.57129
36.257	-0.59082
36.456	-0.69824
36.654	-0.58105
36.851	-0.50781
37.053	-0.52246
37.252	-0.48828
37.45	-0.50293
37.649	-0.53711
37.848	-0.62012
38.047	-0.5957
38.246	-0.80078
38.445	-0.66406
38.644	-0.69336
38.843	-0.64941
39.044	-0.67871
39.243	-0.72754
39.444	-0.5127
39.643	-0.63965
39.843	-0.62988
40.044	-0.63965
40.243	-0.5957
40.443	-0.62988
40.643	-0.63965
40.843	-0.71777
41.044	-0.72754
41.243	-0.61523
41.443	-0.66406
41.641	-0.54688
41.841	-0.61035
42.042	-0.73242
42.245	-0.71289
42.447	-0.52246
42.648	-0.55176

42.849	-0.61035
43.053	-0.47852
43.255	-0.61523
43.456	-0.79102
43.653	-0.63477
43.853	-0.47852
44.053	-0.47852
44.252	-0.47363
44.454	-0.53711
44.654	-0.51758
44.854	-0.48828
45.058	-0.62988
45.26	-0.58594
45.463	-0.64941
45.665	-0.41504

Column1	
Mean	0.219772
Standard Error	0.00704
Median	0.219727
Mode	0.219727
Standard Deviation	0.072825
Sample Variance	0.005303
Kurtosis	0.671002
Skewness	-0.26996
Range	0.424805
Minimum	-0.04395
Maximum	0.380859
Sum	23.51563
Count	107

0.820802 (+/-.15)

Column2	
Mean	-0.60103
Standard Error	0.007723
Median	-0.60303
Mode	-0.63965
Standard Deviation	0.081002
Sample Variance	0.006561
Kurtosis	-0.63062
Skewness	0.020175
Range	0.385742
Minimum	-0.80078
Maximum	-0.41504
Sum	-66.1133
Count	110

For the forth measurement at 90 V, the recorded result is 0.967189+/- 0.16 quad-cell voltage.

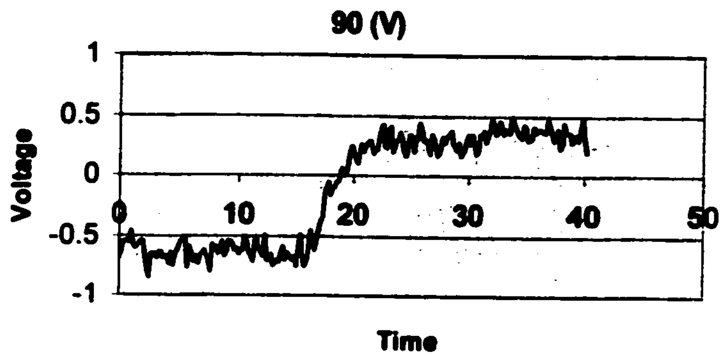

4th Measurement at 90 V

(X1 + Y1) - (X2 + Y2)

Time (s)	Voltage (V)
0.001	-0.68359
0.201	-0.63477
0.4	-0.56152
0.601	-0.54688
0.8	-0.55664
1.001	-0.4541
1.2	-0.57617
1.401	-0.61035
1.601	-0.58594
1.801	-0.53711
2.001	-0.54199
2.202	-0.67383
2.404	-0.79102
2.604	-0.85938
2.805	-0.65918
3.005	-0.65918
3.206	-0.68848
3.412	-0.63477
3.615	-0.63965
3.816	-0.69336
4.016	-0.67871
4.217	-0.74219
4.42	-0.63965
4.621	-0.75195

4.822	-0.6543
5.022	-0.62988
5.223	-0.54199
5.425	-0.53711
5.626	-0.50293
5.827	-0.77148
6.03	-0.5957
6.23	-0.71777
6.432	-0.66895
6.633	-0.73242
6.834	-0.66895
7.034	-0.6543
7.234	-0.62988
7.435	-0.69824
7.636	-0.80566
7.836	-0.58105
8.037	-0.62988
8.237	-0.5957
8.437	-0.6543
8.638	-0.54199
8.839	-0.66406
9.04	-0.63477
9.24	-0.54199
9.441	-0.54199
9.642	-0.61523
9.842	-0.60547
10.042	-0.64941
10.243	-0.61523
10.444	-0.62988
10.641	-0.50293
10.843	-0.64453
11.045	-0.66895
11.245	-0.72266
11.445	-0.54688
11.642	-0.51758
11.844	-0.60059
12.044	-0.66895
12.243	-0.49316
12.445	-0.71289
12.646	-0.69824
12.847	-0.65918
13.047	-0.76172
13.247	-0.70313
13.449	-0.72754
13.649	-0.64941
13.851	-0.59082
14.05	-0.69824
14.248	-0.63477
14.448	-0.69336
14.647	-0.70313

14.847	-0.66895
15.078	-0.76172
15.277	-0.49316
15.477	-0.66895
15.675	-0.75195
15.873	-0.71777
16.075	-0.62988
16.273	-0.45898
16.474	-0.62012
16.674	-0.52734
16.876	-0.44434
17.078	-0.38086
17.279	-0.34668
17.483	-0.15137
17.681	-0.04395
17.88	-0.15625
18.079	-0.09766
18.278	-0.10254
18.479	-0.05371
18.679	-0.04883
18.879	0.058594
19.076	0.024414
19.272	0.019531
19.47	0.097656
19.666	0.200195
19.864	0.253906
20.062	0.136719
20.26	0.102539
20.458	0.195313
20.658	0.258789
20.857	0.200195
21.056	0.249023
21.254	0.288086
21.451	0.268555
21.651	0.180664
21.849	0.214844
22.046	0.214844
22.244	0.307617
22.441	0.429688
22.642	0.239258
22.841	0.224609
23.04	0.390625
23.239	0.405273
23.438	0.200195
23.64	0.288086
23.839	0.292969
24.039	0.356445
24.237	0.317383
24.436	0.219727
24.637	0.170898

24.836	0.341797
25.035	0.307617
25.233	0.200195
25.432	0.332031
25.633	0.307617
25.832	0.439453
26.033	0.302734
26.233	0.297852
26.432	0.283203
26.637	0.175781
26.836	0.341797
27.036	0.3125
27.235	0.166016
27.434	0.200195
27.635	0.263672
27.834	0.322266
28.033	0.283203
28.232	0.322266
28.43	0.375977
28.639	0.258789
28.838	0.244141
29.038	0.209961
29.237	0.27832
29.436	0.170898
29.638	0.229492
29.837	0.292969
30.036	0.341797
30.235	0.263672
30.435	0.341797
30.637	0.175781
30.836	0.209961
31.035	0.341797
31.236	0.327148
31.434	0.380859
31.635	0.27832
31.835	0.380859
32.034	0.46875
32.233	0.424805
32.432	0.336914
32.634	0.366211
32.833	0.454102
33.032	0.336914
33.231	0.400391
33.43	0.366211
33.633	0.361328
33.832	0.488281
34.031	0.429688
34.232	0.356445
34.432	0.332031
34.633	0.3125

34.833	0.419922
35.032	0.410156
35.231	0.297852
35.429	0.307617
35.631	0.410156
35.83	0.361328
36.029	0.375977
36.228	0.395508
36.428	0.375977
36.63	0.366211
36.831	0.473633
37.032	0.405273
37.237	0.361328
37.45	0.292969
37.654	0.395508
37.854	0.229492
38.063	0.268555
38.271	0.43457
38.475	0.356445
38.68	0.356445
38.881	0.27832
39.079	0.3125
39.282	0.351563
39.481	0.302734
39.681	0.478516
39.879	0.317383
40.077	0.19043

Column1	
Mean	-0.64215
Standard Error	0.008994
Median	-0.64941
Mode	-0.66895
Standard Deviation	0.080443
Sample Variance	0.006471
Kurtosis	-0.13304
Skewness	0.003614
Range	0.405273
Minimum	-0.85938
Maximum	-0.4541
Sum	-51.3721
Count	80

Column2	
Mean	0.325039
Standard Error	0.008703
Median	0.332031
Mode	0.341797
Standard Deviation	0.07833
Sample Variance	0.006136
Kurtosis	-0.36042
Skewness	-0.16104
Range	0.322266
Minimum	0.166016
Maximum	0.488281
Sum	26.32813
Count	81

0.967189 (+/-.16)